



THE UNIVERSITY OF ASTON IN BIRMINGHAM

THE
RATES OF CRYSTALLIZATION
OF
COPOLYAMIDES.

EDWARD DOUGLAS HARVEY

A THESIS FOR THE Ph.D. DEGREE.

DEPARTMENT OF CHEMISTRY · AUGUST 1970.

678.7013

HAR

133294

Summary.

A group of polymers and copolymers based upon polyhexamethylene adipamide (66 nylon) have been prepared. The comonomer ingredients included 6-amino hexoic acid (for 6 nylon) , the salt of terephthalic acid with hexamethylene diamine (for 6T nylon), and a blend of trimesic acid with the diamine acting as a branching agent. The polymeric materials were characterised by solution viscometry.

Apparatus for studying the rates of crystallization of polymers and the published information for polyamides and copolymers is reviewed. The construction of a hot stage attachment for a polarising microscope is described, and the results from this equipment of the crystallization rates and melting behaviour of the copolyamides are reported. The results can be grouped into three series; 1. copolymerisation of 66 nylon with 6 nylon resulted in a loss of crystallinity together with a reduction in the melting temperatures and the temperatures for observing crystallization behaviour; 2, copolymerisation with 6T nylon resulted in a moderate retention of crystallinity, due to isomorphous crystallization; and 3, copolymerisation with a branching agent resulted in both a loss of crystallinity and deviation from the normal kinetic behaviour of polymer crystallization.

Observations on the melting of materials showed that the microscopy technique is complementary with differential thermal analysis. Some of the theories of the melting of polymers and copolymers have been introduced in an attempt to explain the experimental data. Quantitative measurements of the heats of fusion and densities of the copolymers are reported.

Acknowledgements.

I wish to thank Dr.F.J.Hybart for supervising this work,and for his assistance and guidance throughout the course of the research. I am indebted to Imperial Chemical Industries,Ltd., for helpful discussions,and for information concerning their hot stage microscope attachments (Plastics Division), a temperature controller (Dyestuffs Division), and for supplying chemicals (I.C.I. Fibres, Ltd., and Plastics Division). I thank Mr.L.Parker (Chief Technician) for assistance with the construction of the hot stage attachments. Some of the thesis figures were redrawn by Mr.W.F.Nash and Mrs.J. Poole,whose help is acknowledged.

I am very grateful to the Science Research Council for the award of a two-year maintenance grant, and to the University of Aston in Birmingham for extending this maintenance for a third year,and for the use of the facilities of the Chemistry Department.

Contents.

Summary	2
Acknowledgements	3
Introduction to the problem	7
Chapter 1, Literature review.	
Crystallinity in polyamides	8
Single crystals, spherulites	8
Copolyamides	10
Isomorphous crystallization	14
Rates of crystallization of polymers	16
Experimental methods	17
Dilatometry, microscopy	17
Differential thermal analysis	19
Other techniques	20
Theoretical treatments of crystallization rates	21
The Avrami analysis	21
The dependence on temperature	23
Observations on rates of polyamides crystallizations	25
Rates of crystallization of copolymers	29
Fusion of copolymers	32
The selection of polymers and apparatus	34
Chapter 2, Apparatus details.	
The design of a hot stage microscope	36
Photocell circuits	40
The temperature control circuits	40
Temperature measurement	44
The operating procedure for the hot stage microscope	46
The DuPont 900 Thermal Analyzer	48
The Differential Scanning Calorimeter cell	49

The hot stage microscope module	49
Temperature calibration of the hot stage and DSC.	53
Heat of fusion calibration of the D.S.C. cell	56
Other apparatus	58
Davenport Density Measuring Apparatus	58
Solution viscosity apparatus	59
Fluidised sand bed apparatus	59
Chapter 3, Materials.	
Commercial polymers	60
Polymerisation reagents	61
Preparation of 66 nylon	61
Polymerisation of 6 nylon and 6.10 nylon	63
66/6 nylon copolymers, preparations	63
characterisation	64
6T copolymers, polymerisation	69
characterisation	70
Branched /cross-linked 66 nylon copolymers	72
Polymer precipitates	73
Chapter 4, Results.	
Depolarised light intensity measurements	75
Rates of crystallization of 66 nylon	76
Copolymers of 66 nylon and 6 nylon	80
Rates of crystallization	80
Temperature programmed crystallization	89
Copolymers of 66/6T nylon and 6.10/6T nylon	92
Melting temperatures	92
Rates of crystallization, 66/6T copolymers	92
6.10/6T copolymers	98
Heats of fusion	101

Branched 66 nylon copolymers, melting temperatures	103
rates of crystallization	103
heats of fusion	106
The melting of various forms of nylon	106
Depolarised light intensity observations	108
D.T.A. observations	112
Chapter 5, Discussion.	
Techniques for studying rates of crystallization	115
Superposability of crystallization isotherms	116
Avrami analysis	122
The dependence of crystallization rates on temperature	127
The Flory equation applied to 66/6 copolymers	139
The isomorphous character of 66/6T copolymers	141
Fusion of 66 nylon, multiple melting endotherms	142
Fusion of copolymers, multiple melting endotherms	148
Chapter 6, Conclusions.	
The crystallization and melting of copolyamides	150
The general importance of nylon polymers	152
The technological implications of the work	153
Recommendations for further work	154
References	156

INTRODUCTION TO THE PROBLEM .

A substantial amount of information has been published concerning the crystallization of polymers. Observations have concentrated upon the growth of crystalline structures from dilute solutions and from supercooled melts. Copolymers have received much less attention, with the exception of some commercially important materials.

Polyamides were chosen for this study, because they are an important class of polymers, and they may be prepared in the form of random copolymers. The physical properties of these copolymers are different from those of the homopolymers, and as a consequence, some copolyamides are of potential importance. The compositions of the copolymers have been selected to include at least one commercial nylon monomer. As 66 nylon (polyhexamethylene adipamide) is the largest tonnage polyamide in the U.K., this polymer has been studied in detail, both as a homopolymer and as a constituent of copolymers.

Theoretical considerations of the kinetics of polymer crystallizations have been reviewed. The interpretations are generally confined to observations of homopolymer crystallizations at isothermal temperatures, and normally exclude copolymers. Although no treatments for the process of crystallization during changing temperature conditions have been published, fast crystallization rates under cooling conditions are the normal commercial practice.

In this thesis, the rates of crystallization of some copolyamides are reported. Although the observations have not been confined to crystallization under isothermal temperature control, most of the measurements have been made using this simplification, in order to obtain the advantageous usage of the established theories.

CHAPTER 1 , LITERATURE REVIEW.

Crystallinity in polyamides.

Attention to observations of the crystalline state of polymers dates from the late 1940's. Two distinct lines of approach were followed over a decade, and both are reviewed extensively by Geil (1).

Single crystals. Observations, using the transmitting electron microscope, of shadowed polymers which had been precipitated slowly from very dilute solutions, confirmed that small single crystals can be produced from polyolefines. The material favoured was linear polyethylene, and although single lamellae were seen, aggregation of platelets was frequently observed. Single crystals of polyamides were observed by Keller (2) and Geil (3), by cooling hot glycerol solutions; more recently, butane diol has been used to dissolve polyamides for single crystal studies.(4).

Spherulites. When polymers are crystallized from more concentrated solutions (over 5% is typical) or from melts, individual single crystals are no longer produced, but aggregated spherical structures are seen. These are termed 'spherulites', and their structure is visible using an optical polarising microscope. The theory of Keith and Padden (5) explaining the physical composition of polymer spherulites has received widespread acceptance, and has three basic concepts:

- i, spherulites consist of fibres or fibrils, separated by as-yet uncrystallized melt;
- ii, depending upon the system, the layers of melt then crystallize slowly or remain amorphous; this process causes lateral coarsening of the existing fibres;

iii, nuclei are bundles of parallel fibres, fanning out like sheaves. Spherulites have been observed in polyamides by many authors (6-9), and classified by Magill (10), on the basis of their appearances under the polarising microscope.

The characteristic Maltese cross pattern, with arms parallel to the directions of the polariser and analyser, can be seen in most polymer spherulites. Positively birefringent spherulites have a greater refractive index along the radius than perpendicular to the radius, and are seen as the usual crystalline form of both 66 nylon and 6 nylon (polycapromide). At higher crystallization temperatures, negatively birefringent spherulites have also been seen for 66 nylon and 6.10 nylon (polyhexamethylene sebacamide). Negatively birefringent spherulites do not form in 6 nylon (11).

Magill and Harris (12) have noticed structures which have the appearances of single crystals in some supercooled polyamide melts, at temperatures close to the polymer melting point. These observations support the concept of spherulites being composed of aligned single crystals, together with amorphous polymer.

With all macromolecular substances, there are structural requirements for accommodating molecules into the crystalline state, and this results in a restriction in the level of crystallinity which can be developed. Keller (13) has shown that folded chains are an essential feature of polyethylene crystals, and folding occurs in 66 nylon crystals (4). An individual molecule may take several folds in the amorphous medium in order to bring about the necessary alignment for the crystalline region. This balance of crystalline and amorphous polymer leads to the characteristic bulk properties of individual polymers, and is discussed by Meares (14).

The strength of the crystalline state of polyamides is

attributable to inter-chain hydrogen bonding. Fig.1 (page 11) shows how the chemical structures of 66 nylon and 6 nylon can each be aligned to produce crystallites which are accommodating hydrogen bonded forces. There is an alternating arrangement of chains within the crystal of 6 nylon, but a parallel arrangement for 66 nylon. These structures were elucidated from X ray crystallographic data by Holmes, Bunn and Smith (15). In earlier work, Bunn and Garner (16) had identified two separate types of stacking of the molecules in 66 nylon crystallites. In the α form, each sheet of extended molecules was found to be displaced 3.55 \AA from the previous sheet to give a stepwise progression in the crystal. In the β form, which appeared to be the less common form, the planes were thought to be arranged alternately. The triclinic unit cell exhibiting α/β polymorphism became the generally accepted structure for 66 nylon, but at temperatures above 160°C , the triclinic structure may be transformed into a hexagonal unit cell structure (17). 6.10 nylon has a similar structure. (16)

For 6 nylon, three crystal forms have been reviewed by Geil (1). The monoclinic unit cell (α form) appears to be the best defined, but the existence of a pseudo-hexagonal cell has been suggested by Vogelsong (18) and Holmes, Bunn and Smith (15). Fewer crystalline forms are reported for most other polyamides. Vogelsong (19) has found that the polyamide from p-xylylene diamine with adipic acid (PXD 6) can exist only in the α configuration, owing to the difficulty in accommodating the aromatic nucleus into the crystal. The aromatic polyamide from hexamethylene diamine with terephthalic acid (6T nylon) may have a similar accommodation requirement.

Copolyamides.

It has been seen that the regular structure of the crystallite requires the close alignment of a nitrogen atom in one polyamide chain with the oxygen atom from an adjacent chain, and this geometric require-

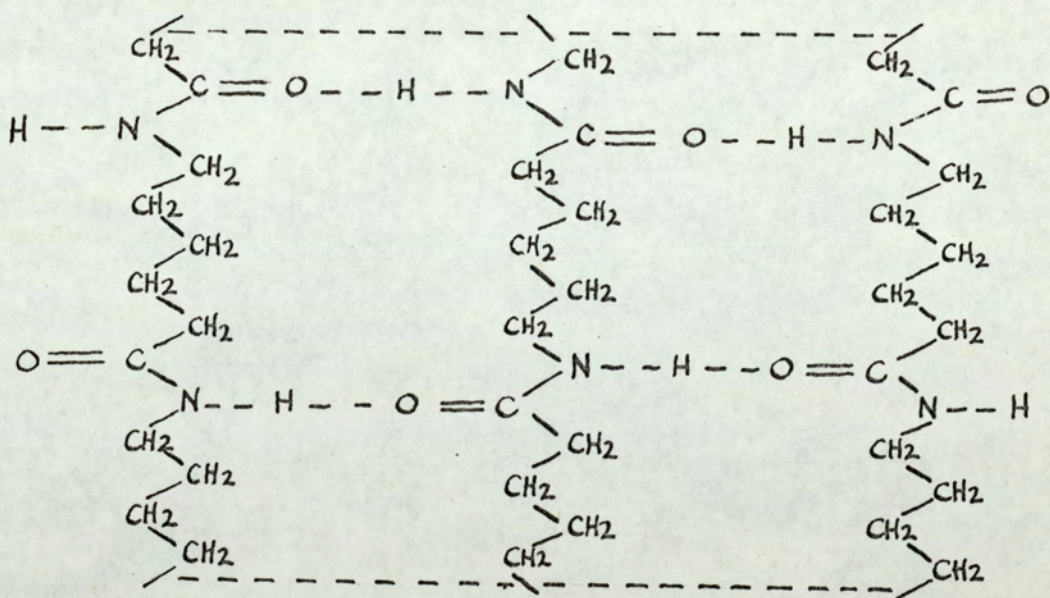
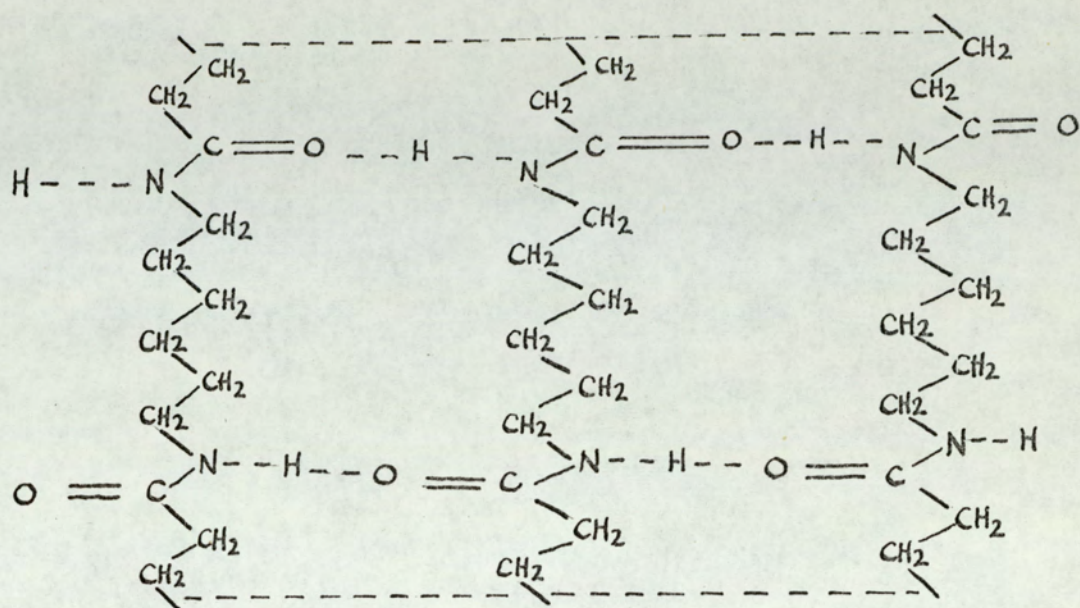


Fig.1. Hydrogen bonding between chains in 66 nylon and 6 nylon. From Holmes, Bunn and Smith (15).

ment may be unsatisfied by the introduction of a structural irregularity. The irregularity may take the form of a main chain side substituent, e.g. an alkyl substituent which may have the effect of producing a totally amorphous polyamide (20), or by means of copolymerisation, a main chain defect may be introduced.

An example of copolymerisation causing a reduction in the percentage crystallinity is the copolymer series formed by 66 nylon and 6 nylon. The melting points of these copolymers have been measured by Catlin, Czerwin and Wiley (21), and separately by Sonnerskog (22). Disagreement in the results is probably accounted for by technique variations; Catlin et al. used a Bloc Maquette and Sonnerskog used a heated capillary tube to observe the temperature of the formation of a melt. A summary of their results is given in table 1.

Table 1. Melting points of copolymers of 66 nylon with 6 nylon.

Weight% 6nylon	0	10	20	30	40	50	60	70	80	90	100
Mole fraction 6 nylon	0.0	0.1	0.2	0.3	0.4	0.5	0.6	0.7	0.8	0.9	1.0
Melting pt, °C, Catlin, ref. 21.	250		215		175	159	154	156	160	175	205
Melting pt, °C, Sonnerskog, (22).	264	234	205	197	188	175	159	176	190	204	214

It can be seen that the melting point-composition curve for copolymers of 66 nylon with 6 nylon passes through a minimum value at 60%(6 nylon)/40%(66 nylon).

Baker and Fuller (23) described the copolymerisation of 66 nylon with 6.10 nylon, and 6.10 nylon with 10.10 nylon (polydecamethylene sebacamide). These authors found reductions in the melting points, hardness and elastic modulus as the comonomer was introduced, and attributed this to crystallinity imperfections. Their observations were supported by a reduction in the intensities of the X ray diffraction patterns

from the copolyamides. Catlin, Czerwin and Wiley found similar results for the copolymers of 66 nylon with 6.10 nylon (21). The 30 : 70, 66 : 6.10 copolymer was judged to be the least crystalline composition, with a melting point of 192°C, compared with 214°C for 6.10 homopolymer. These authors have also examined the terpolymers composed of 66, 6.10 and 6 nylons. The lowest softening terpolymer had the composition ratio 66/6.10/6 nylons as 10/45/45, and melted at 145°C.

A reduction in the percentage crystallinity of a polymer may be obtained by crosslinking. With 66 nylon, crosslinks may be produced by high energy irradiation (24), and density measurements on irradiated nylon have shown a loss in crystallinity. Deeley, Woodward and Sauer, (25) have measured both the crystallinity and the crosslink content of irradiated nylon. Their results are summarised in table 2.

Table 2. The properties of crosslinked 66 nylon. Data of Deeley, Woodward and Sauer.(ref.25).

Molecular wt, Mn.	17,000			
Radiation dose, neutrons, nvt x 10 ⁻¹⁸	0	0.3	2.8	5.5
Density, g/ml	1.150	1.150	1.143	1.152
% crystallinity	57	47	10	-
% crosslinked	0	4.0	9.5	10.0

Molecular wt, Mn	15,600			
Radiation dose, neutrons, nvt x 10 ⁻¹⁸	0	0.04	0.14	γ dose
Density, g/ml	1.144	1.147	1.150	1.150
% crystallinity	53	47	--	--
% crosslinked	0	--	2.8	3.1

The surprising retention of density accompanying loss of crystallinity was probably due to the polymer remaining in the same crystal lattices

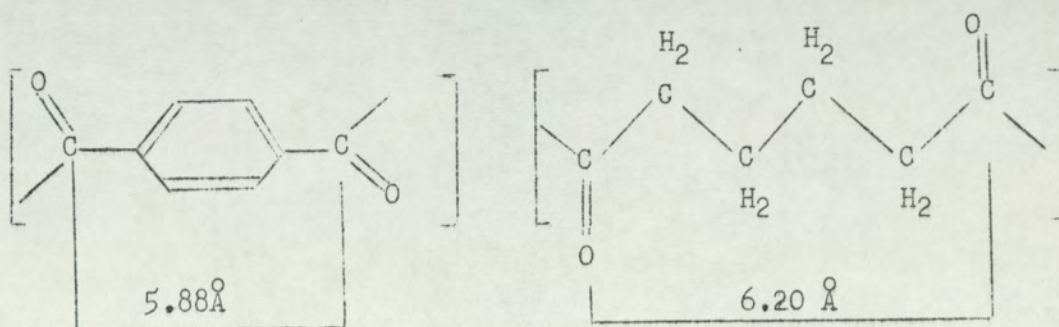
after irradiation. It is likely that recrystallized samples would have shown lower densities. The graphical data of these authors showed that after irradiation there was a small reduction in the melting point value, but the melting onset commenced much earlier, (30°C earlier for a 4% crosslinked sample.).

The use of chemical agents which produce crosslinks in condensation polymers has received theoretical attention. Flory (26) has predicted the gel point of the polyester formed by condensation polymerisation of adipic acid with diethylene glycol, when a 10% level of tricarballic acid is present. The polymerisation of 66 nylon may be similarly modified by addition of tricarballic acid.

Isomorphous crystallization.

A particular example of main chain substitution by copolymerisation is the replacement of one group in the chain with another different group which has an approximately equal length. In these circumstances, the normal crystal may still form, and may incorporate some of the foreign units, to form an isomorphous crystal. A number of polymeric examples have been found, and these have been reviewed by Allegra and Bassi (27). Particularly interesting are the copolymers of 4 methyl pentene-1 with linear α olefins, (n. hexene-1, n. butene, n. octene and n. decene), where the unit cell dimensions allow for co-crystallization. Polyethylene and polypropylene show less tendencies for co-crystallization. Examples of isomorphous copolyesters have also been reviewed by Allegra and Bassi (27). A surprising case of isomorphism was reported by Howard and Knutton (28). Copolymers of 66 polyester with 10.10 polyester showed heats of fusion which were representative of co-crystallization, but their melting points showed minimum values which indicated the presence of an increased level of amorphous polymer. This anomalous behaviour does not appear to have been resolved.

Edgar and Hill (29) and Plimmer, Reynolds et al (30) discovered that 66 nylon formed an isomorphous copolymer with 6T nylon (polyhexamethylene terephthalamide). An explanation of this is to be seen by a consideration of the carbonyl group separations in the adipic and terephthalic linkages :



These separation distances were calculated from published bond distances and angles (31). The values are in agreement with the calculations of Allegra and Bassi (27), but disagree with Edgar and Hill (29) who calculated 5.49 Å for the carbonyl separation in the adipic linkage. The isomorphous state was observed by the retention of melting point and increase in density as the aromatic groups were incorporated. Edgar and Hill used a penetrometer method for the melting points shown in table 3 :

Table 3. Copolymers of 66 nylon with 6T nylon, physical properties. Data of Edgar and Hill (29).

Mole fraction 6T nylon.	0	.094	.128	.283	.383	.482
melting pt, °C.	264	267	272	278	285	296
density, g/ml	1.141	1.149	1.155	1.157	1.166	1.172

The 66 nylon crystallite has been able to accommodate some 6T nylon, although there is a group separation difference of 0.41 Å. However, by contrast, replacement of 6.10 nylon with 6T nylon was not found to show isomorphism, as the crystal cannot accommodate the larger

group separation distance of 4.0 \AA . The melting point /composition graph shows a minimum at 20% 6T/ 80% 6.10.

A similar isomorphous system which is discussed by Yu and Ewans (32) exists with the 10.6/10.T nylon copolymers.

An extensive study of other isomorphous copolyamides was made by Cramer and Beaman (33). They considered copolymers originating from the following monomers :- heptamethylene diamine (7-), bis (3 amino - propyl) ether (303-), adipic acid (-6) and terephthalic acid (-T) Good isomorphous replacements were observable for copolymers of 303.6 nylon with 7.6 nylon ,and for 303.T nylon with 7.T nylon. However, although 7.6 nylon was found to be fairly highly isomorphous with 7.T nylon, copolymers of 303.T nylon with 303.6 nylon showed only slight isomorphous tendencies. With these semi-isomorphous copolymers, there were deviations from linearity on the composition/property graphs, with low melting points and high solubilities characteristic of reduced crystallinity. A further example of partial isomorphous behaviour was shown by Yu and Ewans (32) for 12.6/12.T copolyamides. The melting point /composition graph showed inflexion points at 30% and 70% molar compositions, although the melting point always increased as the 12.T content was increased. The meta xylylendiamine adipamide and terephthalamide (MXD.6 and MXD.T) are not isomorphous. This has been attributed to the unsymmetrical meta substituted component, which cannot be placed at random in the chains without destroying crystallinity.(27).

Rates of crystallization of polymers.

In addition to the work on the structure of the crystalline state of polymers, a substantial effort has been made on the process of polymer molecules entering the crystalline state, and the literature has been reviewed by Sharples (34) and Mandelkern (35). With simple substances,

crystallization from the melt is well understood, and rates of crystallization are frequently limited only by the rate at which the latent heat of crystallization can be removed from the system. With polymers, crystallization is a lengthy process involving the formation of nuclei of a critical size, which results in the initiation of the spherulite growth process. Both experimental and theoretical interest has been invoked in this process.

Experimental methods.

Three methods are predominant in the experimental determination of crystallization rates of polymers. In reviewing these for the present work, consideration is given to (a) adaptability of the method for high melting point polyamides and (b) sensitivity, for use with copolymers of low crystallinity.

Dilatometry. The basic method of following the contraction in volume of a piece of polymer held in a mercury-in-glass dilatometer had been used in this laboratory (36,37,38) and had formed the method for measurement of crystallization rates in three short projects. Good temperature control is required, and for 66 nylon the crystallization temperatures correspond to the upper operating limit for the most stable silicone oils. Platt (39) attempted to study the melting and crystallization of 66 nylon, but found that re-equilibration of water vapour took place rapidly in molten polymer, and this precluded measurements of the polymer volume changes. The method is sensitive to small changes of volume, and is the basis of much established data. Crystallization rates of low melting polyamides have been measured dilatometrically by Kahle (8) and Inoue (40). A useful idea for an automatic measuring apparatus was described by Allen (41).

Microscopy. Observations of the growth of spherulites may be made using an optical polarising microscope with a hot stage attachment.

For many polymers, including polyamides, the growth of spherulites may be observed over a wide range of temperatures, but measurement of the spherulites' sizes may be difficult owing to fast growth rates. Burnett and McDevit (9), Magill (7) and McLaren (42) have overcome this measurement problem by means of a cine-camera attachment to the microscope eyepiece. A photometric method was invented by Magill (43) to provide a more straightforward method for measuring fast crystallization rates. The original photocell was a hot cathode type, with the depolarised light intensity signal displayed on an oscilloscope. A similar apparatus providing a coupled melting stage attachment adjacent to the hot stage was recently described by Binsbergen and deLange (44). The method may be simplified by using a low voltage photocell and a pen recorder, with adequately fast response for the slower rates of crystallization. This simplification has been used by Teitelbaum and Palikhov (45) and Barrall et al (46). These papers (44-46) were received after the instruments described in Chapter 2 had been constructed. Good temperature control for the hot stage attachment is necessary, as discussed by Hay (47). A modern integrated circuit temperature controller which would be ideal for hot stages will shortly become available, and is described by Ireland (48). An interesting instrument described by Miller and Sommer (49), is a hot stage microscope incorporating a differential thermal analysis unit; in this instrument the thermocouples have been used both as temperature measuring elements, and also for heating the sample.

Magill (50) has given a theoretical justification for using the depolarised light intensity signals as a measure of the optical retardation of the polymer. The depolarised light intensity is also shown to be a measure of the birefringence of spherulitic films of uniform thickness. The intensity of light transmitted by a uniformly thick anisotropic film using crossed polars, I_c , is given by

$$I_c = a^2 \sin^2 2\alpha \sin^2 \left(\frac{\pi R}{\lambda} \right) \quad \text{----- 1.1.}$$

where a is the amplitude, α the angle between the polariser and the axis of the crystal, R is the optical retardation and λ the wavelength of light used. With parallel polars,

$$I_p = a^2 \left[1 - \sin^2 2\alpha \sin^2 \left(\frac{\pi R}{\lambda} \right) \right] \quad \text{-----1.2.}$$

Now the total beam is given by $I_o = I_c + I_p$,

$$\text{whence, } \frac{I_c}{I_o} = \frac{\sin^2 2\alpha \sin^2 \left(\frac{\pi R}{\lambda} \right)}{\lambda} \quad \text{---1.3.}$$

For a two dimensional spherulite, the contribution of all orientations to the transmitted light intensity is given by $8 \int_0^{\frac{\pi}{4}} \sin^2 2\alpha \, d\alpha$

where $0 < \alpha < \frac{1}{4}\pi$, then $\frac{I_c}{I_o} = \sin^2 \left(\frac{\pi R}{\lambda} \right) \cdot 8 \int_0^{\frac{\pi}{4}} \sin^2 2\alpha \, d\alpha$

$$= \pi \sin^2 \left(\frac{\pi R}{\lambda} \right), \text{ or in general,}$$

$$\frac{I_c}{I_o} = k \sin^2 \left(\frac{\pi R}{\lambda} \right) \quad \text{----- 1.4}$$

This simply implies that R is proportional to $\sin^{-1} \left(\frac{I_c}{I_o} \right)^{\frac{1}{2}}$.

Binsbergen and deLange (44) also considered the depolarisation, d , in terms of the birefringence Δn . For a specimen of polymer having F small crystals of thickness ω

$$d = 4\pi^2 \frac{F\omega^2 (\Delta n)^2}{15\lambda^2} \quad \text{-----1.5}$$

This expression may then be considered in the normal crystallization treatment.

Differential thermal analysis.(D.T.A.). The technique involves the detection of a temperature differential between the thermocouple imbedded in or in contact with a sample, and another thermocouple similarly placed in a reference material. A DuPont 900 Thermal Analyzer was already in use in the laboratory, and has been used for the DTA.

studies. A similar technique, differential scanning calorimetry, has the alternative procedure of separately heating the sample and reference materials to the same temperature, and recording the differential of the heater voltages required for this. The DuPont D.S.C. cell does not use the latter technique, but is a standard sensitive D.T.A. apparatus.

Inoue (40) has used differential thermal analysis to study the crystallization of 6 nylon, but found that the technique was insufficiently sensitive. Inoue's results were confined to fast rates of crystallization under isothermal temperature or programmed cooling conditions. The D.S.C. technique has been used for much more lengthy crystallization rates by Booth and Hay (51).

Other techniques. The general requirement for following a polymer crystallization is to monitor a property which changes continuously as the process takes place.

Allen (52) has adapted a density balance method for studying 66 nylon, but this requires silicone oil in contact with the polymer.

Buchdahl et al (53) have used the crystallinity bands in the infra red absorption spectrum of polyethylene for following rates of crystallization. The method requires good temperature control of a sample inside a spectrometer.

Sazhin and Podosenova (54) have used the electrical conductivity of a polymer as the physical property which changes during crystallization. The technique appears to be confined to polymers which do not equilibrate water in the melt, and has been suggested by DuPont Instruments Division (55). The method has not been well received, and is not adequately documented in the literature.

Theoretical treatments of polymer crystallization kinetics .

The Avrami analysis.

The kinetics of phase change developed by Avrami (56) were applied to polymers by Morgan and co-workers in Britain (34). For a system at constant temperature, the basic Avrami equation for the primary crystallization process is

$$\Theta = e^{-Zt^n} \quad \text{----1.6}$$

where Z is the rate constant, n is the Avrami integer constant, and Θ is the fraction of polymer which has not crystallized at time t , but which will enter the crystalline state before the process is completed. For volumetric monitoring, the non-crystallized fraction is characterised by

$$\Theta = \frac{V_t - V_\infty}{V_0 - V_\infty}$$

where V_t is the volume fraction at time t , and V_0 and V_∞ are the initial and final volumes. For dilatometry, the usual expression is:

$$\Theta = \frac{h_t - h_\infty}{h_0 - h_\infty}$$

where h is the height of mercury in the dilatometer.

An understanding of the type of crystallization process occurring may be obtained by taking a graph of the natural logarithm of $(-\log \Theta)$ versus $\log t$, when the slope is the Avrami exponent, n . Table 4 gives the interpretation of the Avrami exponent for various types of nucleation and growth processes.

Table 4. Interpretation of Avrami exponents. (34).

exponent, n	interpretation
4	spherulitic growth from sporadic nuclei
3	spherulitic growth from instantaneous nuclei
3	disc like growth from sporadic nuclei
2	disc like growth from instantaneous nuclei
2	rod like growth from sporadic nuclei
1	rod like growth from instantaneous nuclei.

At the half completion point of the process, the time is referred to as the crystallization half time, $t_{\frac{1}{2}}$. Since at $t_{\frac{1}{2}}$,

$$\ln \theta = \ln \frac{1}{2} = -Z t_{\frac{1}{2}}^n$$

whence
$$t_{\frac{1}{2}} = (\ln 2 / Z)^{1/n} \text{ -----1.7}$$

The application of the Avrami equation to experimental data from polymer crystallizations has been widely practiced, but deviations resulting in a decreasing n value as crystallization becomes nearly complete are frequently noticed. Fractional Avrami n values have been reported, e.g. $n = 3.587 \pm 0.008$ for polydecamethylene terephthalate, (57). Microscopic observations on polyethylene oxide show that crystallization proceeds by spherulite growth processes, although the Avrami n value of 2 implies that non-spherulitic crystallization occurs. (58).

For the spherulite growth process, measurements of the growing radius, G , lead to the rate constant, Z by the equations:-

for instantaneous nucleation, $n=3$, $Z = \frac{4}{3} \pi G^3 N$ -----1.8

for sporadic nucleation, $Z = \frac{4}{3} \pi G^3 k_n$ -----1.9

where N is the number of nuclei per unit volume, and k_n is the rate of increase of nuclei per unit volume and time.

An allowance for secondary crystallization is included in a modified Avrami - type equation developed by Gordon and Hillier (59,60).

The process is considered in two parts:

i, the primary process, commencing at time 0, with a volume fraction of

$\frac{\psi}{\psi} \text{ (prim.t)}$ at time t occupied by spherulites; and the primary $\psi \text{ (prim, } \infty)$

Avrami equation which is :-

$$\frac{\psi \text{ (prim.t)}}{\psi \text{ (prim. } \infty)} = 1 - \theta = 1 - e^{-Z t^n} \text{ ----1.10}$$

ii, the secondary process, which may be considered as commencing at a

time, τ , which is between time 0 and time t . Secondary crystallization relies upon some primary crystalline material being formed, so it has a different time base of $(t - \tau)$, and the crystallinity contribution from the secondary process to the volume contraction leads to the secondary Avrami equation :-

$$\frac{(\text{sec}, t - \tau)}{(\text{sec}, \infty)} = 1 - e^{-Z_2 (t - \tau)^{n_2}} \quad \text{---1.11}$$

The dependence of crystallization rates on temperature.

The fundamental nucleation theories in liquid-solid transformations were developed by Turnbull and Fisher (61) using the concept of a free energy barrier which must be overcome for the formation of a stable nucleus. Burnett and McDevit (9) assumed that growth is limited by the formation of monolayers. The rate of nucleation of a spherulite, N , is then given by

$$N = N_0 e^{\left[\frac{-E_D}{kT} - \frac{\Delta F^*}{kT} \right]} \quad \text{----1.12}$$

where k is the Boltzmann constant and N_0 is another constant;

or for growth, the similar expression may be employed for the radial increase, G :

$$G = G_0 e^{\left[\frac{-E_D}{kT} - \frac{\Delta F^*}{kT} \right]} \quad \text{----1.13}$$

where ΔF^* is the energy barrier for the formation of nuclei, which is estimated by geometrical considerations, E_D is the energy of activation for viscous flow for the transport of a polymer segment across the liquid-spherulite interface, and T is the temperature.

For a disc shaped nucleus with thickness l and radius r , the free energy of formation is

$$\Delta F_{\text{disc}} = 2\pi r l \sigma_s - \pi r^2 l \Delta f_0 \quad \text{-----1.14}$$

where σ_s is the interfacial free energy/unit area, Δf_0 is the bulk free energy of fusion, per unit volume. Δf_0 can be equated

to $\left[\frac{\Delta T}{T_m} \right]^{\Delta h_u}$, where T_m is the thermodynamic melting point of the polymer and Δh_u is the heat of fusion, to give

$$G = G_0 e^{\left(\frac{-E_D}{kT} - \left[\frac{\pi l \sigma_s^2}{k \Delta h_u} \right] \frac{T_m}{T \Delta T} \right)} \quad \text{----- 1.15}$$

hence a graph of $\log G$ against $T_m / T(\Delta T)$ should be linear, with a slope proportional to $\sigma_s^2 / \Delta h_u$

A complete treatment of the temperature dependence of polymer crystallization was given by Mandelkern, Flory and Quinn (62). For several situations, theoretical developments were given for the spherulite growth rates, G , and rate constants, Z . It is necessary to invoke the interfacial free energies σ_s, σ_e for cylindrical and end surfaces, and the latent volume change of crystallization,

$$\rho^* = \text{amorphous density} / \text{crystalline density.}$$

(i) For a spherical nucleus promoting spherical growth,

$$Z_{\text{spher}}^{\text{spher}} = \left(\frac{\pi}{3\rho^*} \right) N_0 G_0^3 e^{\left[\frac{-4E_D}{kT} - \frac{16\pi \sigma_s^3}{3 \Delta h_u^2} \frac{T_m^2}{kT(\Delta T)^2} \right]} \quad \text{1.16}$$

(ii) For a disc nucleus promoting disc growth,

$$Z_{\text{disc}}^{\text{disc}} = \left(\frac{\pi}{3\rho^*} \right) l c N_0 G_0^2 e^{\left[\frac{-3E_D}{kT} - \frac{8\pi \sigma_s^2 \sigma_e}{(\Delta h_u)^2} \frac{T_m^2}{kT(\Delta T)^2} \right]} \quad \text{1.17}$$

(iii) For a disc nucleus promoting spherical growth,

$$Z_{\text{spher}}^{\text{disc}} = \left(\frac{\pi}{3\rho^*} \right) N_0 G_0^3 e^{\left[\frac{-4E_D}{kT} - \frac{8\pi \sigma_s^2 \sigma_e}{(\Delta H_u)^2} \frac{T_m^2}{kT(\Delta T)^2} \right]} \quad \text{1.18}$$

In these expressions N_0, G_0 are defined as in equations 1.12 and 1.13.

A simplification of 1.16 - 1.18 is the expression-

$$\ln Z = \ln Z_0 - f \left[\frac{T_m^2}{T (\Delta T)^2} \right] \quad \text{-----1.19}$$

where f is dependent upon the precise nature of the nucleation and growth processes. Also, the half crystallization time, $t_{\frac{1}{2}}$, may be considered, introducing equation 1.7 into 1.19,

$$\ln \frac{1}{t_{\frac{1}{2}}} = \frac{1}{n} (\ln Z_0 - \ln \ln 2) - f' \left[\frac{T_m^2}{T (\Delta T)^2} \right] \quad \text{-----1.20}$$

Hence a plot of $\ln l/t_{\frac{1}{2}}$ versus $T_m^2/T(\Delta T)^2$ should be linear with a slope f' . The mean interfacial free energy, $\bar{\sigma}$, is then obtainable from this slope term by $f' = \frac{8 \pi \bar{\sigma}^3}{\Delta h u}$.

Hoffman's equation for the 'driving force' of a crystallization with temperature change is (63),

$$\Delta F = \left[\frac{\Delta H_f \Delta T}{T_m} \right] \left[\frac{T}{T_m} \right] \quad \text{---1.21}$$

This involves the assumption that a monolayer nucleus initiates growth, and can be considered for non-spherulitic processes. The theory was developed for polytrifluoro chloro ethylene, which appeared to crystallize without spherulitic formation.

Mandelkern (35) took the data of Flory and McIntyre for polydecamethylene sebacate, which unquestionably represented a spherulitic growth process, and found straight lines on plotting $\log Z$ against $T_m/T(\Delta T)$. Mandelkern (66) therefore stated that no definite conclusions can be drawn from data of this type with regard to the type of nucleus involved in the crystallization process.

Observations on the rates of crystallization of polyamides.

Early studies on the kinetics of crystallization of polyamides were published by Morgan (64), Allen (52) and Hartley, Lord and Morgan (65), using the density balance method. In these papers, rates of crystallization of 66 nylon were measured at temperatures 15-20°C below the melting point. The crystallization curves have a sigmoidal shape, and were found to consist of three zones: (a) an induction period, during which the polymer equilibrated at the new temperature, but no crystallization was observed, (b) a main crystallization period, during which the main volume contraction due to crystallization occurred, and (c) a secondary period, which terminated in the

establishment of an equilibrium between amorphous and crystalline material. Allen (52) noticed that if a sample was cooled to room temperature and then reheated to the crystallization temperature, the equilibrium density attained was higher than the level before cooling. This indicated that either crystallization at the elevated temperatures was taking an extremely long time to reach equilibrium, or that some further crystallization could be introduced at the lower temperatures.

Burnett and McDevit (9) measured spherulite growth rates for 66 nylon and 6 nylon, using various melt temperatures. The same spherulite growth rates for 66 nylon were found after melting for 30 seconds at 330°C, 315°C, 300°C and 290°C, indicating that the residual crystallinity was destroyed by these melting processes. Spherulite growth rates of 66 nylon at temperatures below 160°C were found to be too fast for measurement, although a more comprehensive temperature range could be taken for 6 nylon.

Magill found that a considerable amount of importance should be attached to the melting conditions for polyamide crystallizations, and McLaren (42) examined this in detail. For 66 nylon with a molecular weight M_n of 8,700, the growth rate of spherulites was reduced from 8.7 μ /min. to 5.7 μ /min. by extending the melting time at 300°C from 5 to 30 minutes. Since the overall rate constant Z , varies as G^3 , applying equation 1.9, Z is decreased from 8.04×10^{-4} to $3.14 \times 10^{-4} \text{ min}^{-4}$, by this extension in the melting time.

The difficulty in the direct measurement of spherulite growth rates of 66 nylon was illustrated in McLaren's results of the numbers of spherulites present. For a slow rate of crystallization, at 252°C, the concentration of spherulites was found to be $3.1 \times 10^6 / \text{cm}^3$; more spherulites (up to $13 \times 10^6 / \text{cm}^3$) were seen for crystallizations at lower temperatures.

Magill (43) ,using depolarised light intensity in place of volumetric or growth measurements,obtained crystallization isotherms following the Avrami pattern by using

$$\theta = \frac{I_c - I_t}{I_c - I_o} = e^{-Zt^n} \text{ ----- } 1.22.$$

where I_c is the output of the photomultiplier at the completion of the crystallization process, I_o is the initial output and I_t the output at time, t . A plot of θ versus $\log t$ was used to minimise the differences arising out of sample thickness variations. The majoritory of the graphs may be brought into coincidence if a log time base is used,by simply shifting the time scale;and this property was shown by Mandelkern (64) to be a characteristic feature of the crystallization of pure homopolymers.In these circumstances,the temperature coefficient and Avrami integer are remaining constant for the range of crystallization conditions.

Linear Avrami isotherms were shown by Magill (43) for 66 nylon crystallized at 201 and 218°C. At 230°C,departure from linearity due to secondary crystallization was seen,but a value of $n = 3$ was attributed with some certainty. If the induction time of crystallization was omitted from the Avrami analysis ,Magill found straight lines with $n = 2$,in agreement with the earlier density balance work of Allen (52). The value of $n = 3$ is not applicable to all polyamides; Kahle (8) has found that 11 nylon crystallizes over a wide temperature range with agreement to the Avrami analysis,and $n = 4$.

Two other parameters affecting crystallization rates are polymer molecular weight and water content. These are not unrelated, as most polyamides re-equilibrate water of condensation polymerisation in the melt. In his study of 66 nylon crystallization kinetics,McLaren (42) found that the spherulite growth rate decreased from 5.7 μ /min to 4.1 μ /min for crystallization at 247.5°C, if the molecular weight

was increased from 10,000 to 14,600. The effect of equilibrium water was shown in the results at 248°C; the overall rate constant, Z , changed from 3.4×10^{-5} for dried polymer to 1.96×10^{-4} for undried polymer. The film thickness was found to be less important for spherulite growth measurements; for films of 60 - 150 μ in thickness, no variation in G or Z was noticed, for films of 30 μ in thickness, G had increased from 1.6 μ /min to 2.1 μ /min for crystallization at 250°C. Film thickness does become important when very thin films are used, and for a 10 μ thick film, G had increased to 8.7 μ /min for the 250°C isotherm. This thickness effect may be due to nucleation from the glass surfaces, or to the restriction upon three dimensional growth in very thin films. The optimum working thickness for polyamide films may be taken as 30 - 100 μ .

Consideration of the induction time parameter in the crystallization of 6 nylon was given by Magill (11). A transition in the graph of the logarithm of the induction time versus the crystallization supercooling temperature (as $\log \Delta T$) was noticed at 190°C. This was attributed to a changeover in the nucleation process. Above 190°C, sporadic nucleation was predominant, whilst below 190°C predetermined (instantaneous) nucleation was observed. For 66 nylon, McLaren noticed a similar transition occurring at 246°C.

The estimation of the thermodynamic melting points, T_m , of polyamides from crystallization kinetics data has been attempted by several authors. The measured melting point of 66 nylon is generally around 264°C, and the graphs of $T_m^2 / T (\Delta T)^2$ or $T_m / T \Delta T$ versus $\log G$ do not provide straight lines for this measured melting point. Burnett and McDevit (9) had to assume a T_m value of 280°C for 66 nylon before obtaining a linear graph; McLaren found 272.5°C to be sufficiently high, and representative of the thermodynamic melting point of a sample of 66 nylon having a molecular weight of $M_n = 14,000$.

No information on the secondary crystallization processes in polyamides has become available. For polypropylene, Hillier (60) concluded that the primary process contributed about 60% of the total crystallinity at the temperature of crystallization, and the secondary process had an Avrami integer value of 2. At higher temperatures, the primary process accounted for a higher fraction of the total crystallinity. As linear spherulite growth rates have been observed for 66 nylon (65) and 11 nylon (8), it may be suggested that Hillier's treatment could be applied to polyamides.

The rates of crystallization of copolymers.

In addition to the effects of diluents and foreign materials, polymer crystallization rates can be modified by structural irregularities, which may take the form of copolymerised units, branch points, crosslinks or end groups. The general effect is a reduction in the rate of overall crystallization, which approximately follows the reduction in melting point.

A great deal of attention has been devoted by physicists to the crystallization kinetics of linear high density polyethylene, on account of its simple chemical structure. Earlier work on low density polyethylene may be considered as studies involving a branched copolymer. Kovacs (67) had realised that branching impaired the development of crystallinity in polyethylene, and this was confirmed by comparison with unbranched polymethylene (68). Buchdahl, Miller and Newman (53) using low density polyethylene containing 3% of the polymer in branch units, found two important differences between branched and linear polyethylene. (i). The crystallization isotherms from branched polyethylene are not superposable by a shift along the logarithmic time axis. This is in contrast to the observations on linear polyethylene of Russell (69), Plate et al (70) and Mandelkern, Quinn and Flory (62), who had found superposable isotherms. (ii) The Avrami

exponent, n , for branched polyethylene has been found to be less than the value for linear polyethylene. The general behaviour observed is an initial n integer value of 4 characteristic of primary spherulitic growth, but this decreases consistently to approach a value of $n = 1$ as the process is completed.

Mandelkern and Quinn (66) have studied the rates of crystallization of polybutadiene prepared by free radical polymerisation. In the polymer, three types of linkages occur, trans 1.4, cis 1.4, and 1.2 vinyl groups, but the sample used contained 80% trans 1.4 linkages. It is this major component that is capable of crystallizing, and a supercooling temperature of 20-40°C from the melting temperature of 37°C was required to induce crystallization. At faster crystallization rates the individual isotherms were nearly superposable by rescaling the logarithmic time axis, but for the more lengthy crystallizations with $t_{\frac{1}{2}}$ of 4 hours and longer, a more perfect crystalline state appeared to be developing, with the consequent increased rejection of the non-crystallizing comonomer linkages. It was suggested that, in an ideal situation, only the trans 1.4 linkages of polybutadiene would enter the crystalline state; but at faster rates some additional linkages are incorporated.

The theoretical treatment of copolymer crystallization kinetics was developed by Gornick and Mandelkern (71). In a copolymer of A and B units, with only A units capable of entering the crystal lattice, the equation for the nucleation rate of a homopolymer (equation 1.12) has to be modified to

$$N = N_0 X_A e^{\left(\frac{-ED}{kT} - \frac{\Delta F}{kT} \right)} \quad \text{----1.23}$$

where X_A is the mole fraction of A units in the molten phase.

As crystallization proceeds, A units are gradually taken into the crystal, with the melt becoming progressively more rich in B units,

and X_A is reduced. At a conversion, θ , there has been a reduction in the concentration of A units from an initial value X_A^0 to a value X_A^θ , and the attenuation of the nucleation rate is shown as

$$\frac{N_\theta}{N_0} = \frac{X_A^\theta}{X_A^0} e^{-\left[\frac{C\Delta H_u}{kT} \right] \left[\left(\frac{T_m}{T_m - T} \right)^2 - \left(\frac{T_\theta}{T_\theta - T} \right)^2 \right]}$$

-----1.24

where C is a constant dependent upon the geometry of the nucleus. For a cylindrical nucleus, C is given by $8\pi \left(\frac{\sigma_u}{\Delta H_u} \right) \left(\frac{\sigma_e}{\Delta H_u} \right)$.

Mandelkern and Gornick have made predictions of the reduction in the nucleation rate for polyethylene containing small amounts of co-ingredient. Insertion of the nucleation expression into an Avrami like equation leads to an expression which cannot be solved directly, but the predicted isotherms have the observed type of expansion along the logarithmic time axis which prevents their superposition. As with the butadiene copolymers, these graphs also show a tendency for approximate superposition at the lower levels of crystallinity, which result from fast crystallization rates. Mandelkern (35) pointed out that the changing concentration of the crystallizable component in the copolymer melt prevents measurements of the accuracy required to enable the experimental isotherms to be compared with the theoretical predictions.

Prior to the commencement of the present work, Hybart and Pepper (38), Harvey (36) and Holmes (37) investigated the effect of copolymerised 6 nylon on the crystallization rates of 11 nylon. Pepper found remarkably good adherence to an Avrami value of 4, for copolymers containing up to 20% 6 nylon, in agreement with Kahle's value for 11 nylon homopolymer (8); and for any given crystallization half time, it was necessary to increase the supercooling temperature as the comonomer content was increased. This was contrary to the previous findings (36) which had indicated the reverse tendency of

reduced supercooling temperatures for the copolymers. Two criticisms which may be placed against these projects are (i) differential thermal analysis peaks were used in the determination of the supercooling temperatures, with low temperature accuracy resulting, and (ii) no molecular weight characterisation of the polymers was carried out. Pepper's preparative method using a mixture of the appropriate monomers was preferable to the previous projects, as more random copolymers probably resulted. Harvey and Holmes had used the amide interchange reactions between the commercial 11 nylon and 6 nylon polymers to bring about random copolymerisation.

Fusion of copolymers.

Flory's equation (72) for the relationship between the melting points of homopolymers and their derivative copolymers has received a great deal of attention, and the observations were reviewed by Mandelkern (35). The derivation of the equation involves a statistical analysis of the probability of a given chain unit being located either in an amorphous state or in a crystalline state containing a sequence of the same units. There is a critical size required for crystallites to exist in equilibrium. The probability, p , of an A group in the copolymer being succeeded by another A group leads to the solution:-

$$\frac{1}{T_m} - \frac{1}{T_m^0} = \frac{-R}{\Delta H_u} \ln p \quad \text{-----1.25}$$

where T_m and T_m^0 are the melting points of the copolymer and homopolymer respectively, and ΔH_u is the heat of fusion of the crystalline region. For a completely random copolymer p is equivalent to the mole fraction of A units present, X_A , hence,

$$\frac{1}{T_m} - \frac{1}{T_m^0} = \frac{-R}{\Delta H_u} \ln X_A \quad \text{-----1.26}$$

For an ordered copolymer, where both A and B may enter the crystalline

state, or a block copolymer, p exceeds X_A . For alternating copolymers where two B units are not encountered in adjacent linkages, p is less than X_A .

Experimental graphs of $\frac{1}{T_m}$ versus $-\ln X_A$ were given by Mandelkern (35). The copolyamide system considered was 66/6 nylon, taking the results of Sonnerskog (22). The equation in practice has frequently led to low values of the heat of fusion, but the values obtained are very sensitive to the method used to detect the disappearance of the last traces of crystallinity during the melting process.

Small increases in the measured melting points have also been observed when more carefully crystallized polymer samples have been heated. Baker and Mandelkern (73) have taken the measured melting points, T_m^\ddagger , of a number of copolymers which had been prepared with different crystallization rates. Copolymers of polymethylene containing up to $6\frac{1}{2}$ mole % of randomly distributed methyl or n-propyl side groups had been synthesized from mixtures of diazomethane with the appropriate diazo-alkane. The apparent melting points, T_m^\ddagger , obtained dilatometrically, using a $2^\circ/\text{min.}$ heating rate, and the previous crystallization temperature T_c , were extrapolated to the point $T_m^\ddagger = T_c$. This was taken to be the equilibrium melting temperature, T_m . On inserting these T_m values into Flory's equation (1.26), comparatively poor agreement was obtained for the methyl substituted polymers, but more satisfactory agreement was seen for the n-propyl copolymers. Baker and Mandelkern concluded that the crystal phase at equilibrium remained pure for the propyl copolymers, but solid solution occurred for the methyl copolymers.

The selection of polymers and apparatus for the problem.

The review of scientific literature resulted in comparatively little information concerning the crystallization kinetics of copolymers, and this is clearly a subject in which more information is needed. Surprisingly, the only paper of direct relevance to the crystallization kinetics of copolyamides had originated from this laboratory (38). The melting point information on copolyamides in the literature shows some disagreements, and gives no indication of the extent of crystallinity which may be developed in the systems. The criterion for isomorphous crystallization may also require closer definition.

The polymers selected for this study were 66 nylon and modifications of 66 nylon formed by copolymerisation with other polyamide monomers. Of the latter, the monomer for 6 nylon was selected for the first copolymer series, with reference to the results of Catlin et al (21) and Sonnerskog (22). As an isomorphous crystallization series, 66/6T copolymerisation was selected, on account of the data of Edgar and Hill (29) and the implications of Cramer and Beaman (33). A third system selected was 66 nylon containing branched chains and crosslinks. Although ionizing radiation has generally been used to provide this, it was considered to be preferable to accomplish branching by chemical copolymerisation using a trifunctional acid monomer. Following a suggestion by A.C. Davis of I.C.I. Fibres Ltd, trimesic acid (benzene 1,3,5 tricarboxylic acid) was chosen as this monomer, in preference to tricarballylic acid, although no papers concerning the use of trimesic acid in polyamide polymerisation were located from the literature search.

On the selection of apparatus for rates of crystallization

measurements, a preference for hot stage microscopy was indicated, on account of the potential high sensitivity of the method, and the allowance for operation above the ceiling temperature of silicone oils. The photometric invention of Magill was particularly favoured, as it provides a fully automatic method, which is useful for lengthy crystallizations. Methods which are sensitive to water re-equilibration (dilatometry, density balance method) were rejected. Consideration to isothermal differential thermal analysis was also given, but this method was unfortunately found to be practically unusable for the high melting polyamides.

The DuPont 900 Thermal Analyzer was available in the laboratory, and this has been used for heats of fusion determinations. The new D.S.C. Cell has made the instrument much more suitable for quantitative thermal analysis measurements.

Standard methods were selected for polymer preparations, and characterisation of materials by viscometry and density determinations.

CHAPTER 2. APPARATUS DETAILS .

The design of a hot stage microscope.

A search through technical literature of microscope manufacturers did not reveal a commercially available hot stage microscope that would be suitable for precision measurements of polymer crystallization rates. Accordingly, it was decided to construct a suitable apparatus, which would involve the conversion of an ordinary polarising microscope.

Immediately prior to commencing the present work, the author discussed this problem with the Physical Chemistry Research section of I.C.I., Ltd. (Plastics Division), who kindly supplied a blueprint of their hot stage microscope apparatus, and also consented to allow the construction of an apparatus based on their design. The diagrams, figs. 2 and 3 show the general construction. The original designs were by J.H. Magill and R.P. Palmer. The features built into the design of the I.C.I. hot stage attachment are described below.

(1) A disc shaped microscope stage of steel, fitted with a symmetrically wound heater, suitable for operation on 50 - 110 volts a.c. or d.c. The stage is mounted in compressed asbestos ('Sindanyo'), which also serves as an electrical and heat insulator, and may be heated to 300°C.

(2) A closely coupled hot plate of similar dimensions to the hot stage with a control piston to allow for rapid transfer of samples from a melting temperature zone to a crystallization temperature zone.

(3) Suitable provision of drilled holes for thermocouples and for a platinum resistance thermometer, and an inlet for nitrogen gas to provide an inert atmosphere for the sample.

The I.C.I. design was modified to allow for operation at

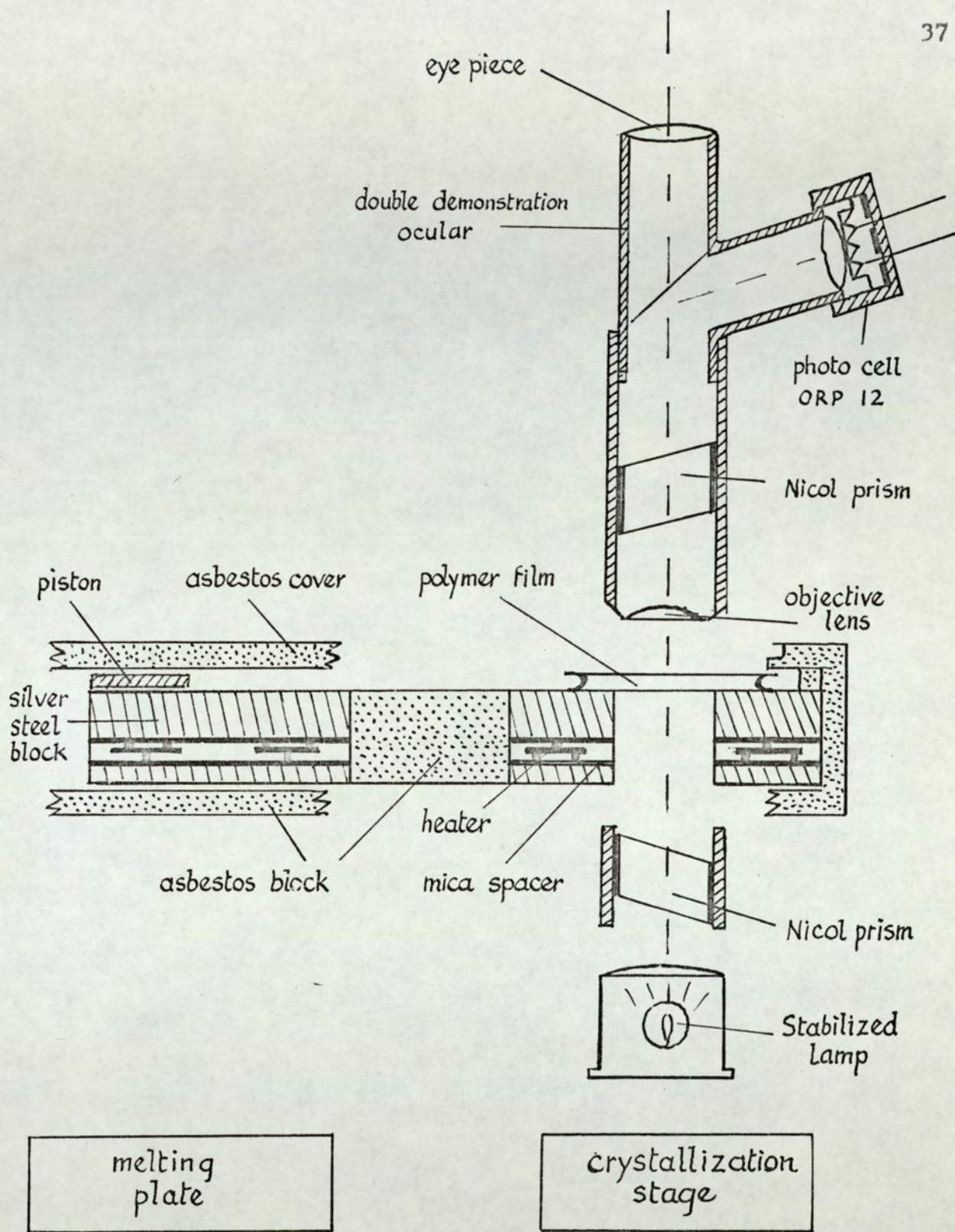


Fig. 2 Modified Swift Microscope (vertical cross-section)

temperatures up to 450°C by increasing the size of the asbestos block, and by fitting larger heaters. The microscope stage and hot plate were turned from silver steel, as stainless steel was not obtainable.

Details of the construction not shown in figs.2 and 3 are described below.

Stage heater:- 24 turns of Eureka heater tape, .025" x .004" x 40", 26 ohms, wound on 2" dia. .01" mica with a .65" dia. central hole.

Hot plate heater:- two heaters, placed one above the other, each 18 turns of the same wire, 17 ohms, wired in parallel on similar formers. The materials were bought from Far Ohm Manufacturing Co., Birmingham, and Midland Micanite Co., Aston.

Insulating spacers:- Circles of .01" mica were interspaced between the heaters and the metal blocks.

Microscope:- A Swift model P polarising microscope was made available for this work by the Geology section of the Chemistry Department.

Although not intended for operation at elevated temperatures, the instrument proved satisfactory after hot stage conversion had been carried out. The normal stage was discarded, and the special stage was fitted, as shown in fig.2. The objective lens used throughout the work was the 1" focal length Swift W319, as supplied with the microscope. The normal eyepiece was removed and a Beck Double Demonstration Ocular, 3778, was fitted. Since the Beck eyepiece has an R.M.S. recommended tube fitting, it was necessary to fit a reduction sleeve into the barrel of the microscope. One arm of the double ocular was left available for optical observations and photography, the other eyepiece was equipped with a photo cell, which was attached by means of a phenolic bottle cap. A Swift pre-focus illuminator was attached to the microscope. The lamp, 6v. 15 watt was supplied from a stabilised mains transformer using the circuit shown in fig.6. A resistor was fitted for dim and bright light intensity operation. The samples were mounted on or between 16 or 19mm. circular

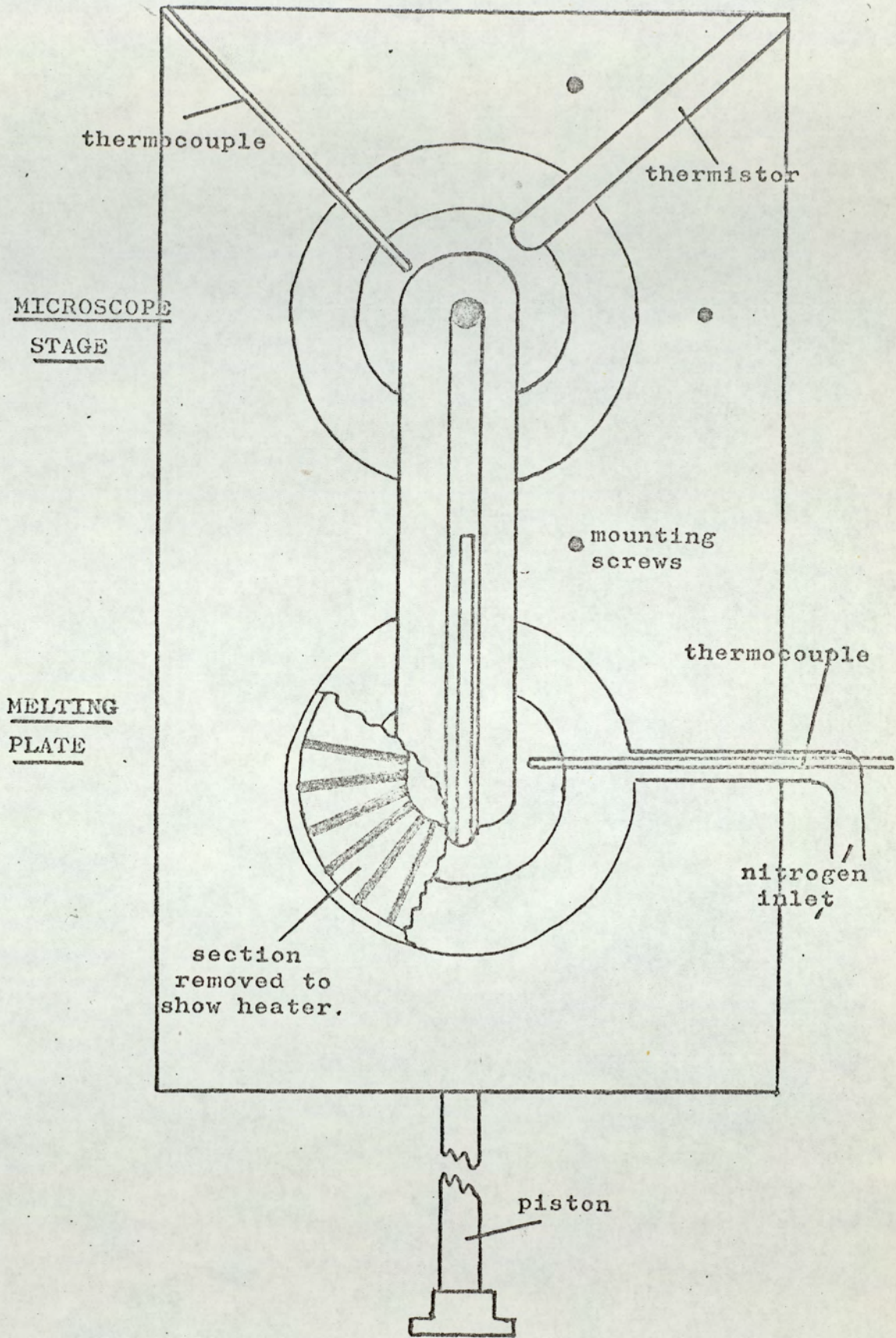


Fig.3 Hot stage for microscope, viewed from above with top cap removed. (Actual size).

glass cover slips ('Chance' grade no.2).

Photocell circuits.

Two photocells were evaluated in connection with this work.

(i) A small selenium /selenium oxide photo-emissive cell (Proops-Soviet import) was suitable for direct connection to a 10 mV recorder , but it gave a fluctuating response. The dimensions of the cell made it difficult to attach the cell to the eyepiece without admitting stray light. (ii) A Mullard ORP 12 cadmium sulphide photoresistor overcame these difficulties, and was consequently preferred. The cell has a photosensitive coil which is behind a glass window. The glass provides some mechanical protection, and serves as a heat shield. The window made an exact contact with the microscope eyepiece, and the cell was then not affected by room lighting variations. The photocell was connected to a supply battery, and used in conjunction with a Bristol's 'Dynamaster' recorder, type R5110, by means of the circuit diagram shown overleaf (fig.4a). This recorder has a 10mV full scale sensitivity, and with the attenuating resistors shown, the apparatus requires the microscope to be set with crossed Nicol prisms. Additionally, a similar circuit (fig.4b) was devised for use with the variable sensitivity recorder system of a DuPont 900 instrument.

The temperature control circuits.

Hot plate control. The hot plate adjacent to the microscope stage was supplied by a mains variable voltage transformer (7 amp. Regavolt) , and gave a temperature control of $\pm 3^{\circ}\text{C}$, as measured using a chromel-alumel thermocouple connected to a Wild-Barfield millivoltmeter .

Hot stage control. Close temperature control to $\pm 0.2^{\circ}\text{C}$ was specified for the hot stage. A design for a 5 watt temperature controller, suitable for a very small cell, was made available by I.C.I. Ltd, (Dyestuffs Division), and this was constructed in the Chemistry Department.

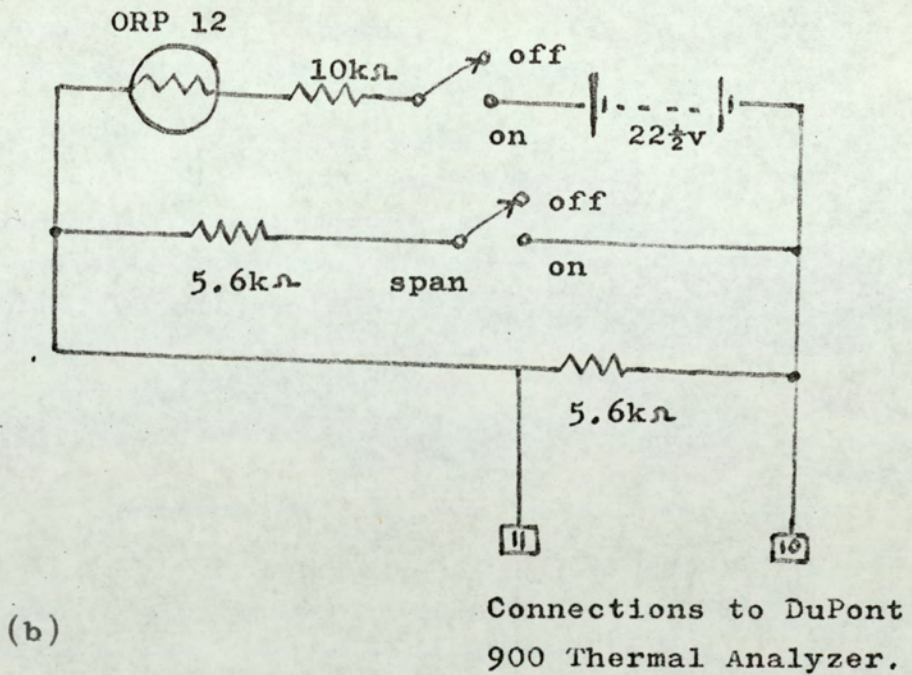
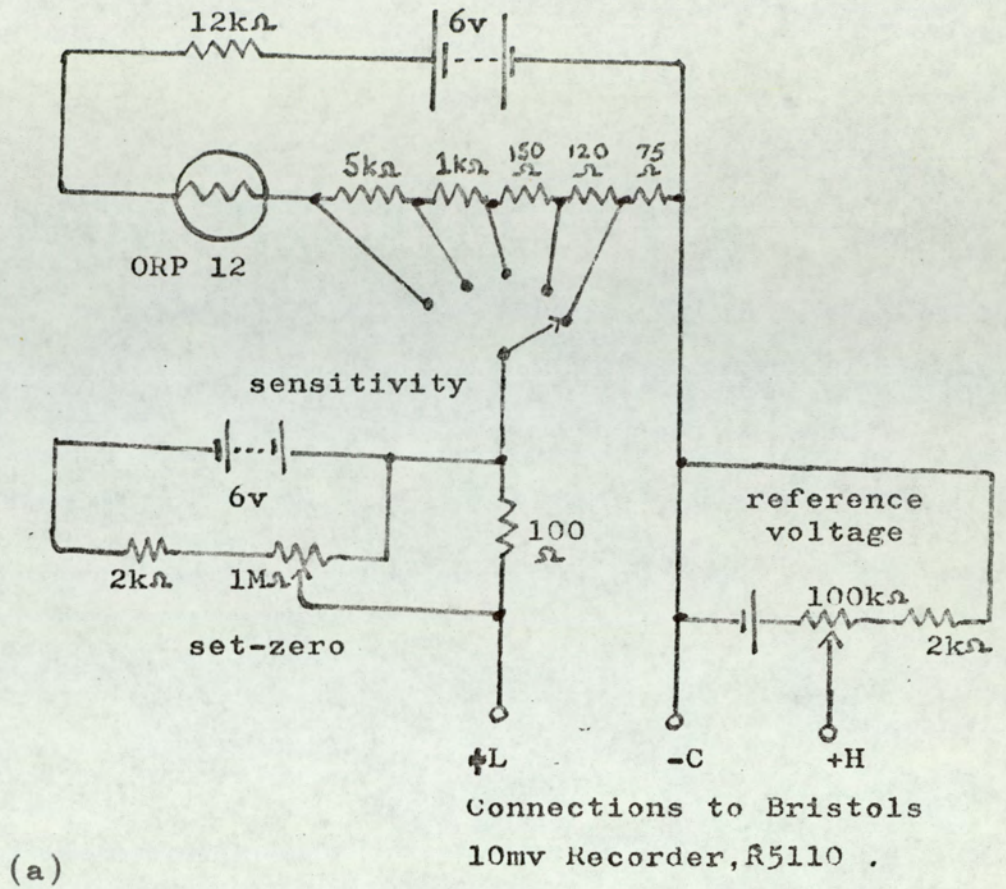


Fig. 4 .The photocell control circuits.

(a)For 'Dynamaster' recorder, (b)For DuPont 900.

The temperature controller required modifications to make it suitable for the hot stage attachment. The Wheatstone's bridge network was formulated to accept a C.N.S. Instruments Ltd. 100 ohm platinum resistance thermistor, and to provide a wider temperature range of 0 -450°C, by means of a range switch. Larger output valves (KT66 in place of EL34) were fitted, to provide 10 watts output into a 200 ohm load. Attempts were then made to convert this controller to 500 watts operation by means of thermal and mechanical relays, but inadequate control resulted. The problem was overcome by means of a thyristor circuit, using the low power from the output valves to operate the thyristor gate. The final circuit is shown in fig.5.

The principle of operation of the temperature controller is described below.

1. A small a.c. from a transformer is fed into a bridge containing the thermistor and the preset balance helipot resistor.
2. The out-of-balance signal is amplified using two pentode valves, and the signal is adjusted with a gain control.
3. This signal is applied to the grids of two large output tetrodes in "push-pull" operation, which are biased by means of dry batteries. The anodes are connected to a mains transformer providing a high secondary potential; this causes a potential to be developed at the cathodes, depending upon the grid voltage.
4. A "cathode follower" circuit is used to deliver current to the thyristor gate terminal. When this voltage exceeds the firing potential (1.5 volts at 60mA), the junction closes, and line mains voltage is applied to the microscope stage heater for the remainder of that mains half cycle.
5. To reduce the load on the thyristor, a diode conducting the inverse half cycles was provided, together with an isolating switch. At higher temperatures (above 200°C) full cycle voltage operation produced

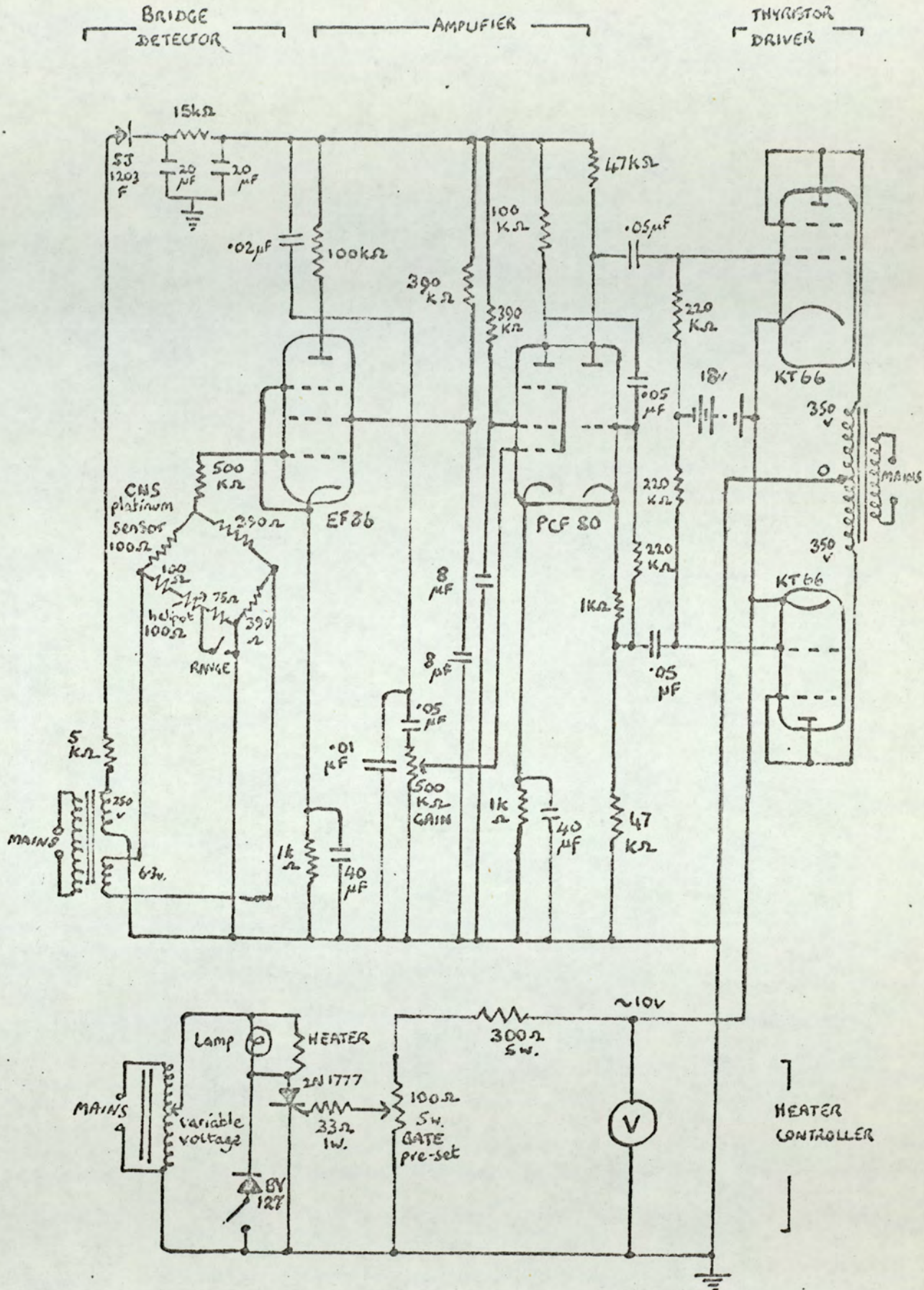


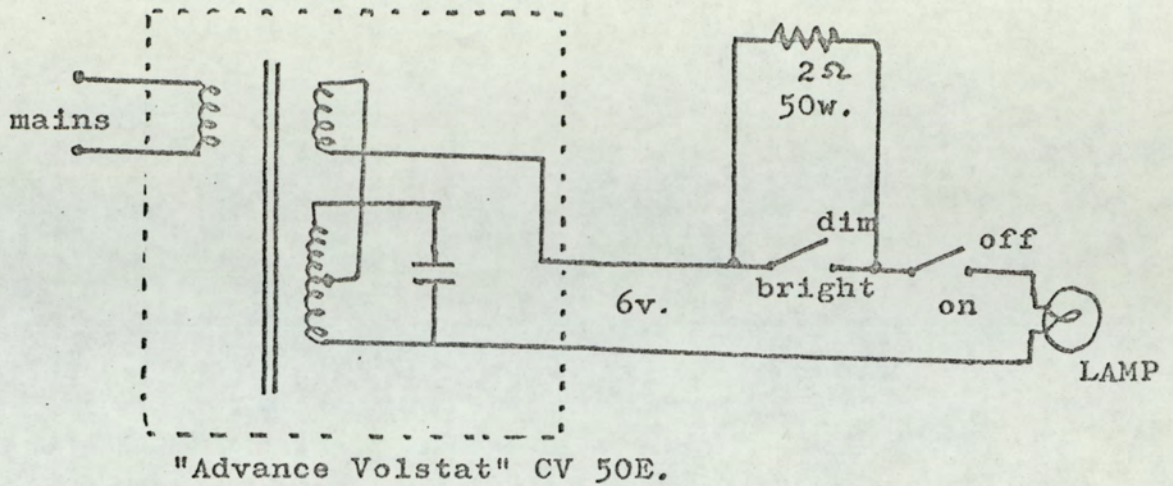
Fig.5 Hot stage microscope temperature controller.

closer temperature control than was attainable by half cycle operation.

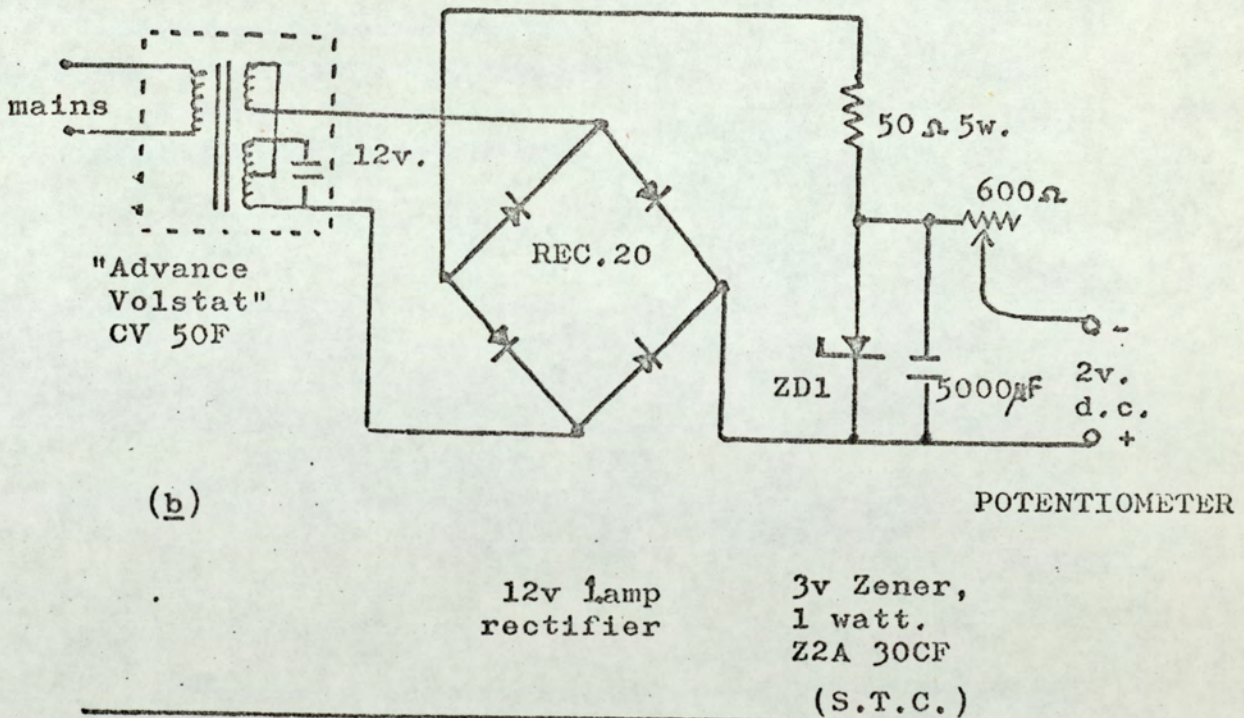
Temperature measurement.

Thermocouples. Analytical quality chromel-alumel thermocouples (DuPont Instruments Ltd., part 900329) were used for the microscope stage and hot plate. The junctions were located in cavities in the metal blocks, and placed as near as possible to the sample. The DuPont thermocouples have ceramic insulators which protect the wires away from the junction, but as an additional precaution against short-circuiting the leads, the microscope stage block was not connected to earth. Compensating cold junctions at 0°C were provided by immersing larger thermocouples (DuPont part 900311) in a mixture of crushed ice and water in a vacuum flask. The thermocouples were connected by soldering the wire ends to a piece of phenolic-laminate printed circuit board located away from the heated parts, in order to eliminate connection voltages. The chromel wires were joined, and copper leads were used to connect the alumel wires to a measuring potentiometer. The conversion of thermocouple voltage to temperature was taken to be as published for chromel-alumel standard thermocouples (74). An occasional check on the condition of the stage thermocouple was made, by comparing the temperature of an oil bath as measured by the thermocouple method, with the reading from a high quality mercury in glass thermometer at the prescribed immersion (Gallenkamp).

Thermocouple potentiometer. A Pye model 7569 P Thermocouple Potentiometer was used for all measurements. The instrument was provided with a 2 volt steady d.c. supply. Initially, two Leclanche cells and a resistor were used; subsequently a mains unit, fig. 6, was built, and this resulted in an improvement to the measuring accuracy of the instrument. Before each temperature measurement, the instrument was standardised against a Weston standard cell, which provides a reference voltage of



(a)



(b)

Fig. 6. The stabilized power circuits: (a) lamp supply, (b) thermocouple - potentiometer supply.

1.0184 volts at 20°C. The reference was itself checked using a certified Weston cell (Parametron) at daily intervals. The thermocouple leads were then connected to the potentiometer, and the voltage was found by potentiometric balance.

The operating procedure for the hot stage microscope.

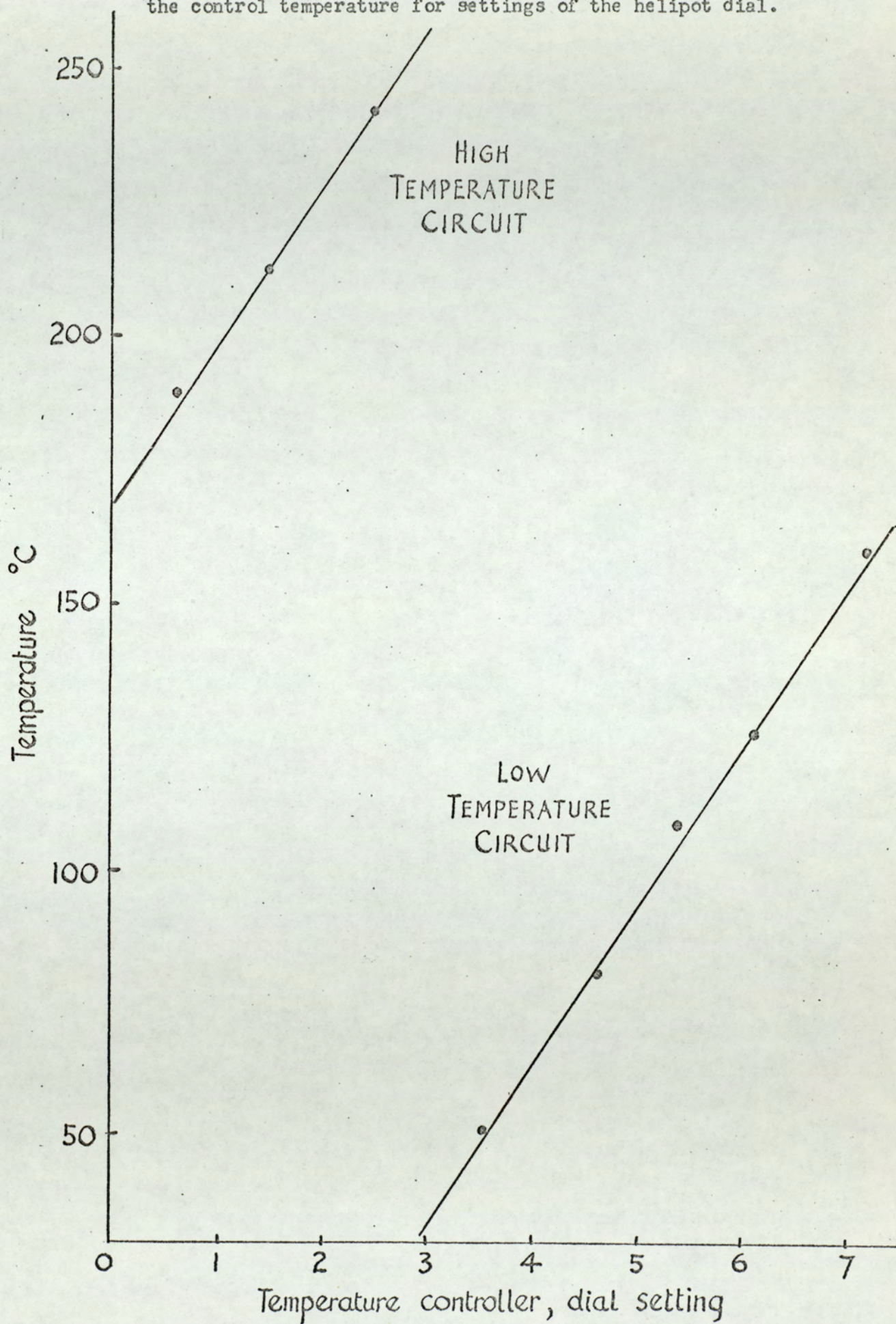
(1). Isothermal temperature control. The hot plate and hot stage are set to equilibrate at the required temperatures. Fig.7 shows the setting for the dial of the temperature controller helipot to produce an isothermal temperature on the microscope hot stage. In addition, the variable voltage transformers are set to pre-determined positions. The hot plate is normally set to a temperature above the melting point of the polymer under study, and the microscope stage is set to a temperature below this melting point.

(2). Optical adjustments. The microscope is set in approximately the correct position for focus, with the Nicol prisms in the crossed planes position. The lamp intensity and photocell monitoring circuits are set to the required sensitivity, and the pen recorder is set to a deflection representing about 5% of the full scale reading.

(3). Polymer melting. A polymer sample is placed between two 16 mm. glass cover circles on the hot plate, and the melt is gently pressed to form a coherent film. Usually, a 2-4 mg. piece of polymer is sufficient. Oxidation in the melt is reduced by increasing the nitrogen flow around the sample, and by pressing the melt into a film between the cover slips without delay.

(4). Polymer crystallization. At the conclusion of the melting time period, the sample is transferred to the microscope stage by means of the piston control rod (fig.3). The focus control is readjusted to bring the film into view. The transfer time is noted, and the development of birefringence in the polymer sample is recorded as a function of time on the pen recorder.

Fig. 7 Temperature controller for the hot stage microscope. Graph of the control temperature for settings of the helipot dial.



The DuPont 900 Thermal Analyzer.

This instrument is basically a temperature controller, a d.c. amplifier, and an X-Y recorder. There is a 36 pin connector (P₄) which gives access to the input and output terminals for these functions, and the instrument accepts interchangeable cells for different aspects of thermal analysis. Each cell has a heater, thermocouples for control and temperature measurement, and a connector (P₄).

Temperature controller. The signal from a thermocouple located near to the heater is converted to a.c., inverted and amplified, and applied to the gates of thyristors working a 0-110 volt mains heater. In addition, a small voltage may be integrated into this circuit to produce a temperature programme, with any heating or cooling rate available from 0 to 25°C/min. Experimentally, the temperature control which can be achieved is not better than $\pm 0.2^\circ\text{C}$ on isothermal control or 2% accuracy in a programme.

X - Y recorder. The Hewlett Packard 135 DTA recorder has a basic response of 0.4 mV/in on the X axis with 10" span, and 4 mV/in on the Y axis with 7½" span. By means of attenuating resistors the response may be reduced to 8mV/in on the X axis and 400mV/in on the Y axis. Only the X axis has the "infinite at null" resistance provision, which is required for precise thermocouple voltage measurements. Chromel-alumel thermocouples are preferred for temperature measurements.

Differential d.c. amplifier. For differential thermal analysis only, this provides a d.c. output which is nominally 1,000 times the d.c. input.

In this study, two cells were used with the DuPont instrument, (a) the Differential Scanning Calorimeter Cell, which was used without modification, and (b) a hot stage microscope module, which was designed specially and built in the laboratory. Both modules operate from 0°C to 500°C.

(a). Differential Scanning Calorimeter Cell.

A schematic diagram showing the construction of the cell is shown in fig.8. It has been necessary to estimate the dimensions of the inaccessible parts of the cell, and the cell has a heat shield which covers the connector pins, but this has been omitted from fig.8 for simplicity. Facilities are provided for operating the cell under vacuum or nitrogen. The samples are contained in aluminium cups with lids, which are placed on a constantan disc which also supports the thermocouples. The front thermocouple is a chromel-alumel junction which is used in connection with a junction at 0°C for temperature measurements. The rear thermocouple is a chromel-constantan junction, and the attenuated signal between this and the chromel-alumel thermocouple is amplified and delivered to the Y axis of the recorder, in the usual style of differential thermal analysis. A Honeywell Elektronik 19 recorder (1 mV full scale deflection) with a fitted Disc Integrator and zero bias control provided more accurate measurements of the D.T.A. peak areas, and enabled thermal effects to be studied as a function of time. The Y axis signal was attenuated and supplied to the Honeywell recorder. The apparatus was used for determining the heats of fusion of polymers. The DuPont handbook (55) gives further details of the methods for operating the equipment, and schematic diagrams of the electrical circuits.

(b). The hot stage microscope module.

The purpose of building an instrument of similar design to the hot stage microscope described earlier (pages 36 to 40) was two-fold :- (i) to explore the variations of birefringence with temperature in crystalline polymers, and (ii) to provide another instrument for studying crystallization rates.

The apparatus was constructed on a second Swift model P microscope, with the hot stage section to the same pattern as described.

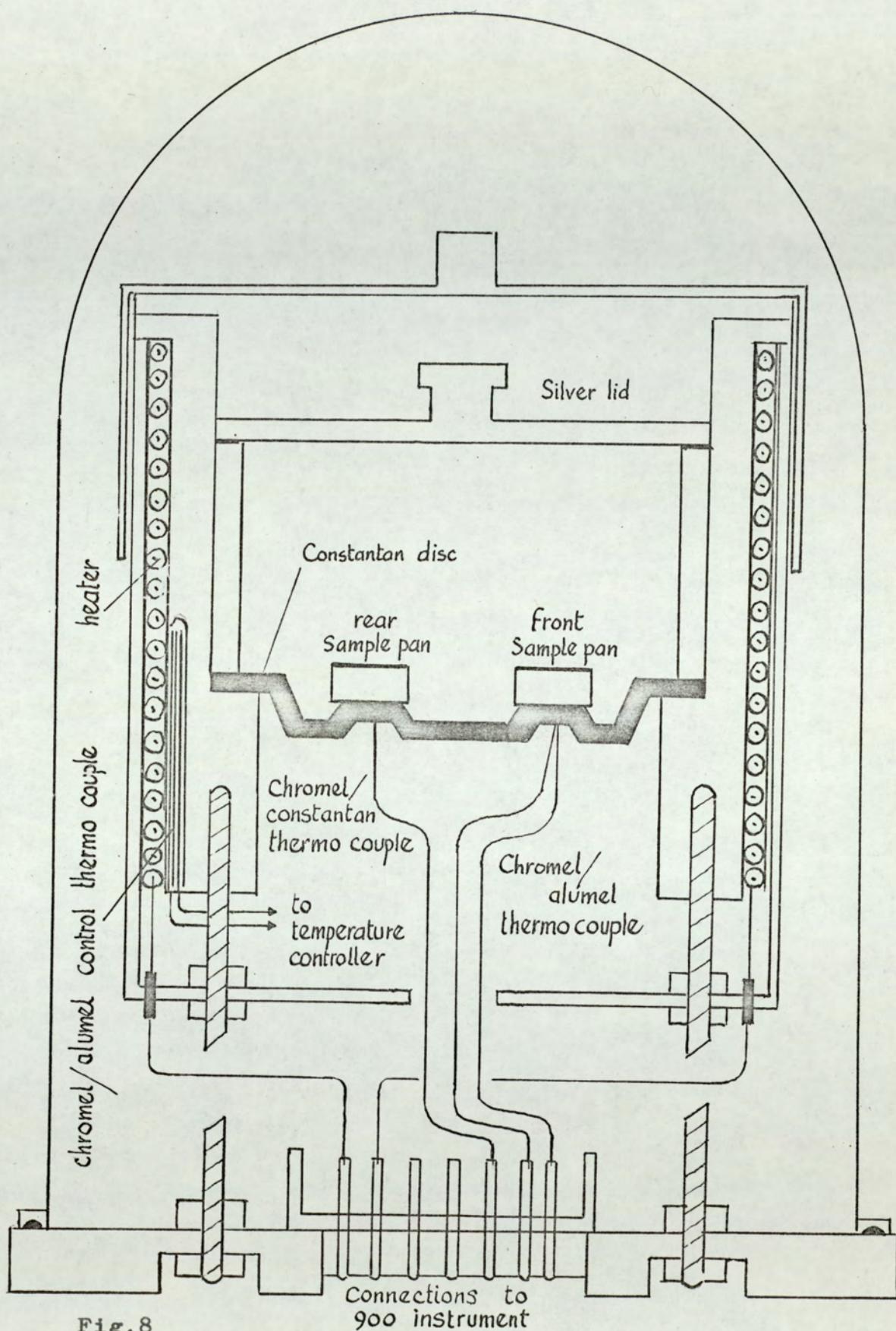


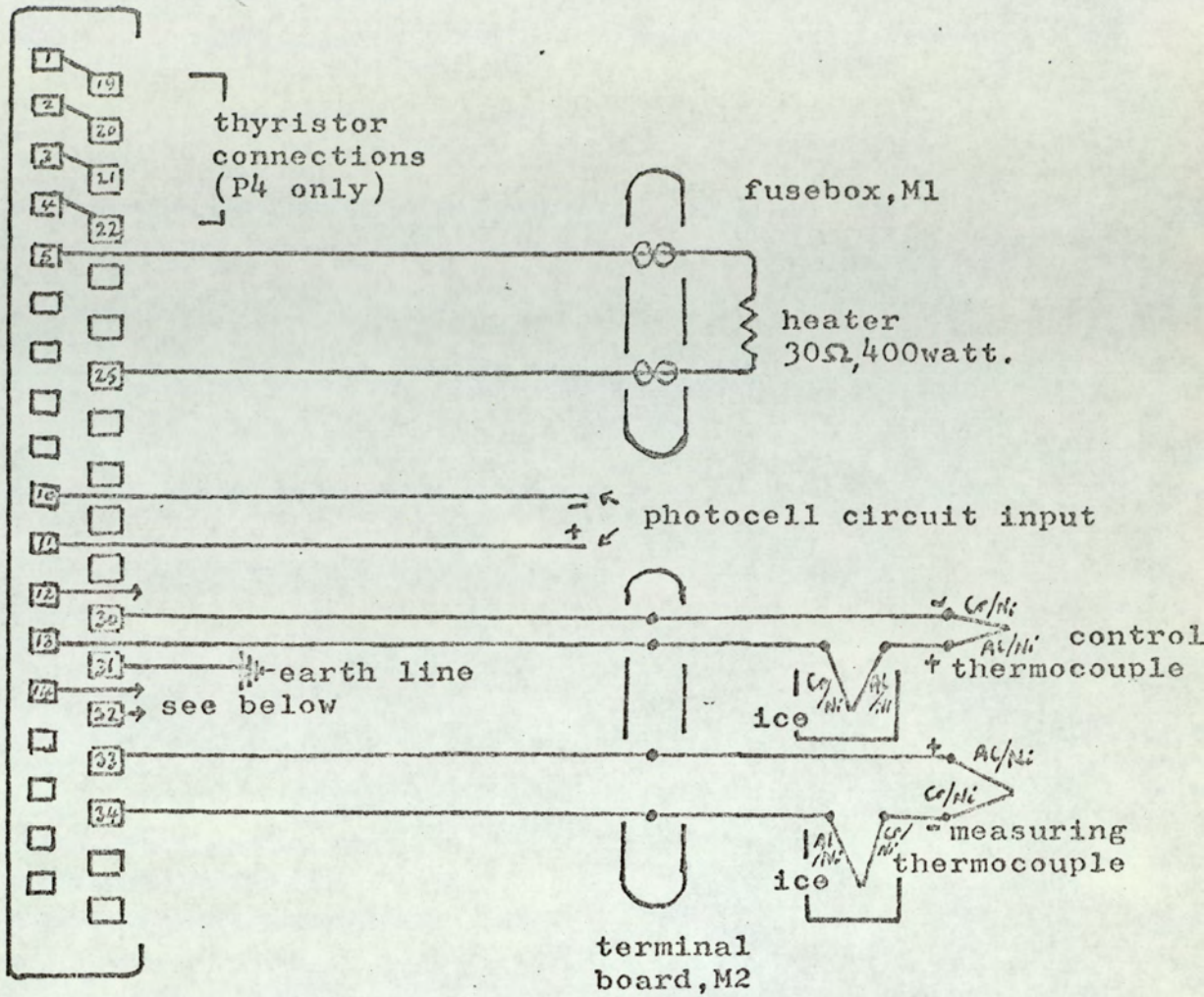
Fig. 8

Du Pont Differential Scanning Calorimeter Cell, 3X actual size.

Stainless steel was used for the stage, and this proved to be much more resistant to corrosion than the silver steel section of the first microscope attachment. A 24 turns heater was fitted, with long tail leads in glass fibre sleeves, to allow for safe operation on the 110 volt supply. The circuit design was concerned with the wiring of the 36 pin Amphenol P4 connector, which is a requirement of the DuPont apparatus. A useful facility of the instrument is a provision for applying a time base generator to the recorder X axis in place of the temperature base, when the instrument is set to 'isothermal'. This was included in the circuit design, and is shown in fig.9, overleaf. The photocell control circuit was modified from the design used on the 'Dynamaster' recorder, to allow for the low sensitivity of the Y axis of the DTA. recorder. The photocell circuit was shown in fig.4b. (page 41). For this microscope, the photocell was supported on a Unitron E.D.E. Demonstration Eyepiece, as this was preferred to the Beck Ocular.

After construction, poor temperature control on the isothermal and hold settings was observed, with temperature variations of $\pm 1^{\circ}\text{C}$. As a result of this, the reproducibility of crystallization / time traces was unacceptable, and no method for improving this was found. The apparatus was much more useful for temperature-programmed traces, with graphs of depolarised light intensity or transmitted light intensity versus temperature. A hot plate near to the instrument was useful for pressing pieces of polymer into films between cover slips.

For sample thickness determinations, a Beck micrometer measuring eyepiece was attached to the microscope by means of another adaptor. The microscope slide was clamped in a vertical position to allow viewing of the edge of the film. An averaged result was obtained by measuring the film thickness at several parts of the edge.



Time base generator:
(panel M3)

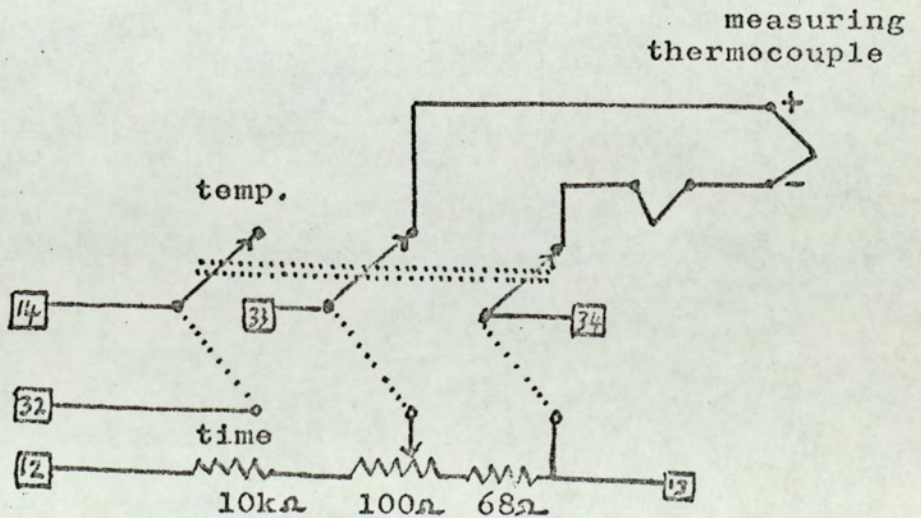


Fig.9 , Schematic diagram for DuPont Microscope Module.

Temperature calibration of the hot stage microscope module and the DuPont Differential Scanning Calorimeter Cell.

The object in calibrating the microscope and D.T.A. equipment was twofold : to provide the best possible temperature accuracy of measurements from the DuPont apparatus, and to permit the comparison of information obtained from the two techniques.

The Hewlett Packard 135 recorder, which is built into the DuPont 900 instrument, was firstly calibrated on the X axis temperature scale. A standard DuPont thermocouple was connected to provide a temperature reading, using a crushed ice/water 0°C reference junction. Since the output of this system is $4.10\text{ mV}/100^{\circ}\text{C}$, and the recorder has a $10''$ span of 4.00 mV , there is a nominal temperature error of 2.2% , which is normally corrected by using the chart supplied with the instrument. A Tinsley 3184 D high accuracy Potentiometer was connected to the instrument to check the temperature response, and it was found to be necessary to draw up a new instrument calibration chart. The corrections for the $20^{\circ}\text{C}/\text{inch}$ scale are shown in table 5.

Table 5. Calibration of the Hewlett Packard recorder, X axis.

Nominal recorded temperature, $^{\circ}\text{C}$; chromel-alumel thermocouples	0	100	120	200	300	400
Correction, $^{\circ}\text{C}$. $20^{\circ}\text{C}/\text{in. scale}$.	+2.5	+0.4	0.0	-0.4	-0.6	-0.8

All temperatures noted hereafter have received the appropriate correction.

The Pye model P. potentiometer, which was used to measure the temperature of the isothermal-temperature microscope, was also standardised against the Tinsley potentiometer. Exact temperature agreement was found for temperature measurements in the range $100 -$

300°C , but the Pye is only accurate to $\pm 0.2^\circ\text{C}$ on account of a less sensitive galvanometer.

The general calibration procedure of Barrall et al (46) for a similar hot stage microscope and DTA equipment was then followed. The hot stage was checked against benzoic acid ('Analar' grade), ammonium nitrate (DuPont Instrument standard sample), and sulphur ('Analar' grade). The graphs of the depolarised light intensity (D.L.I.) versus temperature for benzoic acid and ammonium nitrate are shown in fig.10. The D.T.A. trace from benzoic acid, for a heating rate of $5^\circ/\text{min}$ in the D.S.C.cell is also shown; the D.T.A. peak is seen to occur at the mid-point of the D.L.I. melting trace, confirming that the sample and thermocouple of the microscope stage are essentially at the same temperature. Differential thermal analysis of ammonium nitrate gave small peaks at 40°C , 91°C and 130°C representative of crystalline transitions, and a large melting peak at 174°C . Because the final crystal form is cubic, it is not birefringent, and the melting was not detected by Barrall et al (46) with their D.L.I. apparatus. Transmitted light intensity shows a sufficient change as melting occurs to enable the transition to be measured (fig. 10). The temperatures of the transitions were found by the D.L.I. method to be 41°C , 86°C , 128°C and 175°C , in reasonable agreement with the D.T.A. temperatures. The crystalline transitions in sulphur were observed using D.L.I. and D.T.A. The rhombic-monoclinic conversion was observed at 111°C (DTA) and 110°C (DLI), and the melting of the monoclinic form was recorded at 122°C (DTA) and 119°C (DLI). A published value for the latter transition is 119.2°C (74).

It was concluded that no calibration in addition to the normal recorder correction need be considered for the hot stage microscope , providing heating rates of $2^\circ/\text{min}$ or less are used. At faster heating rates, the temperatures became unreliable, and melting appeared early.

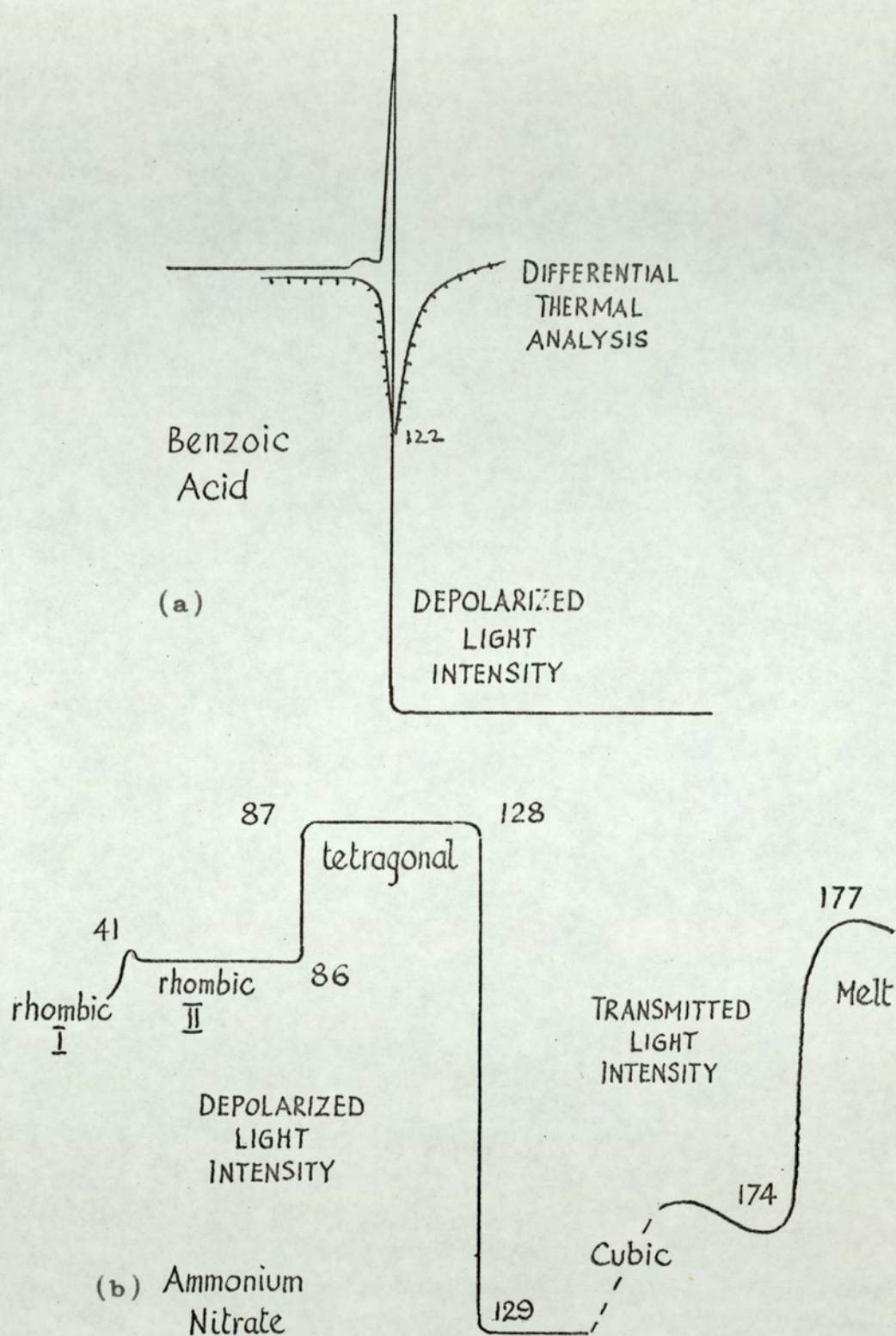


Fig.10. Depolarised light intensity traces for benzoic acid and ammonium nitrate. Heating rate $2^{\circ}/\text{min}$. (Numbers are temperatures in $^{\circ}\text{C}$)

This is probably due to the proximity of the sample to the heater , by comparison with the position of the thermocouple. Also, the thermocouple junction is located in an air cavity, and it consequently attains the block temperature slowly. With differential thermal analysis, the temperatures recorded at fast heating rates are normally above the correct temperature for the transition. $5^{\circ}\text{C}/\text{min.}$ is the preferred programme rate for the DuPont D.S.C. cell. When thermal melting takes place over a wide temperature range, e.g. in the analysis of the melting of polymers, the average melting temperature corresponds approximately to the D.T.A. peak (46).

The calibration of the DuPont D.S.C. Cell for heats of fusion measurement.

The cell was calibrated according to the detailed instructions given in the Handbook (55), using the known heats of fusion of metal standards. The calorific calibration is slightly temperature dependent, due to an increase in the heat losses from the cell at the higher temperatures.

For all measurements, the Honeywell Elektronik recorder was used to display and integrate the D.T.A. peaks. The differential signal was attenuated to 1/17th of the total signal to suit the 1 mV recorder, which then had a sensitivity of 0.69°C for full scale deflection. A heating rate of $5^{\circ}\text{C}/\text{min.}$ was used throughout, and a reference sample pan containing 5mg. glass beads was placed in the cell on the front platform. This is immediately above the chromel-alumel thermocouple, which serves as the temperature measurement element. The rear thermocouple platform supported the sample pan, containing a flat granule of the pure metal standard. During the melting peak, the Disc Integrator was made to draw an oscillatory trace, which could be counted in half cycles. The integrator has a nominal response of 12 cycles per mV.min. The instrument was calibrated using tin as the first standard. The

results are shown in table 6.

Table 6. D.S.C. cell calibration using tin.

Sample :- 0.710 mg.tin. The same sample used for three determinations.
Heating rate, $5^{\circ}/\text{min}$. Chart speed $1''/20 \text{ sec}$. Recorded melting pt, 235°C .

Run no.	1	2	3
D.T.A. signal, cycles from Disc integrator.	1.80	1.75	1.85
D.T.A. signal, cycles/mg.	2.53	2.45	2.60
D.T.A. signal, mV.sec/mg.	12.6	12.3	13.0

From these results, taking the published heat of fusion for tin (55) as 14.2 cal/g , the cell calibration at 235°C is obtained as

$$1 \text{ cycle} = 5.56 \text{ m.cal} \quad \text{or} \quad 1 \text{ mV sec} = 1.11 \text{ m.cal.}$$

The calibration was then repeated using indium as the standard. The results are shown in table 7.

Table 7. D.S.C. cell calibration using indium.

Sample, 1.520 mg.indium; same sample used for each of 3 determinations.
Heating rate, $5^{\circ}/\text{min}$. Chart speed $1''/20 \text{ sec}$. Recorded melting pt. 159°C .

Run no.	1	2	3
D.T.A. signal, cycles from Disc integrator	2.45	2.50	2.40
D.T.A. signal, cycles/mg	1.61	1.64	1.57
D.T.A. signal, mV sec/mg	8.05	8.20	7.85

Taking the published value for the heat of fusion of indium, 6.79 cal/g (55), the cell calibration for 159°C is obtained as

$$1 \text{ cycle} = 4.20 \text{ m.cal} \quad \text{or} \quad 1 \text{ mV sec} = 0.85 \text{ m.cal.}$$

The melting points of these two metals (159 and 235°C) are in the same range as the melting points of most of the polymers under

consideration. The DuPont Handbook has an equation which can be used to extend the calibration to other temperature rates:

$$\Delta H = \frac{E A \Delta T_s T_s}{M a}$$

where E is the calibration coefficient in m.cal/°C min, A is the peak area in sq.in, ΔT_s is the Y axis sensitivity setting, °C/in, T_s is the X axis sensitivity, M is the sample mass and a the heating rate. The equation is discussed by Platt(39), but it has little theoretical basis, as it assumes that heat losses from the cell and the amplifier response are both linear and constant for all heating rates. In this work, the DuPont equation has been regarded as unacceptable ; consequently it has been necessary to programme all the heating for heats of fusion determinations at the standard rate of 5°C/min. The DuPont recommendation of assuming a linear variation of the cell's calorific response with temperature has been assumed.

Other apparatus.

Davenport Density Measuring Apparatus.

The principle of the determination of density by the flotation of bodies in partially mixed liquids is attributed to Galileo (75). In a thermostatted bath at 23°C, a blend of xylene (density 0.88) and carbon tetrachloride (density 1.59) is placed in a tube, to provide a column of liquid having a density gradient. Calibrated glass floats are placed in the column, using a slowly moving gauze basket to reduce mixing of the liquids. The equilibrium heights of the floats may then be compared with the heights of small pieces of polymer samples, and the polymer density can be obtained from a height versus density graph. The columns used were in the density range 1.02 - 1.25 g/ml, and had an average lifetime of useful operation of about three months.

Solution viscosity apparatus.

Three Ubelohode viscometers (76) having different capillary bore sizes were used. The viscometers were mounted in a water bath, which was controlled to $25^{\circ}\text{C} \pm 0.1^{\circ}\text{C}$, by a Tecam controller.

Fluidised sand bed apparatus.

For carrying out polymerisation reactions, a high temperature bath ($200 - 300^{\circ}\text{C}$) with good temperature control was required. The Techne fluidised bed apparatus was preferred to the vapour-bath technique (77), and gave a temperature control of $\pm 5^{\circ}\text{C}$. The temperature could be preset to the required range by means of adjusting a bimetal switch.

CHAPTER 3 , MATERIALS.

In this chapter, details are given of the materials used in the subsequent study of crystallization rates and melting processes. Details of the commercial polymers and the materials for preparing laboratory polymers are given. The copolymerisation techniques are described, and the polymers and copolymers are characterised by their solution viscosities.

Commercial polymers.

66 nylon. A large sample was obtained from I.C.I. Fibres, Ltd., and is identical with the sample used extensively by Platt (39) in a study of the melting of 66 nylon using differential thermal analysis. The sample was supplied with the following details: code, XP 10257, chip with no TiO_2 , contained 0.5 mole % acetic acid as a molecular weight stabiliser; solution viscosity for an 8.4% solution of nylon in 90% formic acid = 32.3; amine end groups = 42.9, carboxyl end groups = 79.0. An approximate measurement of molecular weight may be obtained from
$$\text{Mn} = \frac{2 \times 10^6}{2 \times [\text{carboxyl end groups}]} = 13,000$$

A sample of 66 nylon of similar molecular weight was obtained from I.C.I. Ltd (Plastics Division) coded A.100.

66 nylon yarn. A reel of 'Bri- nylon' yarn, 30 denier, 10 filament yarn, TiO_2 content 0.3%, average tenacity 4.5 g/denier, solution viscosity 35, was also kindly supplied by I.C.I. Fibres, Ltd.

66 nylon tyre cord. A sample was sent by the Olympic Tyre and Rubber Co., Australia. Code: 5260 nylon Roll 137.

6. nylon. A sample of chip containing no additives was provided by I.C.I. Fibres, Ltd.

6.10 nylon. A sample of chip coded B.100 was supplied by I.C.I. Ltd.

Polymerisation reagents.

Hexamethylene diamine. Laboratory grade hexamethylene diamine (B.D.H) was distilled twice at atmospheric pressure, from a flask fitted with a side air condenser. The fraction distilling at 200-205°C was collected.

Sebacic acid. Laboratory grade sebacic acid (B.D.H) was recrystallized from water.

6.10 nylon salt. A 20% solution of 6.10 nylon salt in water was supplied by I.C.I.ltd, (Plastics Division). The solution was evaporated on a steam bath to give a solution of about 40% salt content. The pH was adjusted to 7.0 by adding sebacic acid. On cooling, 6.10 salt crystallized out. The salt was filtered off and recrystallized from water.

66 salt and 6T salt were supplied by I.C.I.Ltd in a form suitable for polymerisation, and the monomers were not further purified.

6-amino hexoic acid and trimesic acid were polymerisation grades (Koch-Light Laboratories), and were used without further purification.

Preparation of 66 nylon polymer.

The salt of hexamethylene diamine with adipic acid (66 salt) is usually polymerised in the laboratory by a two stage process (77). In the first stage, the salt is converted to a prepolymer by heating it in a sealed tube. This prevents the loss of hexamethylene diamine by volatilisation before a polymer is formed. The second stage involves converting the prepolymer to a high molecular weight polymer, by extended heating at a temperature above the polymer melting point.

The two stage process was carried out for 12g. nylon salt in a Carius tube. Nitrogen was first passed over the salt for $\frac{1}{2}$ hour, then the tube was evacuated to 10mm Hg, and sealed at the constriction. The tube was placed in a steel sleeve for safety reasons, and this was heated by immersion in the fluidised sand bath at 215°C for $1\frac{1}{2}$ hours.

The tube was cooled, and broken open with the usual precautions. The prepolymer was placed with 1 ml distilled water in a "Quickfit" test tube (code MF 24/2/6), which was clamped in the fluidised sand bath. The test tube was equipped with a 6" reflux air-condenser, and a slow nitrogen flow over the polymer was provided by passing the gas through a "Quickfit" T piece at the top of the condenser. These precautions ensured a steam/nitrogen atmosphere for the polymerisation, with oxygen excluded. The condensation polymerisation was carried out for $3\frac{1}{2}$ hours at 285°C , with controlled heating. The polymerisation was judged to be completed when the melt showed a bubbled appearance, indicating that the viscosity was too high to prevent the free escape of water vapour. No further vacuum stage was necessary.

It was found that the polymerisation could be carried out in a single stage process without the separate prepolymer formation stage. A slurry of 12g.66 salt and 2ml distilled water was placed in a "Quickfit" test tube fitted with an 18" air-condenser, and a 2% excess of purified hexamethylene diamine was added. Condensation polymerisation commenced at 200°C when a prepolymer formed rapidly. The melt was then formed and maintained at 285°C for 4 hours under steam/nitrogen. On cooling, a solid piece of polymer formed, which was removed by breaking the test tube.

By carrying out the polymerisation in an oxygen-free atmosphere, no appreciable yellowing of the product was noticed. The polymer was broken into small pieces by immersing it in liquid nitrogen, followed by mechanical action. The pieces were placed in boiling distilled water for 15 minutes to remove any residual monomers; followed by drying in a vacuum oven for 48 hours at 1mm Hg pressure, 60°C . The samples were stored in stoppered bottles.

Polymerisation of 6 nylon.

Initial attempts to prepare 6 nylon by the melt polymerisation of caprolactam showed that the polymerisation proceeds slowly, and a satisfactory molecular weight was not achieved without a lengthy reaction time. Degradation during polymerisation was also a severe problem.

6 amino hexoic acid was much more convenient for polymerisation, as it could be conveniently converted to polymer in a single stage polymerisation reaction at 285°C under steam/nitrogen, with a reaction time of 3 hours. Attempts to prepare prepolymers from 6-amino hexoic acid all resulted in the Carius tubes exploding, as the melt condensation polymerisation proceeds rapidly in the early stages of polymer formation.

Preparation of 6.10 nylon.

Polymerisation of 6.10 nylon was carried out by heating the salt in the steam / nitrogen atmosphere for 5 hours at 270°C .

Preparation of 66/6 nylon copolymers.

A blend of 66 salt and 6.amino hexoic acid was produced by grinding the required quantities of the monomers in a mortar. Most polymerisations were then carried out by the two-stage process, except where 6.amino hexoic acid was the major constituent, when a single stage process was used. Details of the copolymerisation conditions for the polymers selected for further study are given in table 8. (overleaf). For the more highly copolymerised samples, longer reaction times at lower temperatures were used. The additional time is necessary at the lower temperatures, as the condensation reaction proceeds more slowly.

Table 8. Copolymerisation of 66 nylon with 6 nylon; experimental conditions for the polymers selected for further study.

Molar composition of feed, % 66 salt (with amino hexoic acid)	Code	Condensation polymerisation stage	
		Time, hours	Temperature °C
100	32	3½	285
97	63	3	285
93	26	2½	275
85	25	3½	275
80	24	5	270
70	33	8	270
60	31	12	265
50	37	12	260
40	27	8	240
27	28	7½	240
15	29	6	260
10	38	6	270
0	30	3	285

Characterisation of 66 nylon and 66/6 copolyamides.

The Mark-Houwink equation is frequently used for molecular weight measurements (76). The relationship is:-

$$[\eta] = K M^a$$

where K and a are constants for a given polymer, solvent and temperature and $[\eta]$ is the intrinsic viscosity, which is obtained from a graph of the concentration dependence of the specific viscosity function,

$$[\eta] = \lim_{c \rightarrow 0} \frac{(\eta)_{sp}}{c}$$

The specific viscosity

is obtained from flow time measurements:

$$\eta_{sp} = \frac{n_{\text{solution}} - n_{\text{solvent}}}{n_{\text{solvent}}}$$

For molecular weight determination $[\eta]$ is obtained from the Y axis intercept of a graph of $\frac{\eta_{sp}}{c}$ versus c , (where c is the concentration in g/100ml).

In this study, an effort has been made to produce copolymers which have approximately the same viscosity average molecular weight as spinning grade nylon, i.e. Mv in the 20,000-25,000 range.

A litre of 90% formic acid was prepared by diluting 98% acid, and standardising against 1 N. caustic soda. 0.1 molar sodium formate was added as a polyelectrolyte suppressor. A solution of 66 nylon was prepared by warming 0.250 g polymer with 25ml solution of sodium formate in formic acid, in a flask fitted with a condenser. The temperature of the solvent was maintained at about 100°C for the minimum length of time required to completely dissolve the polymer (15 mins.). The cooled solution was filtered using a no.3 glass sinter.

Viscosity measurements were carried out using an Ubbelohde viscometer placed in a 25°C water bath. Before filling, the viscometer was cleaned with chromic/sulphuric acid, distilled water, and alcohol, and dried in an oven. The flow time for the solvent was determined, the viscometer was recleaned, and the flow time for 5ml of a 1% solution was determined. Successive dilutions of the formic acid solvent were then made and the graph of $\frac{\eta_{sp}}{c}$ versus c was drawn. A group of measurements for 66 nylon (XP 10257, commercial chip) is shown in table 9. This data has been plotted graphically in fig.11, to determine $[\eta]$. Fig.11 also shows a similar plot for a copolymer of 85% 66 nylon. Intercepts of 0.58 and 0.56 were obtained for these polymers. These values are now expressed as limiting viscosity numbers

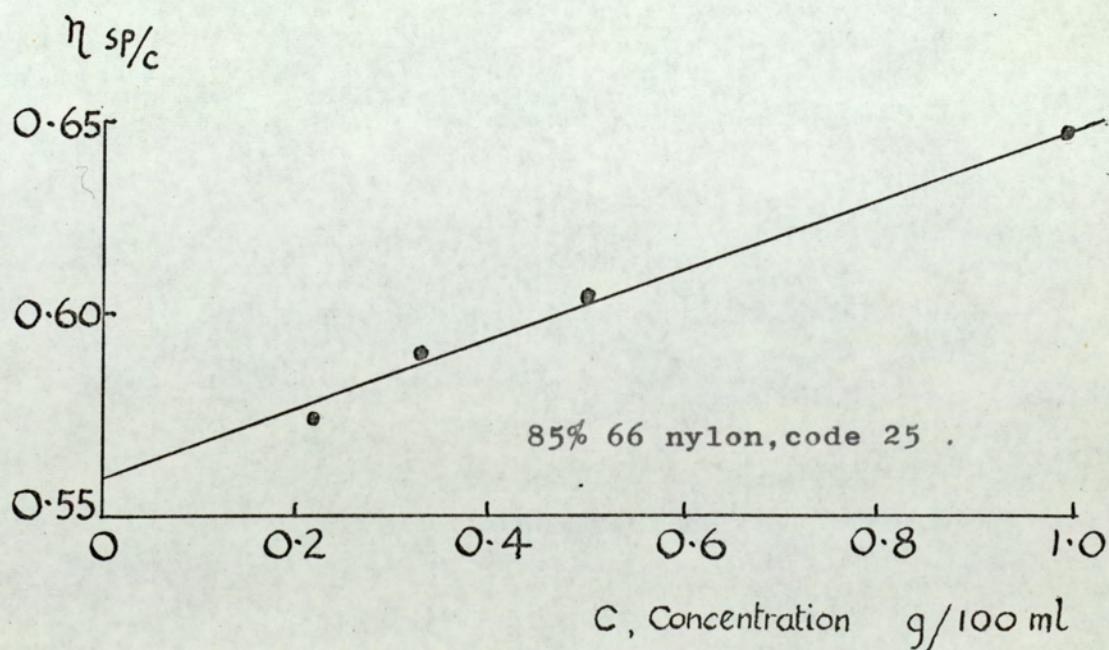
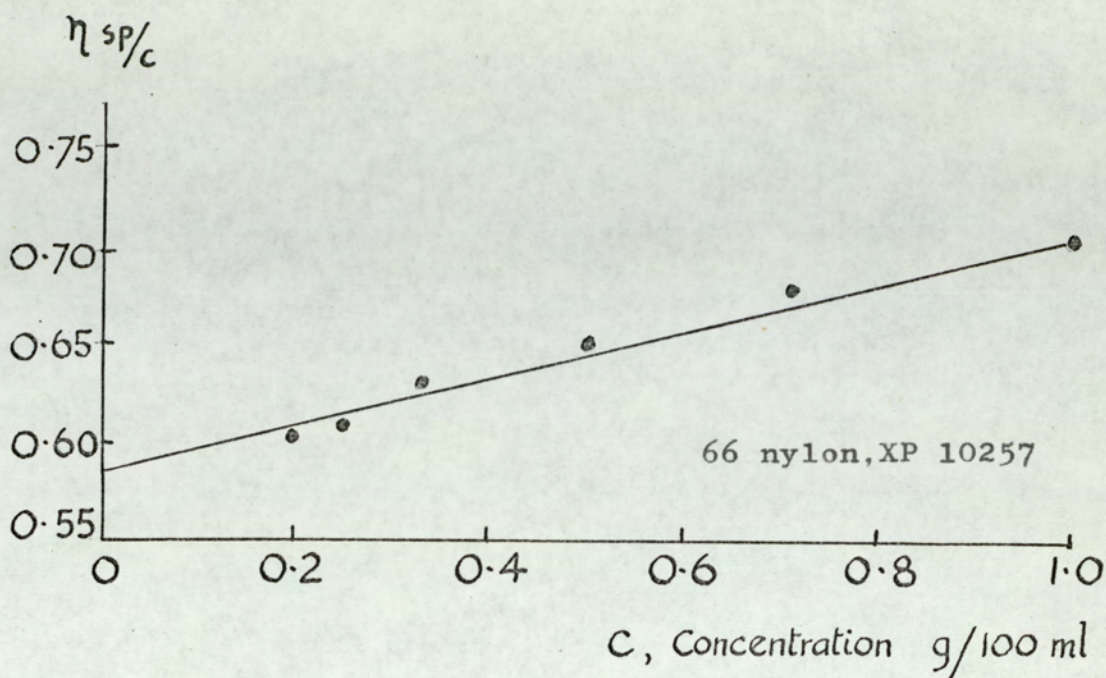


Fig. 11. Solution viscosity measurements in 90% formic acid. 66 nylon and a copolymer containing 85% 66 nylon .

of 58 and 56 ml/g. (Limiting viscosity no = 100 x inherent viscosity).

Table 9. Viscosity measurements for commercial 66 nylon, sample XP 10257. Solvent, 90% formic acid with 0.1 molar sodium formate.

Solvent flow time 298.0 sec.

Concentration g/100ml	Individual flow times,secs average	η_{sp}	$\eta \frac{sp}{c}$
1.0	510.0, 511.0, 510.8 510.6	0.714	0.714
0.71	444.4, 444.5 444.4	0.492	0.688
0.50	396.6, 395.0 395.8	0.325	0.651
0.33	361.0, 361.0 361.0	0.211	0.634
0.25	343.6, 344.0 343.8	0.154	0.615
0.20	334.5, 334.6 334.5	0.122	0.612

Conversion of viscosity results to molecular weights is usually accomplished by using published values for the constants in the Mark-Houwink equation. Elias and Schumacher (78) using light scattering methods for their absolute molecular weight determinations gave the equation

$$[\eta] = 0.10 \cdot 51.6 \times 10^{-5} M^{0.687}$$

for 66 nylon in the formic acid solvent at 25°C. Burke and Orofino (79), using light scattering and osmometry, in a detailed appreciation of the same system, gave

$$[\eta] = 87.7 M^{0.65}$$

There is a difference in the molecular weight values which are obtained using these two relations. For the commercial sample of 66 nylon, XP 10257, with a limiting viscosity number of 58, the values for the molecular weight are 26,900 (ref.78) and 21,800 (ref.79).

No published solution viscosity / molecular weight relationships were found for 66/6 copolyamides, and the two expressions for 66 nylon homopolymer have been assumed to be approximately correct for these copolymers. The expression of Bennewitz (80) for 6 nylon

in 85% formic acid at 20°C was obtained by end group analysis, and is

$$[\eta] = 75 M^{0.70}$$

This expression is very similar to Burke and Orofino's expression for 66 nylon. An attempt was made to determine an intrinsic viscosity value for 6 nylon using 85% formic acid at 20°C. Very poor linearity on the η sp/c versus c graph was obtained, indicating that polyelectrolyte effects were interfering with the flow time measurements. The relationships for 66 nylon have consequently been assumed to be approximately correct for 6 nylon, and 90% formic acid with sodium formate has been used as solvent.

Table 10 shows the intrinsic viscosities (as limiting viscosity numbers) and the corresponding molecular weights for the 66/6 copolyamides. For convenience, the densities are also shown here.

Table 10. Molecular weights and densities of 66/6 copolyamides.

Molar composition, % 66 nylon	Code	Density g/ml, 23°C	Limiting viscosity number	Mv (ref.78)	Mv (ref.79)
100	32	1.157	58	26,900	21,800
97	63	1.154	51	22,250	18,600
93	26	1.151	58	26,900	21,800
85	25	1.145	56	25,500	20,800
80	24	1.139	58	26,900	21,800
70	33	1.134	60	28,500	23,000
60	31	1.130	68	32,000	26,000
50	37	1.126	66	32,500	25,000
40	27	1.128	55	24,000	20,100
27	28	1.129	62	29,700	24,200
15	29	1.135	58	26,900	21,800
10	38	1.136	62	29,700	24,200
0	30	1.152	57	26,200	21,500

The density measurements shown in table 10 were obtained using the Davenport apparatus. The samples had been crystallized from the melt using a cooling rate of $2^{\circ}/\text{min.}$ to room temperature.

Copolyamides containing terephthalic acid - "6T copolymers".

Two series of polymers were produced: (i) copolymers of 66 nylon with 6T nylon and (ii) copolymers of 6.10 nylon with 6T nylon. In each series, copolymers containing up to 20% 6T were prepared.

Polymerisation.

A summary of the preparations of copolymers selected for further study is given in table 11.

Table 11. Preparations of copolymers containing 6T nylon.

Molar composition		Code	Condensation polymerisation	
% 6T nylon	other nylon		time, hours	Temperature C
1	66 nylon	65	3	290
2		55	3	290
5		47	4	290
10		43	$2\frac{1}{2}$	300
15		49	$2\frac{1}{2}$	305
20		50	$2\frac{1}{2}$	305
0	6.10 nylon	61	5	300
10		62	6	300
15		67	3	290
20		69	5	300

The molar weights for 66 nylon salt, 6T nylon and 6.10 nylon salts were taken as 262g, 282g and 318g respectively. The single stage polymerisation procedure was followed as for 66 nylon preparation, but higher temperatures were necessary as the 6T concentration was increased, as shown in table 11. Copolymers containing more than 20% 6T in

66 nylon could not be prepared without incurring an appreciable amount of thermal degradation. Particularly lengthy polymerisations were necessary for 6,10 nylon and 6.10/6T copolyamides.

Characterisation.

A summary of the limiting viscosity numbers, molecular weights and densities of the copolymers from the preparations listed in table 11 are given in table 12.

Table 12. Limiting viscosity numbers, molecular weights and densities of 66/6T copolyamides and 6.10/6T copolyamides.

Mole % 6T with 66 nylon	Code	Density g/ml, 23°C	Limiting viscosity no. (formic acid, 25°C)		Mv (ref.78)
1	65	1.152	-		-
2	55	1.152	44		20,000
5	47	1.153	53		23,600
10	43	1.161	47		20,800
15	49	1.168	46		20,600
20	50	1.174	48		26,900
Mole % 6T with 6.10 nylon	Code	Density g/ml 23°C	Limiting viscosity numbers 25°C formic acid m.cresol		Mv (ref.81)
0	61	1.115	41	131	14,100
10	62	1.114	35	73	7,600
15	67	1.118	31	75	7,900
20	69	1.126	34	65	6,800

No published information concerning the molecular weight determination for these copolymers was found. The polymers were soluble in the 90% formic acid solvent, although longer times (2-3 hours) were necessary to dissolve the more highly aromatic copolymers. No values for converting the formic acid solution viscosity values of 6.10

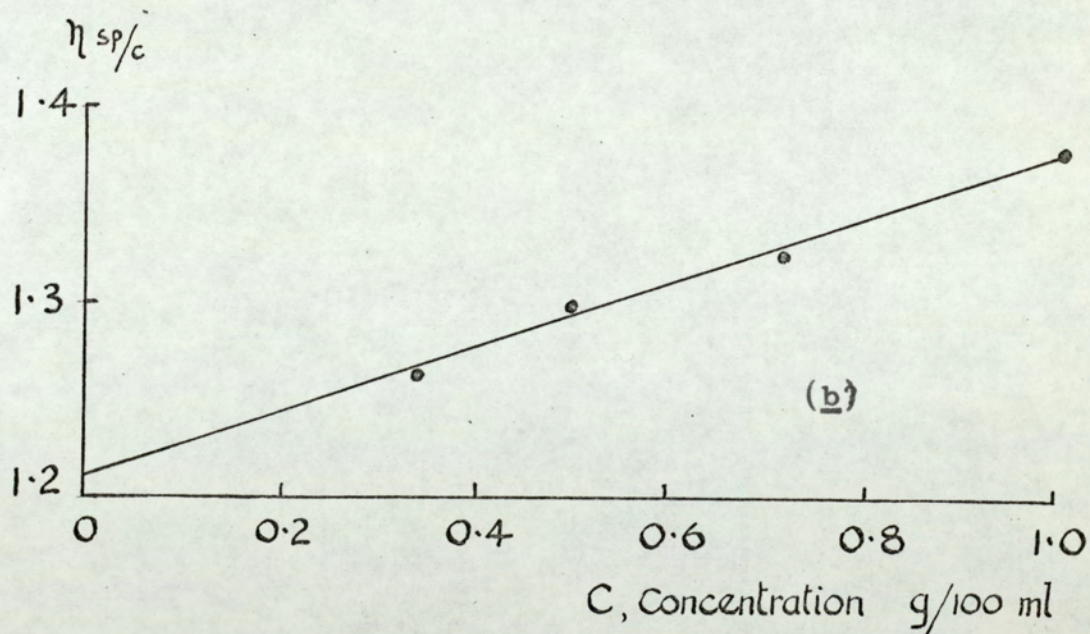
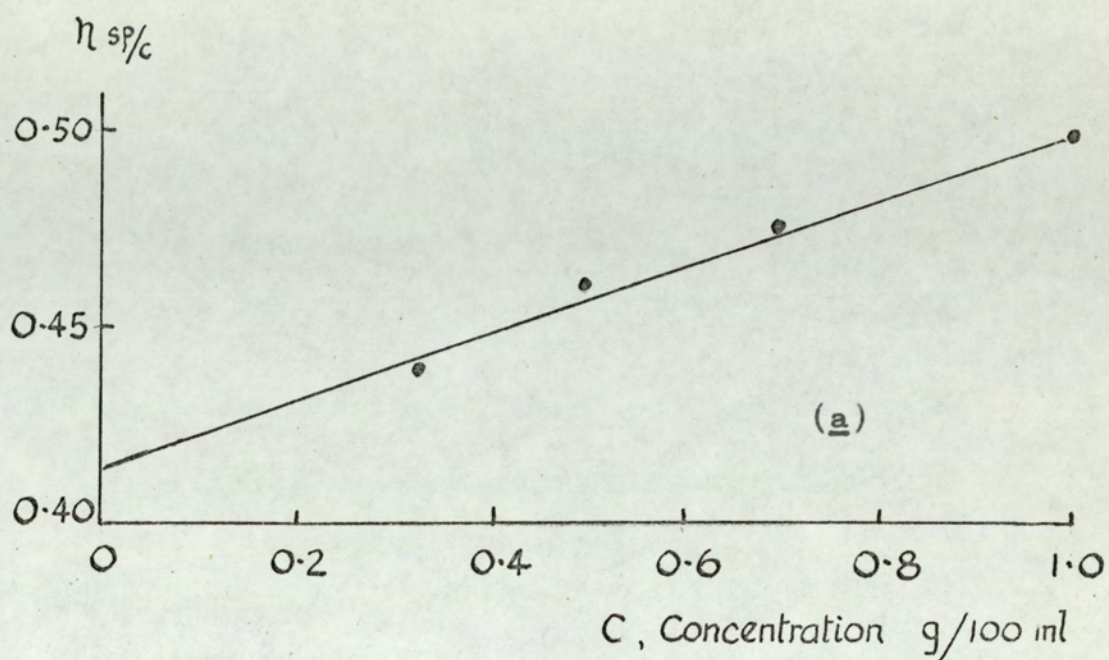


Fig.12. Solution viscosity measurements for 6.10 nylon in (a) 90% formic acid and (b) m.cresol.

nylon to molecular weights were available. Morgan and Kwolek (81) gave the Mark Houwink constants for 6.10 nylon in meta cresol as:-

$$[\eta] = 13.5 M^{0.96}$$

The copolymers including 6.10 nylon were therefore characterised by solution viscosity measurements in m.cresol. Fig.12 shows the η_{sp}/c versus c graphs which were obtained for 6.10 nylon using (a)formic acid and (b) m. cresol. Conversions to molecular weight in table 12 (page 70) have used the values for K and a constants of Elias and Schumacher (78) for 66 nylon and 66/6T copolyamides, and Morgan and Kwolek (81) for 6.10 nylon and 6.10/6T copolyamides. The densities of the polymers shown in table 12 were determined on samples which had been crystallized from the melt at 2°/min to room temperature.

Branched /cross-linked 66 nylon copolymers.

Preparation. An attempt to make a salt of trimesic acid with hexamethylene diamine was not successful, because the product could not be isolated. A finely powdered blend of trimesic acid with hexamethylene diamine in a 2:3 molar ratio ("6X monomer") was used in place of the salt. An allowance for the trifunctional nature of 6X monomer was made when calculating the molar proportions for copolymerisation. Copolymers containing up to 3% 6X with 66 nylon could be made using a single stage polymerisation at 300°C. The reaction was regarded as complete when a highly bubbled melt had formed. The polymers were cooled to room temperature at 2°/min. and density determinations were made. The results are shown in table 13 (page 73).

Characterisation. A solution of each copolymer resulted after digestion for 4 hours in hot formic acid, and the solution viscosities of the copolymers were measured without particular difficulty. The results are shown in table 13. The limiting viscosity numbers have not been converted to molecular weight values, as the intrinsic

viscosity-molecular weight relationships for 66 nylon are probably not applicable with any accuracy to these copolymers.

Table 13. Chemically branched /cross-linked 66 nylon. Preparation details, solution viscosities and densities of 6X/66 copolyamides.

Mole % 6X monomer (with 66 salt)	Code	Polymerisation time, hours at 300°C	Density g/ml 23°C	Limiting viscosity number in formic acid
1	53	1½	1.161	64
2	54	2	1.160	57
3	52	1½	1.156	54

Polymer precipitates.

Products from the polymerisations were normally white solids, and were generally used for further study of rates of crystallization without purification by precipitation. Small quantities of precipitates were prepared for melting studies, using the techniques described below.

1. A sample of 66 nylon was precipitated from a 5% solution of the polymer in 98% formic acid, by adding excess methanol with vigorous stirring. The precipitate was filtered and refluxed with methanol to remove adhering acid traces, then filtered and dried in a vacuum oven for 12 hours at 60°C/10mm Hg. The precipitate had a fibrous appearance, and was only slightly birefringent when viewed under a polarising microscope.

2. A 1% solution of 66 nylon in aqueous formic acid was prepared by dissolving the precipitate from section 1 (above) in boiling 70% formic acid. The flask was transferred to a 65°C water bath, and a mechanical stirrer was started. A precipitate formed overnight, which appeared to be similar to the shish ke-bab type described by Keller

(82) for polyethylene. The precipitate was highly birefringent when examined under the polarising microscope.

3. A 1% solution of 66 nylon in hot butane diol was produced, again starting from the fibrous precipitate. The solution was allowed to cool slowly to room temperature, without stirring. Excess alcohol was added to assist filtration, and the precipitate was boiled in methanol, refiltered, and dried in the vacuum oven. Microscopic examination showed brightly birefringent specks, suggesting that aggregated single crystals had been formed.

An attempt was made to examine the precipitates from the second and third methods by electron microscopy. These samples were thought to be composed of single crystals, possibly similar to the crystals which Geil(3) had obtained from glycerol solutions of polyamides. Using a Philips E.M.200 electron microscope, with the usual grid preparation procedure, no isolated crystals were seen, although some of the aggregates appeared to contain lamellae.

CHAPTER 4 RESULTS.

Depolarised light intensity measurements (D.L.I.).

Optical depolarised light intensity measurements of polymer crystallization have the same general shape as dilatometric graphs (34-38). The crystallization process has been regarded as commencing at the instant of transfer of the polymer melt to the stage of the microscope. Under conditions of very rapid crystallization, induction times as short as 10 seconds have been encountered, indicating that the sample quickly attained a temperature close to the temperature of the microscope hot stage.

The crystallization process commences with an induction period, during which any nuclei which form are not visible at the optical microscope magnification (about 200 x). At the time t_i , the trace of the photocell output begins to show a signal due to the appearance of birefringent entities. The main primary spherulite growth process takes place, and the crystallization terminates at a time t_f . At the completion of crystallization, there appears to be an equilibrium between the crystallized fraction and the remaining amorphous medium. In the latter stages of the process, secondary crystallization predominates, with a perfection process taking place in the already-formed spherulites. The D.L.I. technique gives a response which includes the perfection process, and the trace is representative of the total crystallinity development in the system. The crystallization half time, $t_{\frac{1}{2}}$, is defined as the time when the depolarisation trace has recorded 50% of the overall change. For further information concerning the shapes of the D.L.I. isotherms, some $t_{\frac{1}{4}}$ and $t_{\frac{3}{4}}$ values have been recorded, and these correspond to the 25% and 75% completion stages. These values allow a reasonable reconstruction of the isotherms from tabulated results.

Rates of crystallization of 66 nylon.

Two samples of 66 nylon, having approximately the same molecular weights, and similar to spinning grade were used for this study, a laboratory sample (code, 32) and commercial polymer (XP 10257). For crystallization rates, all samples of these polymers were melted for 5 minutes at 300°C, followed by transfer to the microscope stage at the preselected temperature. It was not considered necessary to repeat the observations of McLaren (42) on different melting conditions. A discussion of these results was given on page 26.

Fig. 13 (page 77) shows three crystallization isotherms for each sample of 66 nylon. The complete results for these polymers are shown below in table 14.

Table 14. Rates of crystallization of 66 nylon.

Laboratory polymer, code 32.					
Temperature, °C	crystallization times, mins.				
	t_i	$t_{\frac{1}{4}}$	$t_{\frac{1}{2}}$	$t_{\frac{3}{4}}$	t_f
247.8	13.3	32.7	47.3	88.7	300
246.7	12.0	31.0	42.0	60.0	160
246.0	8.0	21.3	28.7	46.0	145
244.0	6.7	16.0	22.3	42.0	120
243.8	4.7	10.0	12.0	18.0	75
242.0	2.5	5.7	8.7	17.0	70
241.5	2.0	3.0	4.0	10.0	70
240.0	1.0	1.5	2.2	5.0	30
Commercial polymer, XP 10257					
Temperature °C	crystallization times, mins.				
	t_i	$t_{\frac{1}{4}}$	$t_{\frac{1}{2}}$	$t_{\frac{3}{4}}$	t_f
251.0	30.0	53.3	65.0	80.0	200
248.8	11.0	26.7	34.0	44.7	100
248.0	10.0	22.0	28.0	39.0	90
246.5	8.0	16.6	22.0	30.0	60

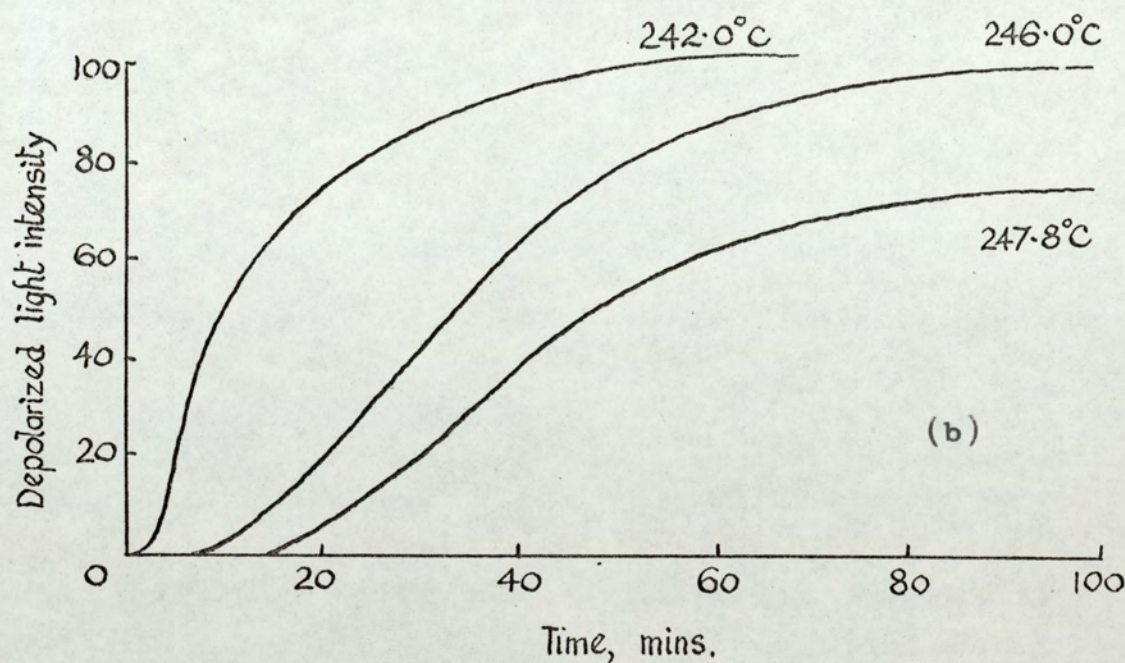
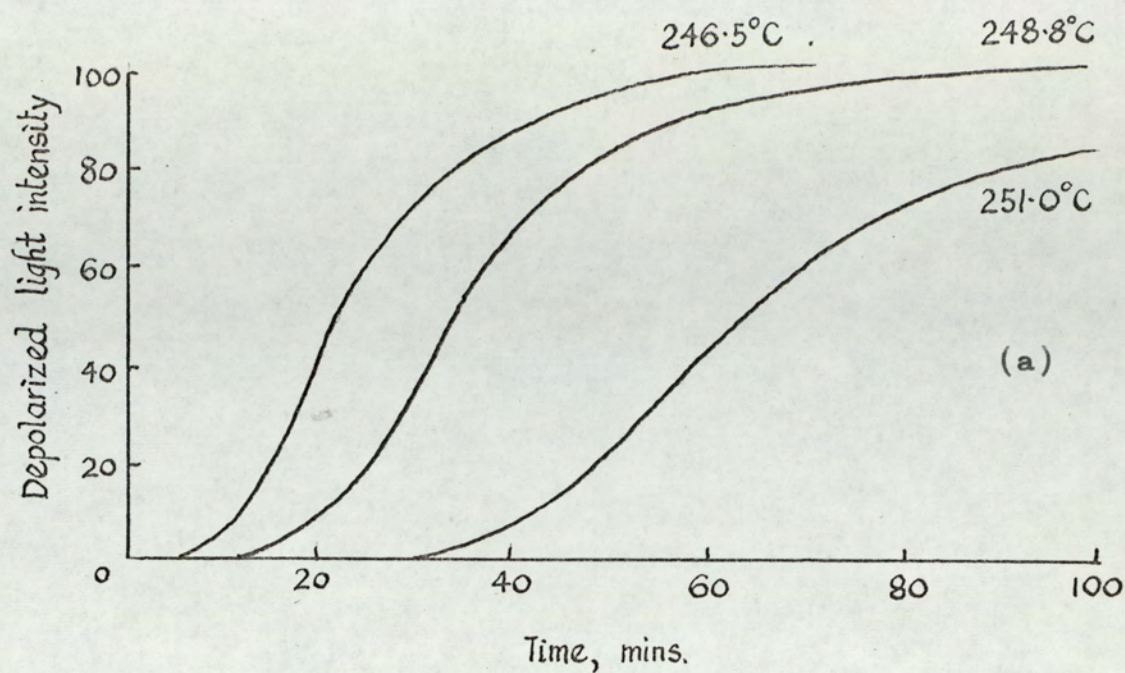


Fig.13. Depolarised light intensity traces for 66 nylon
 (a) commercial sample (b) laboratory sample.

With the present microscope equipment, it was not possible to record a crystallization having a half time of less than 3 minutes with accuracy, due to the slow response time of the recording equipment. Additionally, a slow crystallization resulted in an excessive time before the infinity D.L.I. value was reached. Typically t_f was found to be $6 \times t_{\frac{1}{2}}$ minutes, and the process was then continued for a further time period to ensure that the infinity value had been reached. A maximum half time of 2 hours was practicable, as for longer processes the equipment occupation time became excessive, and the temperature control usually showed unacceptable variations due to inadequate long term stability of the d.c. amplifier. For 66 nylon, the crystallization time limitations were found to be equivalent to a working temperature range of 240-248°C for the laboratory polymer, and 243-251°C for the commercial polymer.

The dependence on temperature of the crystallization rates of commercial and laboratory 66 nylon were found to be slightly different. For a given crystallization rate, the commercial polymer crystallized at a temperature about 3°C higher than laboratory produced polymer. This is illustrated in fig. 14 (overleaf), which shows the crystallization rates for 66 nylon samples at various temperatures. The difference in the crystallization behaviour of these two samples was found to be more significant than could be attributed to water content variations, as discussed by McLaren (42). Further experiments which could have explained the effect were not carried out, as the difference is marginal compared with copolymer effects. Additionally, the effects of molecular weight, film thickness, melting time and melt temperature are well documented for samples of commercial 66 nylon. (42, 43).

The melting points of the polymers were determined using samples

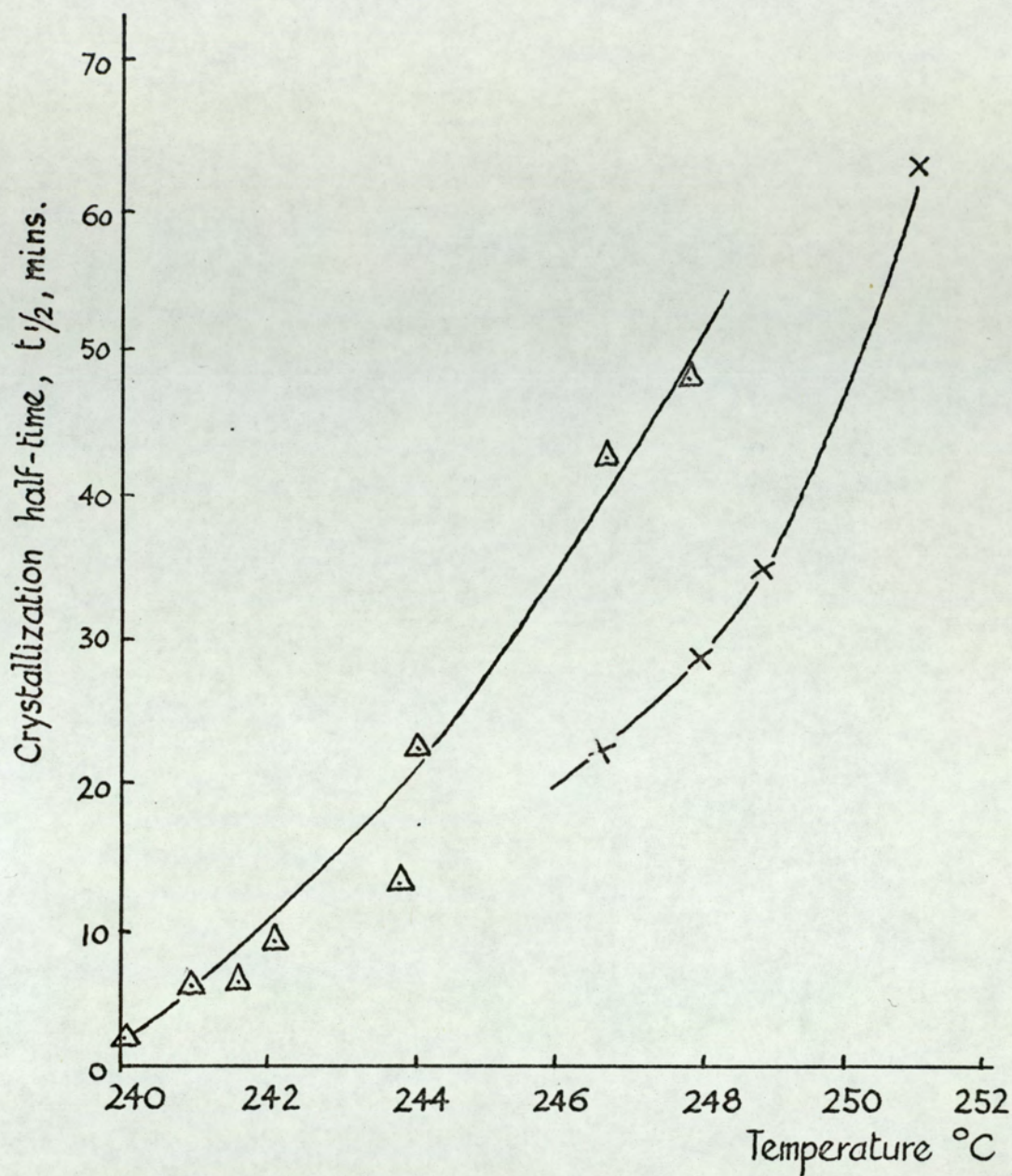


Fig. 14. Crystallization of 66 nylon, $t_{1/2}$ versus temperature.

- Δ Laboratory sample, code 32.
 \times Commercial sample, XP 10257.

which had been produced from the more lengthy crystallizations. Using a programmed heating rate of $2^{\circ}/\text{min.}$ and the microscope module of the DuPont 900 Analyzer, the temperature at which the last traces of birefringence disappeared from the sample was recorded. The method is known to lead to high values for melting points (83), although it has received recent analytical attention (46) which confirms its accuracy for polymer melting points. After the usual corrections, the values obtained for the melting points of 66 nylon samples were found to be 269.5°C for commercial grade polymer, and 268.0°C for the laboratory sample. The melting point determined by this method was reproducible to $\pm 0.5^{\circ}\text{C}$.

Copolymers of 66 nylon and 6 nylon.

A summary of the materials used for this study was given in table 10 (page 68). No commercial copolyamides were available, but the copolymers had approximately the same molecular weights as the commercial forms of 66 and 6 nylons.

Rates of crystallization.

The depolarised light intensity traces for the copolyamides have the same general shape as the curves for 66 nylon. As expected (21,22), the crystallization temperatures have to be reduced as the comonomer content is increased. For convenience, the copolymer series is considered in two parts, on either side of the minimum melting composition.

The results for copolymers containing between 3 and 50% 6 nylon content, with 66 nylon as the main ingredient are shown in table 15. (overleaf). Results of initiation time (t_i), $t_{\frac{1}{4}}$, $t_{\frac{1}{2}}$, $t_{\frac{3}{4}}$ and t_f are shown for five temperatures for each of the seven copolymers. The melting points have been noted in table 15, and the melting conditions were taken as 5 mins. at $T_m + 30^{\circ}\text{C}$ for each sample.

Table 15. Crystallization measurements at various temperatures for copolymers containing 3-50% 6 nylon in 66 nylon.

Code 63, 97% 66 nylon; melting point 263.5°C, melting condition 5min/290°C.

Temperature °C	t_i	$t_{\frac{1}{4}}$	$t_{\frac{1}{2}}$	$t_{\frac{3}{4}}$	t_f	times, mins.
242.2	12.0	29.0	39.6	65.3	200	
241.2	10.0	23.3	34.0	60.0	170	
240.5	7.0	12.0	16.7	30.0	80	
240.0	4.0	8.0	13.3	30.0	70	
238.8	2.0	7.3	10.0	15.3	60	

Code 26, 93% 66 nylon ; melting pt 256.0°C., melting condition 5min/280°C.

Temperature °C	t_i	$t_{\frac{1}{4}}$	$t_{\frac{1}{2}}$	$t_{\frac{3}{4}}$	t_f	times , mins.
236.5	20.0	36.8	56.0	103.3	280	
234.8	14.0	28.8	38.0	58.0	160	
234.0	8.0	14.0	21.0	30.0	120	
233.5	6.6	10.7	13.3	16.7	47	
231.5	2.1	6.6	9.3	15.3	30	

Code 25, 85% 66 nylon; melting pt.235.0°C, melting condition 5min/265°C.

Temperature °C	t_i	$t_{\frac{1}{4}}$	$t_{\frac{1}{2}}$	$t_{\frac{3}{4}}$	t_f	times, mins.
223.2	27.0	49.3	73.0	120	250	
221.8	12.0	25.3	33.3	43.0	140	
219.2	9.3	18.2	24.0	34.7	120	
217.5	3.3	8.0	13.3	22.0	70	
211.0	1.3	3.0	4.0	6.0	15	

Code 24, 80% 66 nylon; melting pt.227.0. melting condition 5mins/260°C

Temperature °C	t_i	$t_{\frac{1}{4}}$	$t_{\frac{1}{2}}$	$t_{\frac{3}{4}}$	t_f	times, mins.
212.0	16.6	37.3	47.3	63.0	113	
211.5	14.0	28.7	37.3	53.0	100	
210.2	10.0	19.3	24.3	33.0	80	
207.2	8.0	16.0	20.0	26.7	60	
204.2	4.0	8.3	10.7	14.0	40	

Table 15 (continued) , crystallization of 66/6 copolyamides.

Code 33, 70 % 66 nylon, melting pt. 210.0°C , melting condition 5 mins/ 240°C .

Temperature $^{\circ}\text{C}$	t_i	$t_{\frac{1}{4}}$	$t_{\frac{1}{2}}$	$t_{\frac{3}{4}}$	t_f	time, mins.
191.7	30.0	66.6	94.6	140	260	
190.6	28.0	62.7	83.3	120	240	
189.2	14.7	28.0	36.6	51.3	95	
187.0	10.0	20.2	26.6	38.0	80	
183.0	4.0	8.0	10.6	15.3	50	

Code 31. 60% 66 nylon, melting pt. 188°C , melting condition 5 mins/ 220°C .

Temperature $^{\circ}\text{C}$	t_i	$t_{\frac{1}{4}}$	$t_{\frac{1}{2}}$	$t_{\frac{3}{4}}$	t_f	time, mins
174.8	20.0	35.4	56.0	100	250	
171.2	10.0	23.2	32.0	60	140	
169.5	8.8	19.0	26.7	38.7	120	
167.5	6.6	13.3	17.3	25.3	80	
166.2	4.0	8.3	11.3	15.3	60	

Code 37. 50% 66 nylon, melting pt. 178°C , melting condition 5 mins/ 220°C .

Temperature $^{\circ}\text{C}$	t_i	$t_{\frac{1}{4}}$	$t_{\frac{1}{2}}$	$t_{\frac{3}{4}}$	t_f	time, mins
160.2	18.0	40.0	52.0	70	180	
157.2	10.7	27.3	37.3	53	120	
155.8	6.0	14.3	19.3	28	87	
153.0	4.7	9.3	12.0	17.3	80	
151.5	3.3	7.3	9.7	14.0	60	

Fig.15 shows the $t_{\frac{1}{2}}$ values at various temperatures for 66 nylon and copolymers of 66 nylon with up to 50% 6 nylon. The $t_{\frac{1}{2}}$ versus temperature curves are approximately superposable by rescaling the temperature axis.

The results for copolymers containing up to 40% 66 nylon copolymerised with 6 nylon are shown in table 16 (page 84). These copolymers show a similar trend, with a temperature reduction as the comonomer content is increased. The $t_{\frac{1}{2}}$ versus temperature curves are shown in fig.16. Again, the curves are approximately superposable by

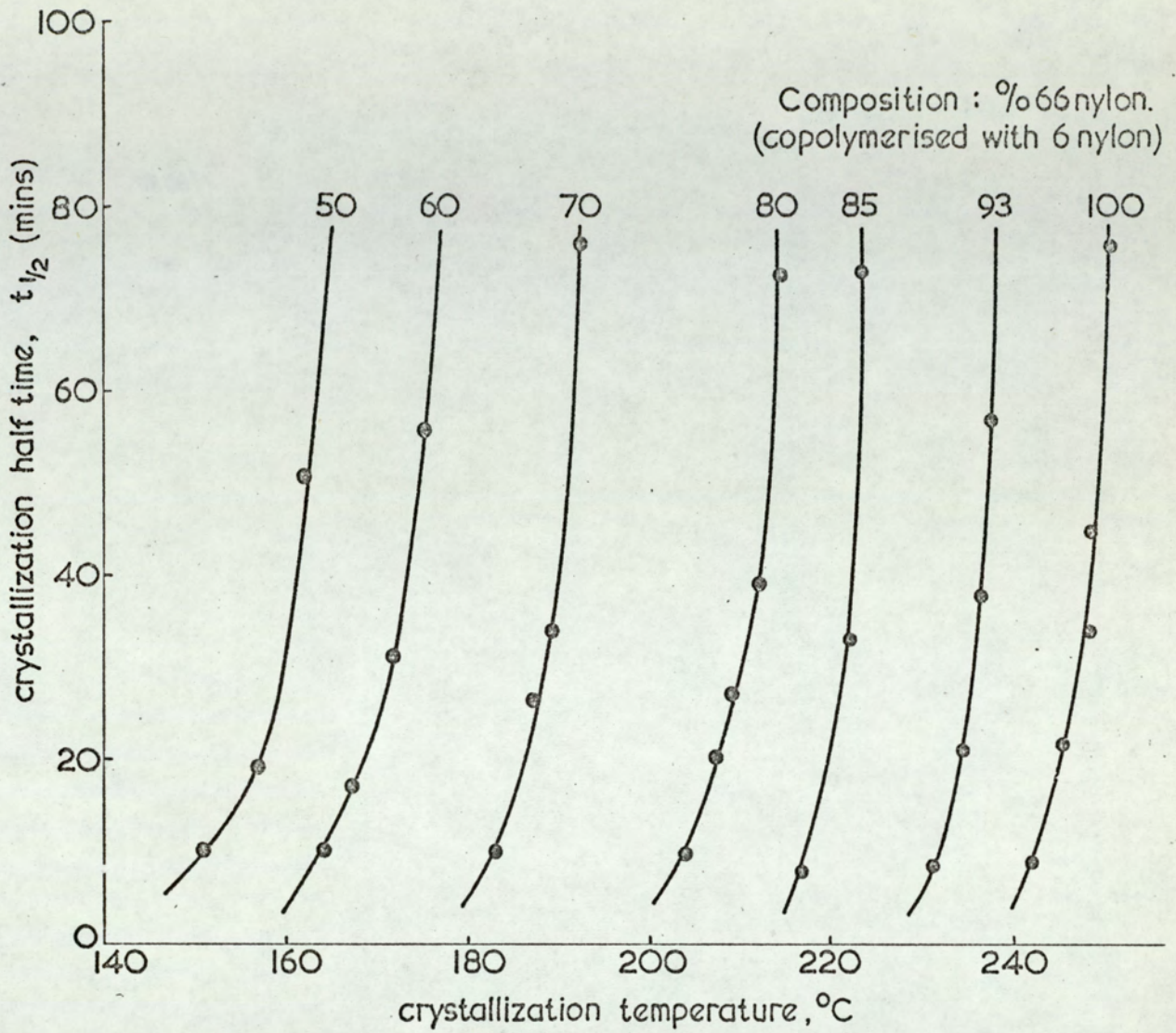


Fig.15 Crystallization half times at various temperatures, for 66 nylon and its copolymers with up to 50% 6 nylon.

Table 16. Crystallization measurements at various temperatures for 6 nylon and copolymers containing up to 40% 66 nylon in 6 nylon.

Code 30. 6 nylon. Melting pt. 221°C, melt condition 5min/250°C.

Temperature °C	t_i	$t_{\frac{1}{4}}$	$t_{\frac{1}{2}}$	$t_{\frac{3}{4}}$	t_f	times, min.
199.5	13.3	30.0	44.7	80.0	180	
198.2	8.6	18.7	24.7	36.7	94	
197.8	8.5	16.0	21.0	30.0	80	
197.5	5.3	11.3	16.0	30.0	80	
196.2	2.0	4.3	6.0	9.3	60	

Code 38, 90% 6 nylon, melting pt. 201°C, melt condition 5min/230°C

Temperature °C	t_i	$t_{\frac{1}{4}}$	$t_{\frac{1}{2}}$	$t_{\frac{3}{4}}$	t_f	times, min.
185.2	38.0	65.3	84.3	100	210	
182.5	14.6	24.7	31.3	43.0	150	
179.5	8.7	16.0	20.0	28.0	117	
177.0	4.7	8.0	10.0	14.0	60	
174.0	2.0	4.0	5.3	7.3	37	

Code 29, 85% 6 nylon, melting pt. 195°C, melt condition 5min/225°C

Temperature, °C	t_i	$t_{\frac{1}{4}}$	$t_{\frac{1}{2}}$	$t_{\frac{3}{4}}$	t_f	times, min.
176.8	23.3	39.0	49.0	69.0	160	
174.2	12.0	22.0	30.0	44.7	100	
173.8	10.0	19.2	24.0	34.7	100	
171.2	6.6	7.6	14.0	20.0	60	
167.6	3.3	5.3	7.6	14.0	50	

Code 28, 73% 6 nylon, melting pt. 179°C, melt condition 5min/220°C

Temperature °C	t_i	$t_{\frac{1}{4}}$	$t_{\frac{1}{2}}$	$t_{\frac{3}{4}}$	t_f	times, min.
157.0	13.3	21.0	27.3	36.0	100	
156.5	8.6	15.3	20.0	28.0	93	
153.5	4.7	9.3	12.0	18.0	70	
150.5	2.7	5.2	6.3	9.3	50	

Code 27, 60% 6 nylon, melting pt. 177°C, melt condition 5min/220°C

Temperature °C	t_i	$t_{\frac{1}{4}}$	$t_{\frac{1}{2}}$	$t_{\frac{3}{4}}$	t_f	times, min.
156.5	40.0	87.3	120	175	300	
155.2	16.0	29.6	38.6	55.3	260	
154.0	13.5	26.6	34.3	50.6	200	
150.8	8.3	15.3	18.7	26.0	120	
148.5	6.0	10.0	11.7	16.6	60	
146.0	2.7	4.3	5.3	7.3	60	

rescaling the temperature axis. (page 86).

Fig.17 (page 87) is a compiled graph ,taking temperatures by estimation from figs. 15 and 16, which would lead to values of the half crystallization time of 10 and 30 minutes. For comparison,the observed melting points are included in this graph.

An additional effect noticed with these copolymers concerned their relative birefringence values. 66 nylon is much less birefringent than 6 nylon under these conditions of crystallization. As the copolymer composition is increased by adding 6 nylon to 66 nylon,the total birefringence developing on crystallization is marginally reduced,reaching a minimum value at 40-50 % comonomer. As the 6 nylon content is increased further,from 50-100 %,the total birefringence increases markedly. It is not possible to obtain absolute values for birefringence with the present microscope,as measurements are obtained as depolarised light intensities. Measurements of birefringence or depolarised light intensity cannot be used for estimating the percentage crystallinity of a polymer without making allowances for the unit cell type.

For measurements of percentage crystallinity of copolymers, the density method was used. The values of the densities of the copolymers were shown in table 10 (page 68) and are shown in fig.18 (page 88) as a function of composition. The conversion of density into percentage crystallinity values may also be estimated by assuming a linear relationship between the reciprocal densities of the crystalline and amorphous fractions of the polymer. Miller (84) has given the relationship between crystalline and amorphous densities as

$$\frac{\alpha}{\rho_c} + \frac{1 - \alpha}{\rho_a} = \frac{1}{\rho}$$

where ρ_c, ρ_a are the crystalline and amorphous densities for the polymer, ρ is the measured density and α the percentage crystallinity.

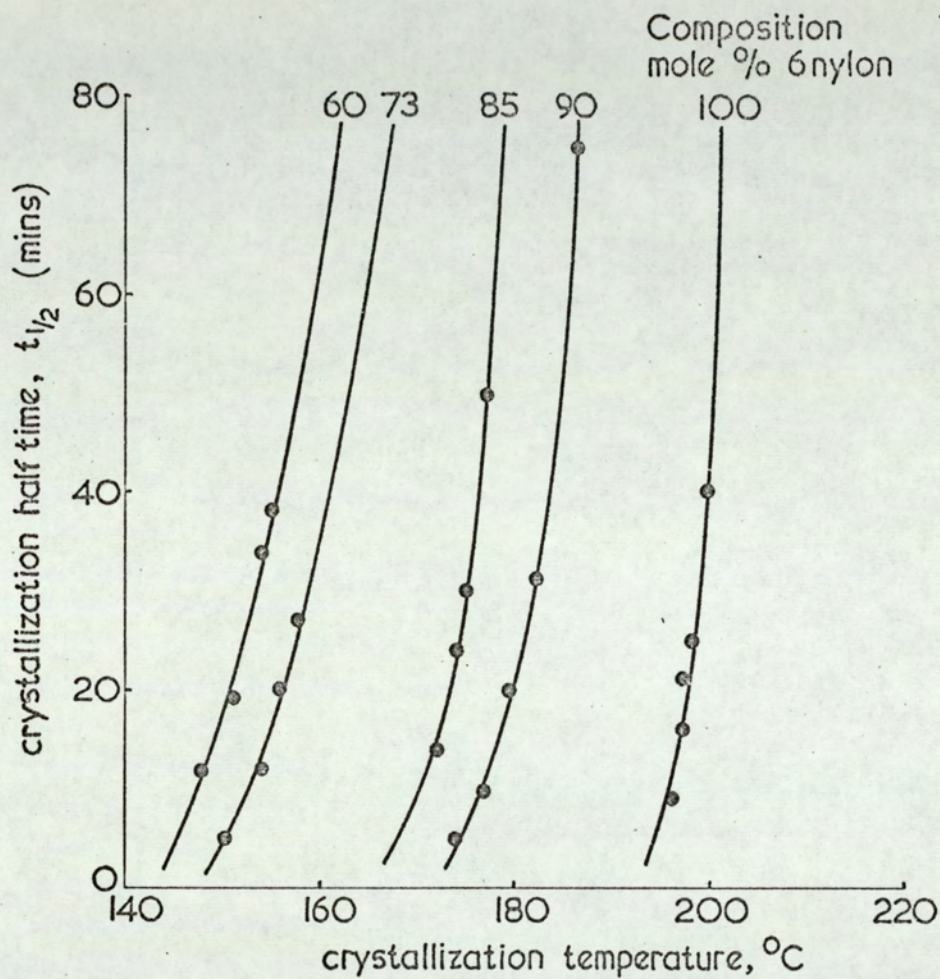


Fig.16. Crystallization half times at various temperatures, for 6 nylon and its copolymers with up to 40% 66 nylon.

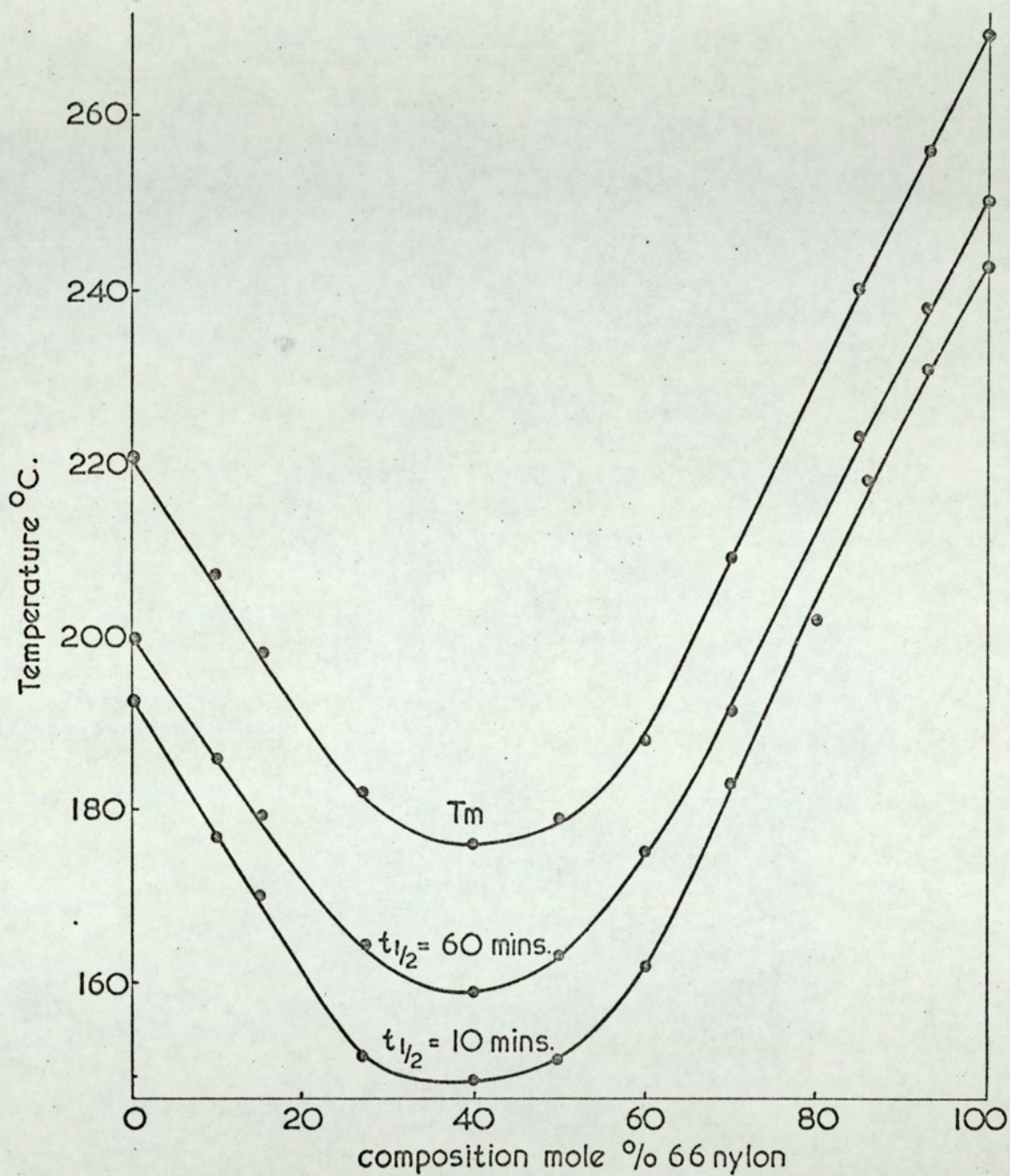


Fig.17. Temperatures for melting and certain crystallization rates for 66/6 copolyamides.

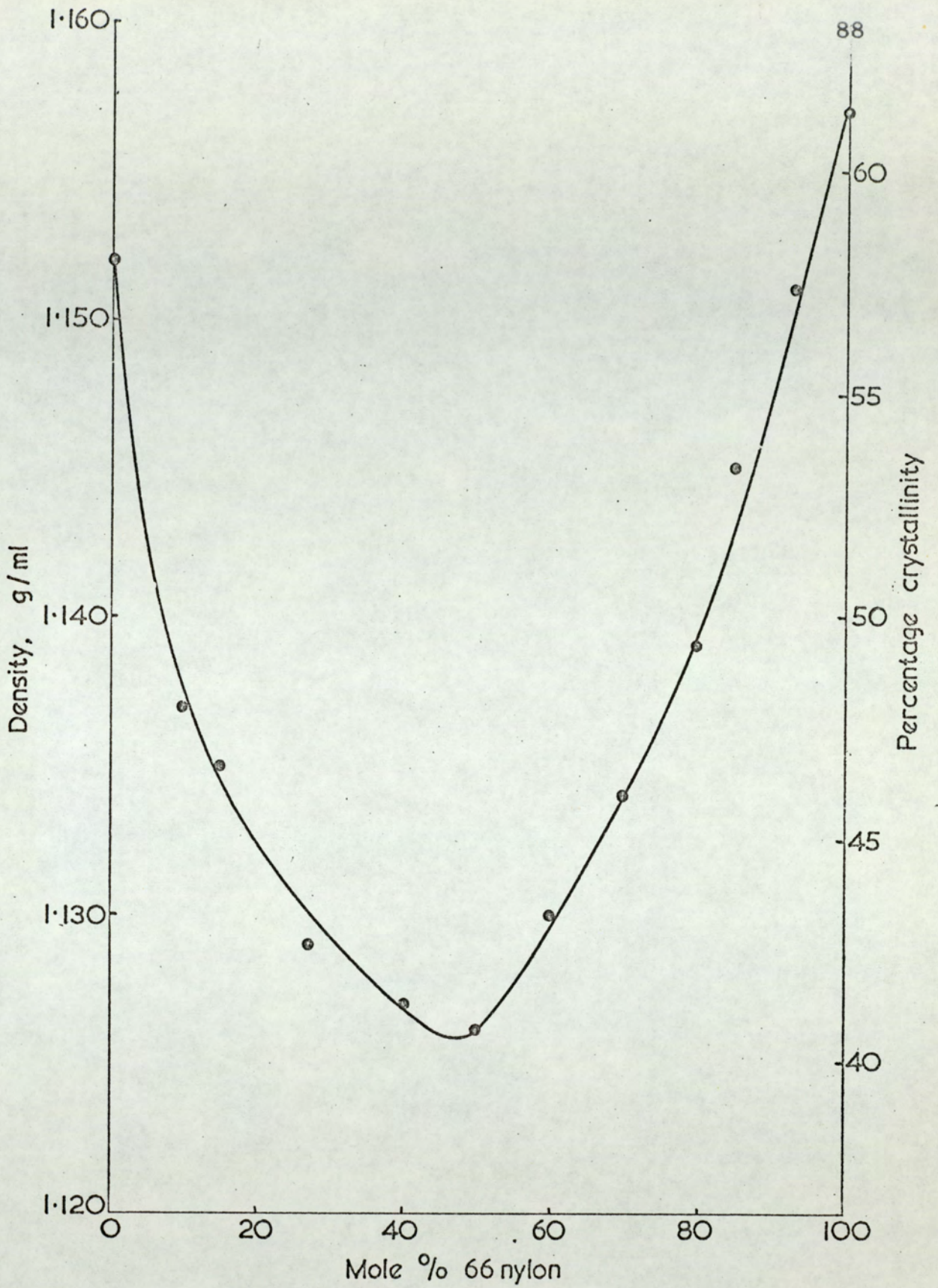


Fig.18. Densities and percentage crystallinities for 66/6 nylon copolymers.

For 66 nylon, Starkweather and Moynihan (85) gave the crystalline and amorphous densities as 1.22 and 1.069 g/ml respectively. For 6 nylon, similar values have been obtained (86) , with the crystalline and amorphous densities as 1.23 and 1.10 g/ml. The percentage crystallinities of the copolymers have been estimated by using the conversion equation (page 85), and have been inserted as an axis to fig.18.

Temperature-programmed crystallization.

In addition to the rates of crystallization determined under constant temperature conditions, a number of temperature-programmed curves were obtained for the 66/6 copolyamides.

The total depolarised light intensity signals have been corrected for film thickness using the expression of Binsbergen and deLange (44) (equation 1.3). In practice, it was convenient to use a film of 50 microns thickness for these studies, and the depolarised light intensities are therefore expressed for a 50 micron film. The results are shown in fig.19 (overleaf).

The shapes of the traces for the two homopolymers were found to be different. 6 nylon developed its birefringence over a narrower temperature range than 66 nylon, and the homopolymers also gave different shaped traces in the 250 - 180°C temperature range. In the lower temperature range of 180 - 60°C, where no signals can be detected using differential thermal analysis, birefringence changes in the polymers are observable.

A similarity between the behaviour of a copolymer and the homopolymer corresponding to the major ingredient can be seen, although the more highly copolymerised samples tended to show very lengthy temperature based crystallizations. As the comonomer content is increased, there is an increase in the recorded supercooling temperature; for these crystallizations the supercooling temperature has

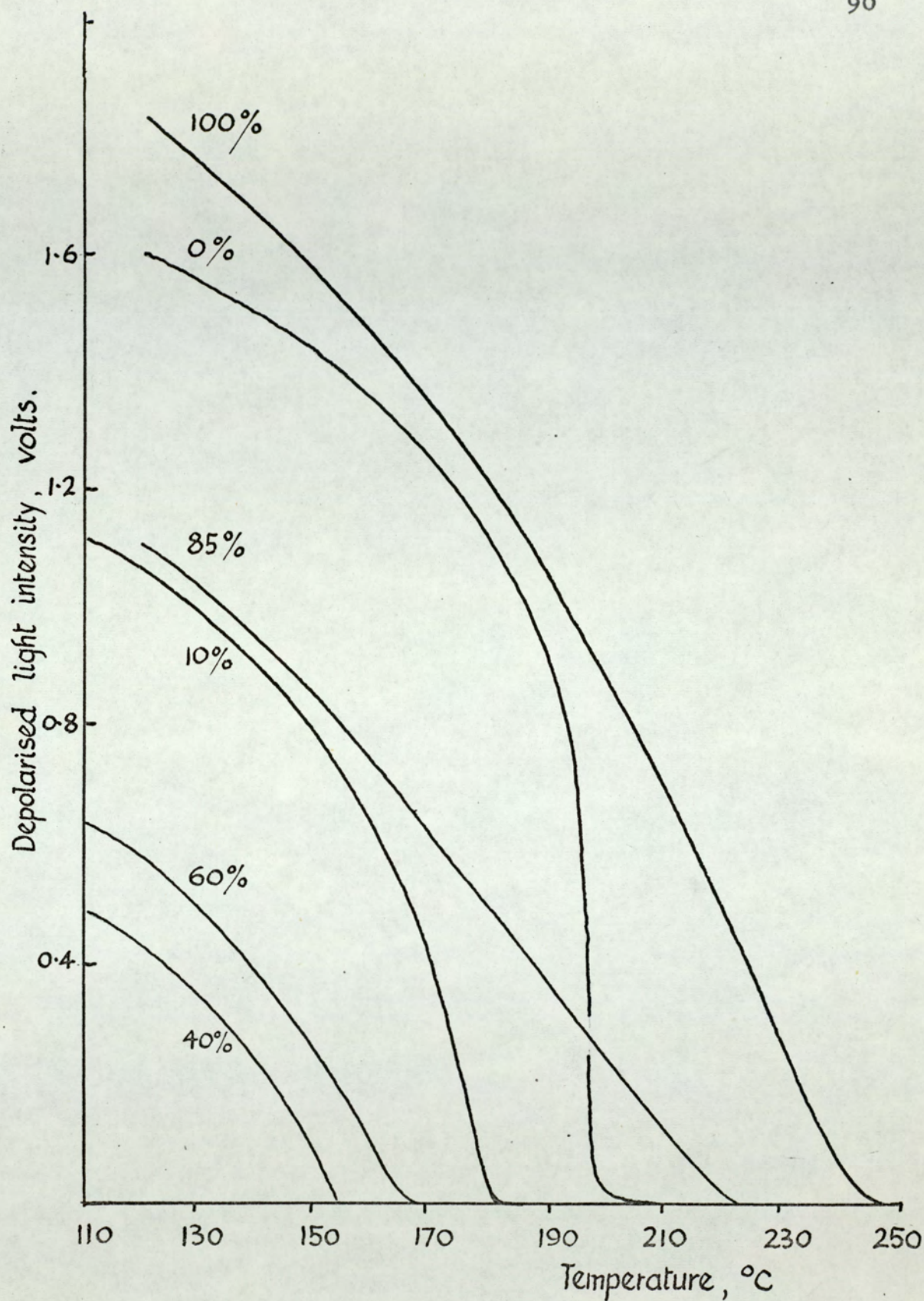


Fig.19. Temperature-programmed crystallization of 66/6 nylon and copolymers. Compositions as %66 nylon. Cooling rate, $2^{\circ}/\text{min}$ from $(T_m + 30)^{\circ}\text{C}$; D.L.I. signal corrected to 50μ film thickness.

been taken as $T_m - T_o$, where T_o is the temperature for the onset of crystallization during a programmed cool at $2^\circ/\text{min}$ from $T_m + 30^\circ\text{C}$.

The temperatures at which 25%, 50% and 75% of the overall depolarised light intensity had developed have been recorded. The onset temperature, T_o , and final temperature for completion of the crystallization process, T_f , have been noted. The results are shown in table 17.

Table 17. Programmed crystallization of 66 nylon, 6 nylon and 66/6 copolyamides. Cooling rate, $2^\circ/\text{min}$ from $T_m + 30^\circ\text{C}$. Temperatures of crystallization onset T_o , completion T_f , and fractional conversion $T_{\frac{1}{4}}$, $T_{\frac{1}{2}}$, $T_{\frac{3}{4}}$ from depolarised light intensity measurements.

% 66 nylon	100	85	60	50	40	27	15	0
code	XP.	25	31	25	27	28	29	30
T_o $^\circ\text{C}$	252	222	161	153	155	156	170	208
supercooling at T_o , ΔT $^\circ\text{C}$.	15	13	15	25	21	22	21	13
$T_{\frac{1}{4}}$ $^\circ\text{C}$	224	200	155	144	151	152	169	205
$T_{\frac{1}{2}}$ $^\circ\text{C}$	189	172	148	136	149	148	168	202
$T_{\frac{3}{4}}$ $^\circ\text{C}$	147	140	125	116	140	139	146	195
T_f $^\circ\text{C}$	80	80	50	40	90	90	80	140

These temperatures are not regarded as reproducible to better than $\pm 1^\circ\text{C}$, under the experimental conditions used, as there is an uncertainty temperature range required before the DuPont programmer can provide the controlled cooling. Also, it is not possible to cool the microscope stage at a rate faster than $2^\circ/\text{min}$ except at much higher temperatures. The programmed temperature results must therefore be regarded as inferior in accuracy to the isothermal crystallization data.

Copolymers of 66 nylon and 6.10 nylon with 6T nylon

A summary of the materials used for this section was given in tables 11 and 12 (pages 69,70).

Melting temperatures.

The measured melting points of the copolymers and homopolymers are shown in fig.20 (overleaf). These were obtained using the hot stage microscope with a programmed heating rate of $2^{\circ}\text{C}/\text{min}$ and the differential thermal analysis equipment (D.S.C.cell) with a $5^{\circ}/\text{min}$ programme. The samples had previously been crystallized by cooling at $5^{\circ}/\text{min}$ from 30° above T_m to 150°C .

In the 66/6T copolyamide series there is a steady increase in the temperature at which the last trace of birefringence disappears, as the comonomer content is increased, in agreement with the results of Edgar and Hill (29). With the D.T.A. peak temperatures, as the comonomer content is increased, there is a constant melting point recorded up to the 15% level of 6T, followed by an increase for the 20% copolymer, (fig.20). Whereas the disappearance of birefringence measures the melting point of the more perfect crystalline material, the peak of the DTA. trace measures an average melting point in the sample, and hence is lower. As the amount of comonomer is increased, the difference between these values is increased, showing a wider range of melting.

In the 6.10/6T nylon copolymers, a steady drop in the melting point is observed as the comonomer is introduced.

Rates of crystallization.

The rates of crystallization of the copolymers have been compared by using the half times for the processes, including secondary crystallization.

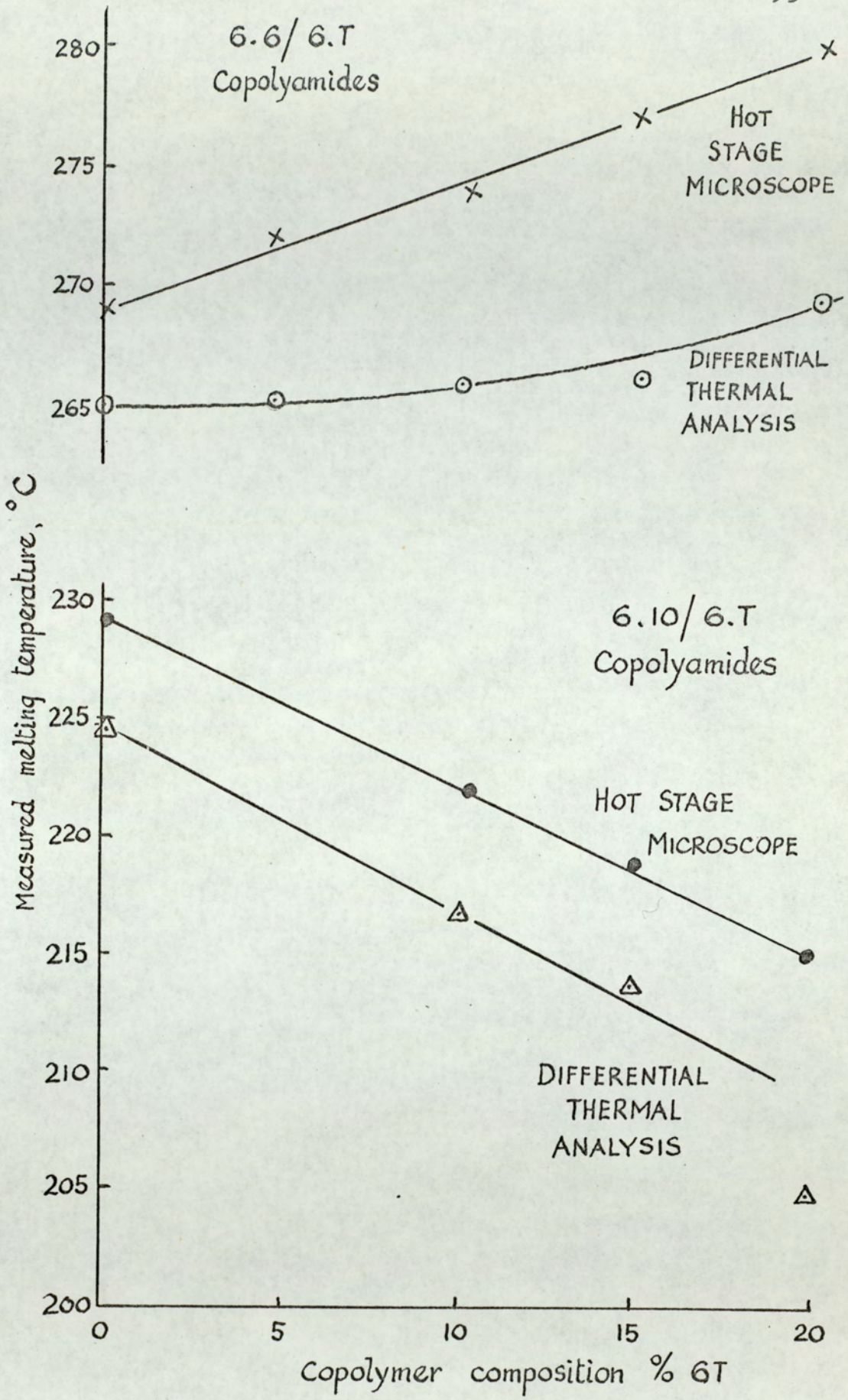


Fig.20. Melting point - composition data for 6.6/6T copolyamides and 6.10/6T copolyamides.

66/6T copolymers . These copolymers have melting points in a similar temperature range as the melting of 66 nylon. The same melting condition as was used for 66 nylon has been selected for these copolymers (i.e. 5mins/300°C). The effect of composition on the rates of crystallization of copolymers containing up to 20% 6T nylon with 66 nylon is shown in fig.21. (page 95).The results for the copolymers are also presented in table 18,together with t_1 , $t_{\frac{1}{4}}$, $t_{\frac{1}{2}}$, $t_{\frac{3}{4}}$ and t_f values. The supercooling temperatures , ΔT ,shown in table 18 have been obtained using programmed hot stage microscopy.

Table 18 Rates of crystallization of 66/6T copolyamides.

Melting condition,5 mins/300°C. Measurements at various temperatures T_c , (copolymers containing up to 20% 6T.).

2% 6T /98 % 66 nylon,code 55. Melting pt.270.5°C

T_c °C	ΔT °C	t_1	$t_{\frac{1}{4}}$	$t_{\frac{1}{2}}$	$t_{\frac{3}{4}}$	t_f min.
246.0	24.0	25.0	49.3	58.7	107	250
245.0	25.0	20.0	34.7	41.3	60	180
244.8	25.2	12.0	27.3	37.3	88	150
244.2	25.8	11.3	20.0	24.0	32	80

5% 6T /95% 66 nylon,code 47. Melting pt.272.0

T_c °C	ΔT °C	t_1	$t_{\frac{1}{4}}$	$t_{\frac{1}{2}}$	$t_{\frac{3}{4}}$	t_f min.
247.5	24.5	20.0	53.0	67.0	90	200
246.0	26.0	20.0	39.5	48.7	68.7	133
244.0	28.0	5.3	14.0	20.0	42	100
242.8	29.2	4.0	8.0	16.0	40	80

10% 6T /90% 66 nylon,code 43.Melting pt.274.0°C.

T_c °C	ΔT °C	t_1	$t_{\frac{1}{4}}$	$t_{\frac{1}{2}}$	$t_{\frac{3}{4}}$	t_f min.
247.0	27.0	14.0	42.0	53.0	73.0	200
246.5	27.5	10.0	27.0	40.0	60.0	180
245.8	28.2	9.0	26.0	35.0	48.0	100
244.5	29.5	8.7	18.0	22.7	29.3	60
240.2	33.8	2.3	5.0	6.6	14.0	60

Continuation of table 18; rates of crystallization of 66/6T nylon copolymers ; times of crystallization for various temperatures.

15% 6T nylon/85% 66 nylon, code 49. Melting point, 277.0°C

T_c °C	ΔT °C	t_i	$t_{\frac{1}{4}}$	$t_{\frac{1}{2}}$	$t_{\frac{3}{4}}$	t_f	min.
249.0	28.0	25.0	52.7	80.0	147	500	
248.0	29.0	20.0	43.3	58.7	93	250	
245.2	31.8	8.0	17.3	22.0	35	200	
243.2	33.8	8.0	14.0	17.7	27	100	
241.8	35.2	4.0	9.3	13.3	26	100	

20% 6T nylon/80% 66 nylon, code 50 .Melting point, 281 °C.

T_c	ΔT °C	t_i	$t_{\frac{1}{4}}$	$t_{\frac{1}{2}}$	$t_{\frac{3}{4}}$	t_f	min.
250.2	30.8	15.0	28.5	37.5	85	250	
248.0	33.0	10.0	20.0	28.0	73	360	
246.2	33.8	9.3	17.3	25.3	50	160	
245.5	35.5	4.0	10.0	14.0	27	130	
243.5	38.5	2.0	6.0	9.3	14.6	57	
242.0	39.0	2.0	4.0	5.0	10.0	30	

For 0%, 2%, 5%, 10% and 15% copolymers, the crystallization temperatures required to produce a certain $t_{\frac{1}{2}}$ value were closely comparable. For the 2% copolymer, these temperatures were lower than the temperatures for 66 nylon homopolymer:- for a 50 minute $t_{\frac{1}{2}}$ the copolymer crystallized at 2.5°C lower than the homopolymer, for a 30 minute $t_{\frac{1}{2}}$ this decrease was 1.5°C, whilst at 243°C nearly identical 15 minute $t_{\frac{1}{2}}$ values were observed (fig.21). The copolymer containing 15% 6T gave a $t_{\frac{1}{2}}$ versus temperature graph which was nearly superposable with the equivalent graph for 66 nylon homopolymer, although the melting point of this copolymer was found to be 9°C higher than 66 nylon. The 20% copolymer behaved significantly different, with higher melting and crystallization temperatures than 66 nylon.

Fig.22 (overleaf) shows the effect of supercooling temperature

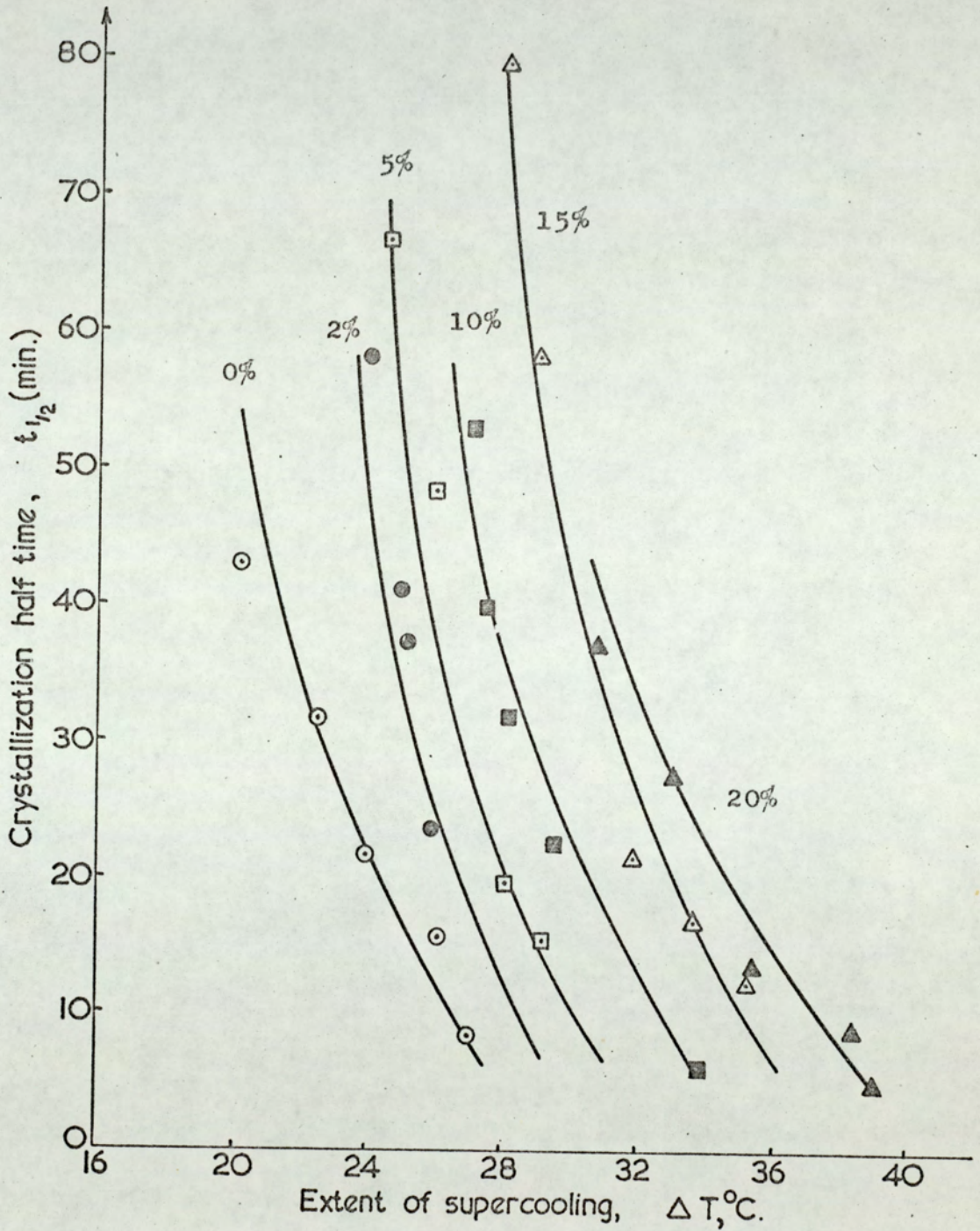


Fig.22. 66/6T copolymers, rates of crystallization as a function of supercooling temperature. Compositions shown as % 6T.

on the $t_{\frac{1}{2}}$ values for the 66/6T copolyamides. A substantial increase in the supercooling temperature was observed as the comonomer content was increased. For a 30 minute crystallization, the supercooling increased from 22°C for 66 nylon to 28°C for the 10% copolymer and to 33°C for the 20% copolymer. Fig.22 shows the half time of crystallization versus supercooling temperature. The curves appear to be approximately parallel in the range studied.

6.10/6T copolymers. Table 19 (overleaf) shows the effect of composition on the rates of crystallization of 6.10 nylon and copolymers containing up to 20% 6T nylon. The spherulites observed for the 20% copolymer were very low in birefringence, and the depolarised light intensity signals were only slightly greater than the 'stray light' intensity which arises through transmitted light in crossed Nicol prisms. It was difficult to study the crystallization of this copolymer using the hot stage microscope apparatus. Edgar and Hill (29) gave the 20% copolymer composition as the minimum in the melting point graph, indicating that this is the least crystalline copolymer in the 6.10/6T copolyamide series.

Fig.23 (page 100) shows the observed $t_{\frac{1}{2}}$ values for various crystallization temperatures for 6.10 nylon and the three copolymers of 6.10/6T nylon. The crystallization temperatures were found to show the normal behaviour when co-crystallization does not occur, as was noticed with the 66/6 nylon copolymers. In the 6.10 series, the supercooling temperature for a 30 minute $t_{\frac{1}{2}}$ value was found to be 16.5°C for the homopolymer, 18.5°C for the 10% copolymer and 20°C for the 20% copolymer. These supercooling temperatures are rather low by comparison with 66 nylon, and also show a smaller increase with copolymerisation than was observed for the 66/6T copolymers.

Table 19. Rates of crystallization of 6.10/6T nylon copolymers.

Melting condition, 5min/275°C. Crystallization times for various temperatures and supercooling temperatures.

6.10 nylon homopolymer, code 61. Melting point, 230°C

Tc °C	ΔT °C	t_i	$t_{\frac{1}{4}}$	$t_{\frac{1}{2}}$	$t_{\frac{3}{4}}$	t_f	mins.
215.0	15.0	47.0	133	177	210	600	
214.0	16.0	20.0	40.0	60.0	85.0	250	
213.2	16.8	13.3	27.0	35.3	53.0	160	
211.0	19.0	5.0	13.3	18.7	24.0	120	
208.0	22.0	2.7	6.7	8.7	11.3	37	

10% 6T nylon/ 90% 6.10 nylon, code 62. Melting point, 222°C

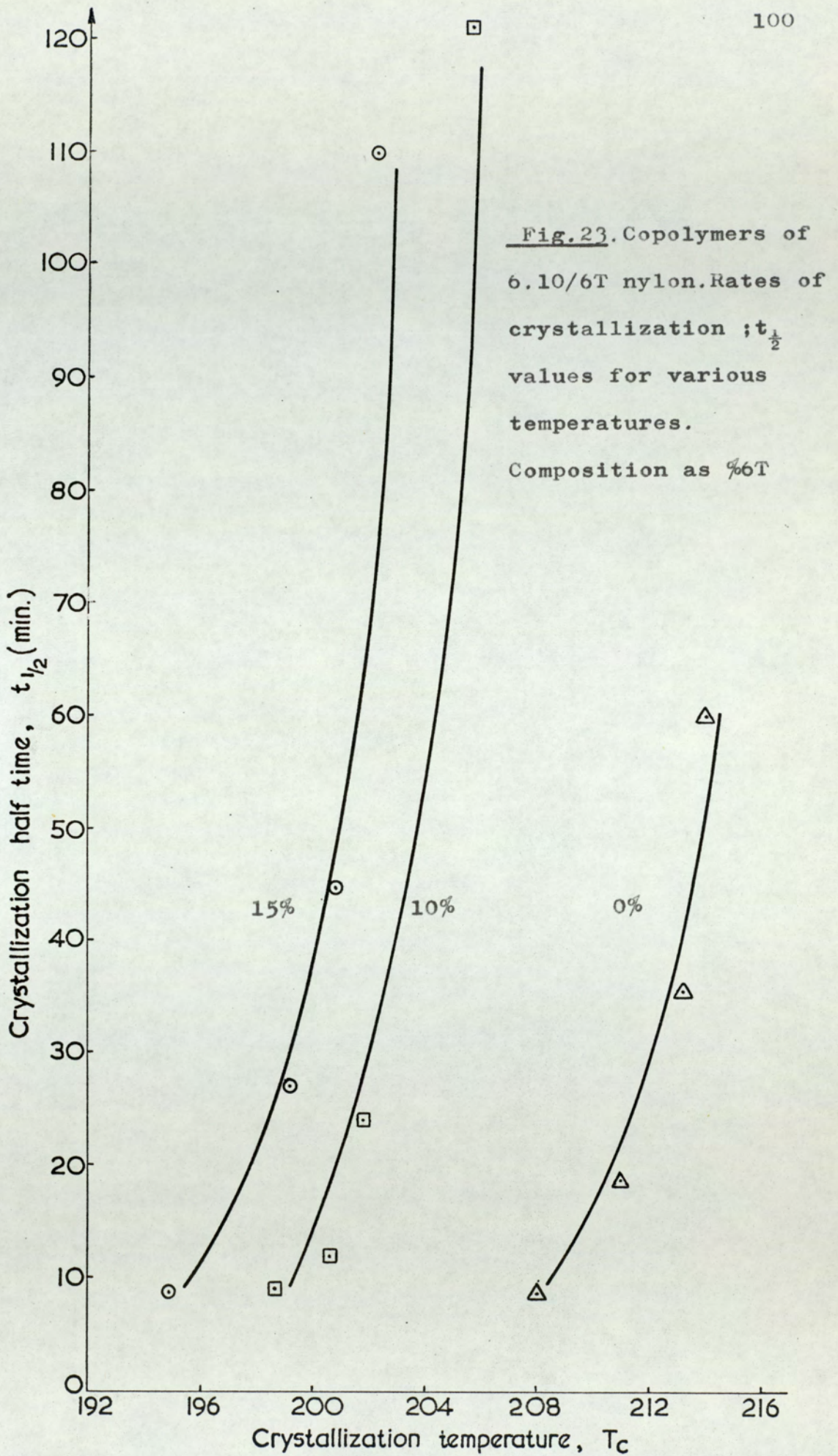
Tc °C	ΔT °C	t_i	$t_{\frac{1}{4}}$	$t_{\frac{1}{2}}$	$t_{\frac{3}{4}}$	t_f	mins.
205.5	16.5	26.5	88.0	121	220	600	
201.8	20.2	5.0	16.3	22.0	34.7	200	
200.5	21.5	4.7	9.7	12.0	16.7	60	
198.5	23.5	4.0	7.0	9.3	12.0	45	
196.0	26.0	2.0	4.7	6.0	8.9	40	

15% 6T nylon/ 85% 6.10 nylon, code 67. Melting point, 219°C.

Tc °C	ΔT °C	t_i	$t_{\frac{1}{4}}$	$t_{\frac{1}{2}}$	$t_{\frac{3}{4}}$	t_f	mins.
202.2	16.8	40.0	93.0	110	133	400	
200.8	18.2	14.0	38.0	45.0	60	150	
199.2	19.8	13.3	22.7	26.6	32	60	
196.8	22.2	6.6	13.0	15.3	18.7	40	
194.8	24.2	3.3	7.3	9.0	12.5	40	

20% 6T nylon/ 80% 6.10 nylon, code 69. Melting point, 215°C

Tc °C	ΔT °C	t_i	$t_{\frac{1}{4}}$	$t_{\frac{1}{2}}$	$t_{\frac{3}{4}}$	t_f	mins.
195.9	19.1	2.7	9.0	15.3	33.7	73	
185.5	29.5	1.3	3.3	5.3	14.7	80	



Heats of fusion of copolymers containing 6T nylon.

In order to obtain a measure of the relative crystallinity changes which are brought about by 6T copolymerisation, the heats of fusion of the copolymers were measured. A weighed sample, up to 10mg. was crystallized under nitrogen by cooling the melt at $5^{\circ}/\text{min}$ to 60° below the melting temperature, using the DuPont DSC cell. The sample was then heated at $5^{\circ}/\text{min}$. in the cell, using the standard conditions for heats of fusion determination, and the melting endotherm was recorded accurately. The area under the melting peak was obtained from the Disc integrator attachment to the Honeywell recorder, as described in Chapter 2. (page 56). The copolymer heats of fusion were obtained by comparing these areas with the calibration areas using pure metals. Repeated fusion of a single polymer sample led to reduced values for the heat of fusion, and this was attributed to oxidation of the material. Samples of the copolymers were also annealed under nitrogen in test tubes, using the fluidised sand bath to produce a controlled temperature. The results of these experiments are shown in table 20 (overleaf). The annealing conditions were selected as 5 hours at approximately $T_m - 25^{\circ}\text{C}$, and were 5 hours at 245°C for the 66/6T copolymers and 5 hours at 200°C for the 6.10/6T copolymers.

Multiple melting endotherms were encountered with the annealed polymers in this series. For calculation of the heats of fusion, the total endothermic contribution has been included. The observations of Hybart and Platt (39) and others on the changes in the D.T.A. melting endotherms of 66 nylon appeared to apply equally to the 66/6T copolymers.

The annealing results (table 20) show that 66/6T nylon copolymers undergo a substantial crystalline perfection process on annealing. The extent of the perfection depends upon composition; for 15%

and 20% 6T/66 copolymers the heats of fusion approximately doubled by 5 hours annealing at 245°C, whereas 66 nylon homopolymer increased from 19.3 to 25 cal/g. only. An anomalous result appeared in the 6.10/6T copolymer series, where much smaller increases in the heats of fusion were noticed in the annealing processes. The 20% 6T/6.10 copolymer gave a large increase in the annealing process. As this copolymer was annealed at a temperature very close to its melting point, a separate sample was annealed at a lower temperature (5 hours at 185°C). This still gave a high heat of fusion (11.0 cal/g). The remaining 6.10/6T copolymers have heats of fusion which fall much more significantly as the copolymer composition is increased, and show only a small recovery of the lost crystallinity on annealing.

Table 20. Heats of fusion of 66/6T copolyamides and 6.10/6T copolymers

66/6T.copolymers.						
%6T nylon	0	5	10	15	20	
Peak temperature	267	265	266	267	268	°C
Heat of fusion (un-annealed)	19.3	17.7	12.6	9.4	7.0	cal/g
Heat of fusion (annealed)	25.1	22.5	20.2	18.3	15.5	cal/g
6.10/ 6T copolymers.						
% 6T nylon	0	10	15	20		
Peak temperature	221	217	214	205		°C
Heat of fusion (un-annealed)	18.9	12.1	7.8	4.6		cal/g
Heat of fusion (annealed)	22.9	15.1	10.8	11.3		cal/g

Branched /cross-linked 66 nylon copolymers (66/6X copolyamides).

A summary of the branched 66/6X copolymers was given in table 13 (page 69) . For this section, it is appropriate to make a comparison between the melting points, crystallization rates and fusion data of copolymers of 66 nylon with 1-3% 6X nylon and 66 nylon copolymerised with 3 or 7 % 6 nylon.

Melting temperatures. The melting points of the materials were determined by heating a thin film on the microscope, with a programmed heating rate of 2°/min, or in the D.S.C. cell with a 5°/min. programme. The results are shown in table 21.

Table 21. Melting points of copolymers of 66 nylon with 6X nylon and 6 nylon.

Comonomer	--- 66 nylon	6X nylon			6 nylon	
		1	2	3	3	7
Melting pt, microscopy °C	269	267½	265	263½	263½	256
Melting pt, D.T.A. °C	265	262	259	257	260	253

The optical melting points correspond to the melting of the more perfect parts, and measurements by this technique show that 3% 6X and 3% 6 nylon copolymers have the same melting points. Branching therefore resulted in no additional loss of melting point in the more perfect regions. However, the melting range of the branched copolymers is increased, as is shown by the D.T.A. peak temperatures. At the 3% comonomer level, branched nylon has a 3° lower average melting point than the equivalent unbranched copolymer.

Rates of crystallization of branched nylon.

The depolarised light intensity traces for the 3%6X copolymer and the 3% 6 nylon copolymer are shown in fig. 24 (overleaf). For a certain $t_{\frac{1}{2}}$ value, cross linked nylon required a significantly larger

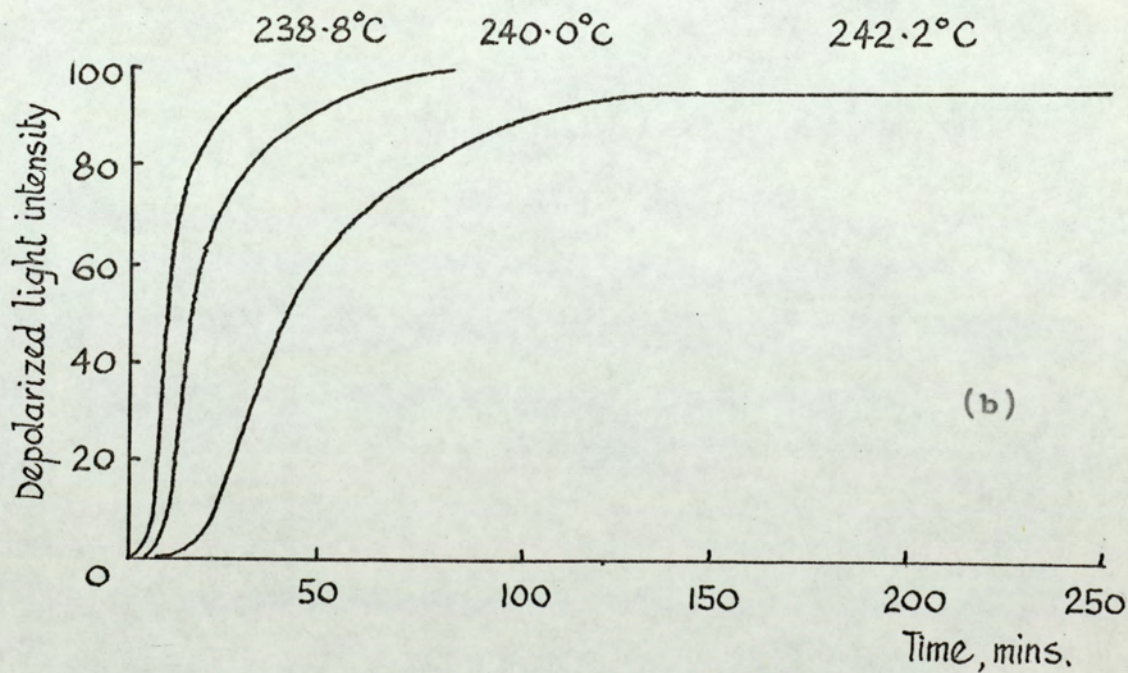
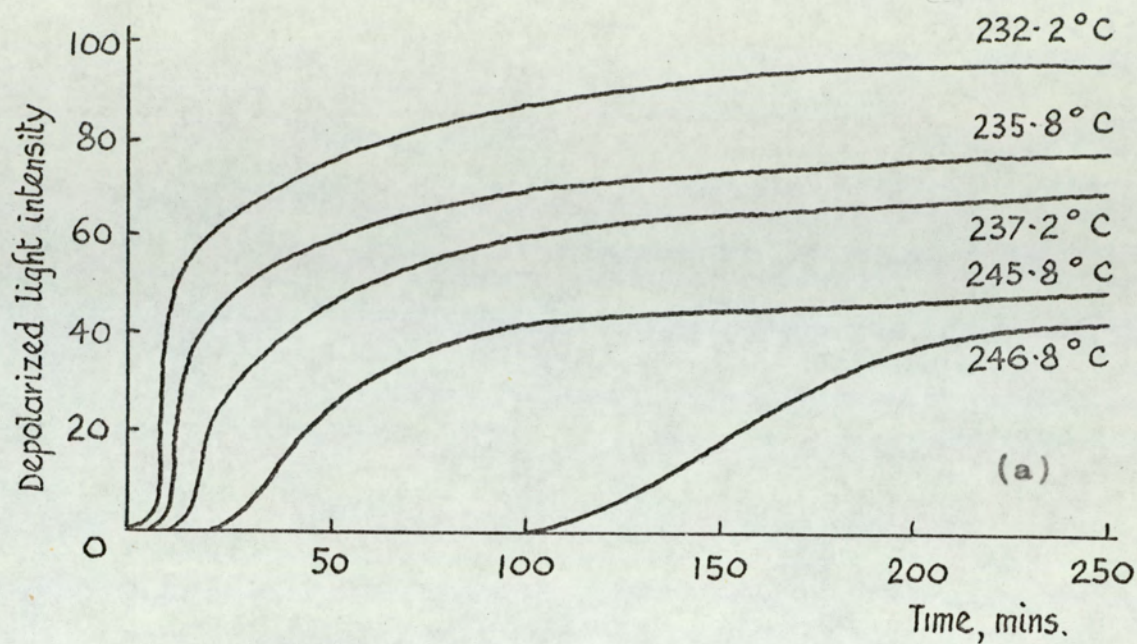


Fig.24. Depolarised light intensity curves for the isothermal crystallization of 66 nylon copolymers (a) 3% 6X nylon copolymer (b) 3% 6 nylon copolymer.

supercooling temperature, and the measured supercooling temperatures for branched nylon increased as the 6X content was increased. The complete crystallization results for the 6X copolymers are given in table 22, and these values may be compared with the rates of crystallization of copolymers of 66 nylon with 3 and 7% 6 nylon, which were included in table 15 (page 81).

Table 22. Crystallization of branched 66 nylon, 6X/66 copolymers.

Crystallization times for various temperatures, T_c , and supercooling temperatures, ΔT .

1% 6X/99% 66 nylon, code 53.

$T_c, ^\circ C$	$\Delta T ^\circ C$	t_i	$t_{\frac{1}{4}}$	$t_{\frac{1}{2}}$	$t_{\frac{3}{4}}$	t_f mins
246.8	20.7	66.0	97.0	130	165	420
245.5	22.0	45.0	79.0	95	126	400
243.5	24.0	8.5	15.0	22.5	75	250
241.5	26.0	7.5	10.5	16.0	90	250
240.0	27.5	3.7	7.5	9.0	33	240
236.0	31.5	1.5	2.0	3.7	27	180

2% 6X / 98 % 66 nylon, code 54 .

$T_c ^\circ C$	$\Delta T ^\circ C$	t_i	$t_{\frac{1}{4}}$	$t_{\frac{1}{2}}$	$t_{\frac{3}{4}}$	t_f mins.
242.8	22.2	28.5	64.5	119	200	500
241.5	23.5	13.5	25.5	43.5	165	760
239.2	25.8	7.5	13.5	22.5	180	600
238.2	26.8	4.0	8.5	10.8	120	400
236.2	28.8	2.5	5.5	7.0	50	200
232.5	32.5	0.6	1.5	3.5	26	120

3% 6X / 97 % 66 nylon, code 52.

$T_c ^\circ C$	$\Delta T ^\circ C$	t_i	$t_{\frac{1}{4}}$	$t_{\frac{1}{2}}$	$t_{\frac{3}{4}}$	t_f mins.
237.2	26.3	9.5	21.0	75	400	-
235.8	27.7	7.5	15.5	31.5	198	600
234.0	29.5	4.5	9.7	15.0	85	390
232.2	31.3	3.0	5.2	8.2	53	330

It was not possible to study copolymers containing more than 3% trimesic acid as their melt viscosities were too high to allow the polymers to be pressed into films without incurring decomposition.

The $t_{\frac{1}{2}}$ versus temperature curves for these copolymers are shown in fig.25 (overleaf). Nearly parallel curves resulted, although the crystallization takes place at high supercooling temperatures. The total times of crystallization are also lengthy, due to a slow secondary process.

Heats of fusion of branched nylon copolymers.

Measurements were made using the D.S.C. cell, with similar experimental conditions to those used for the 6T measurements. The results are shown in table 23.

Table 23. Heats of fusion of 66/6X copolymers and some 66/6 copolyamides.

Comonomer	-	6X nylon			6 nylon		
Mole% comonomer	0	1	2	3	3	7	15
Code	32	53	54	52	63	26	25
Heat of fusion, cal/g.	19.3	13.6	10.8	8.6	14.4	12.4	11.2

The effect of copolymerising 6X with 66 nylon resulted in a more pronounced loss in the heat of fusion than was obtained for the 66/6 copolymers. The crystalline state is less readily entered by the branched copolymers, and the heats of fusion may be considered to indicate a significant loss in the percentage crystallinity.

No measurements have been made on annealed samples of 6X/66 copolymers.

The melting of various forms of nylon.

This is a section of miscellaneous results on the fusion of 66 nylon and the copolymers used in the crystallization studies. For optical microscopy, programmed heating rates of 2°/min. have normally

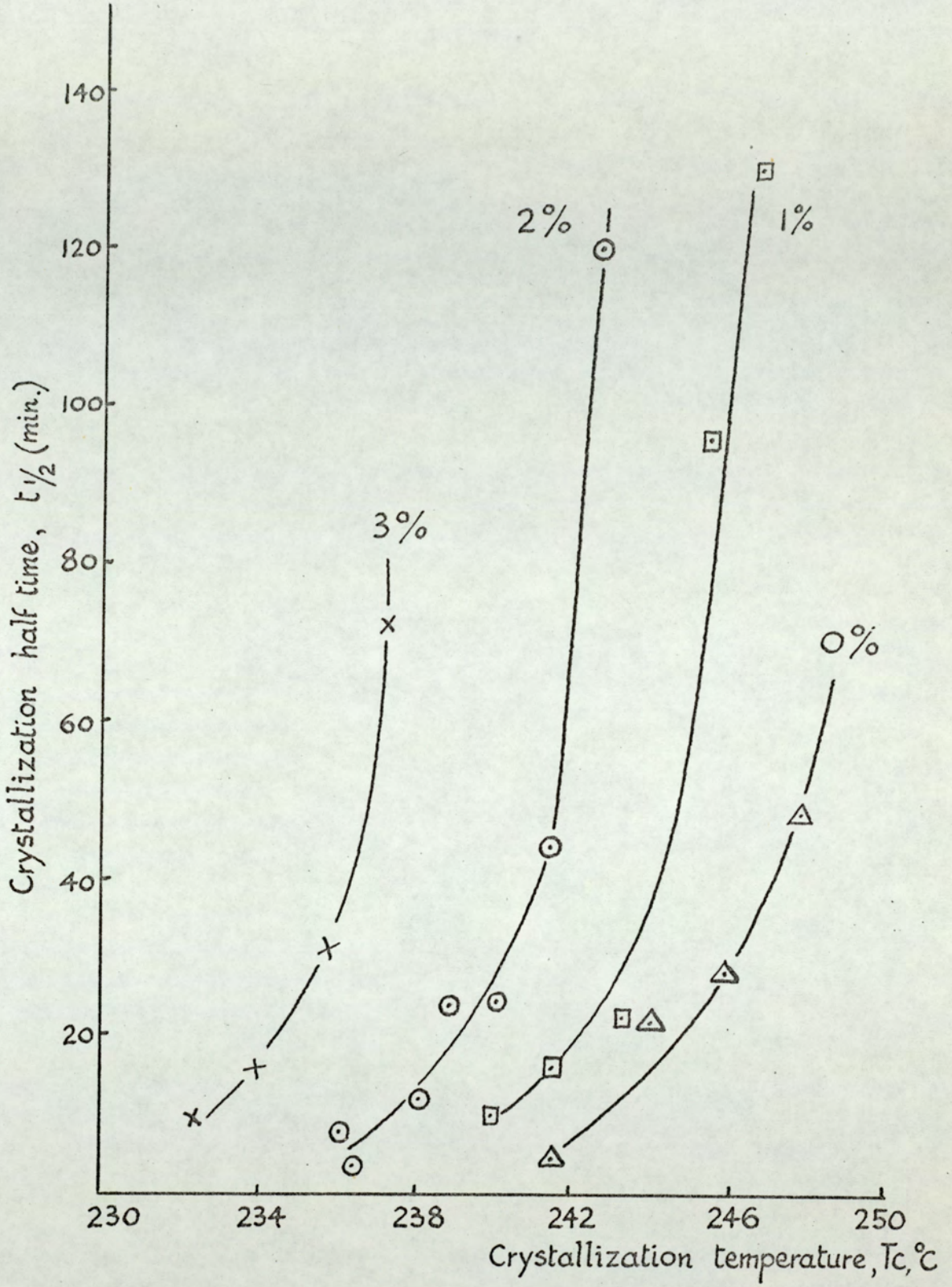


Fig.25. Rates of crystallization of 66/6X nylon copolymers, showing $t_{\frac{1}{2}}$ values for various temperatures. Compositions shown as % 6X in copolymer.

been used. For differential thermal analysis, the D.S.C cell in a $5^{\circ}/\text{min}$ heating programme has formed the basic condition, as slower programming leads to small peaks and irregularities due to inaccurate programming.

Depolarised light intensity observations. The melting of 66 nylon, sample XP 10257, using optical depolarised light intensity is shown in fig.26, overleaf, for three forms of the polymer. Sample A consists mainly of highly crystalline single crystals, obtained from slowly crystallizing a 1% solution of 66 nylon in butane diol. The onset of melting temperature is high, with practically no loss of birefringence below 160°C , followed by a section ($257-263^{\circ}\text{C}$) where melting is sharp. The comparatively low melting point is thought to be attributable to residues of butane diol, which are very difficult to remove completely from the crystals. B and C are samples of commercial 66 nylon crystallized from the melt using rapid and slow conditions of crystallization. The rapidly crystallized sample (B) has a wide melting range, commencing at about 85°C ; melting takes place in the range $85-268^{\circ}\text{C}$, but there is a large loss of birefringence in the range $257-268^{\circ}\text{C}$. The slowly crystallized sample (C) has a comparatively large loss of birefringence over the temperature range $30-250^{\circ}\text{C}$ and the intensities of the spherulites' Maltese cross patterns decrease in this process. Experiments on heating and cooling 66 nylon at the same programmed rate of $2^{\circ}/\text{min}$, showed that the gain and loss of birefringence in the $25-200^{\circ}\text{C}$ range is reversible with temperature. The slowly crystallized polymer finally entered the fully molten state in the range $263-269^{\circ}\text{C}$. Visually, the destruction of spherulites takes place in this process. There is a very small D.L.I. signal change after melting has been completed, due to the slow response of the photocell in attaining a baseline. Fig.26 shows an extrapolation of baselines to allow for this.

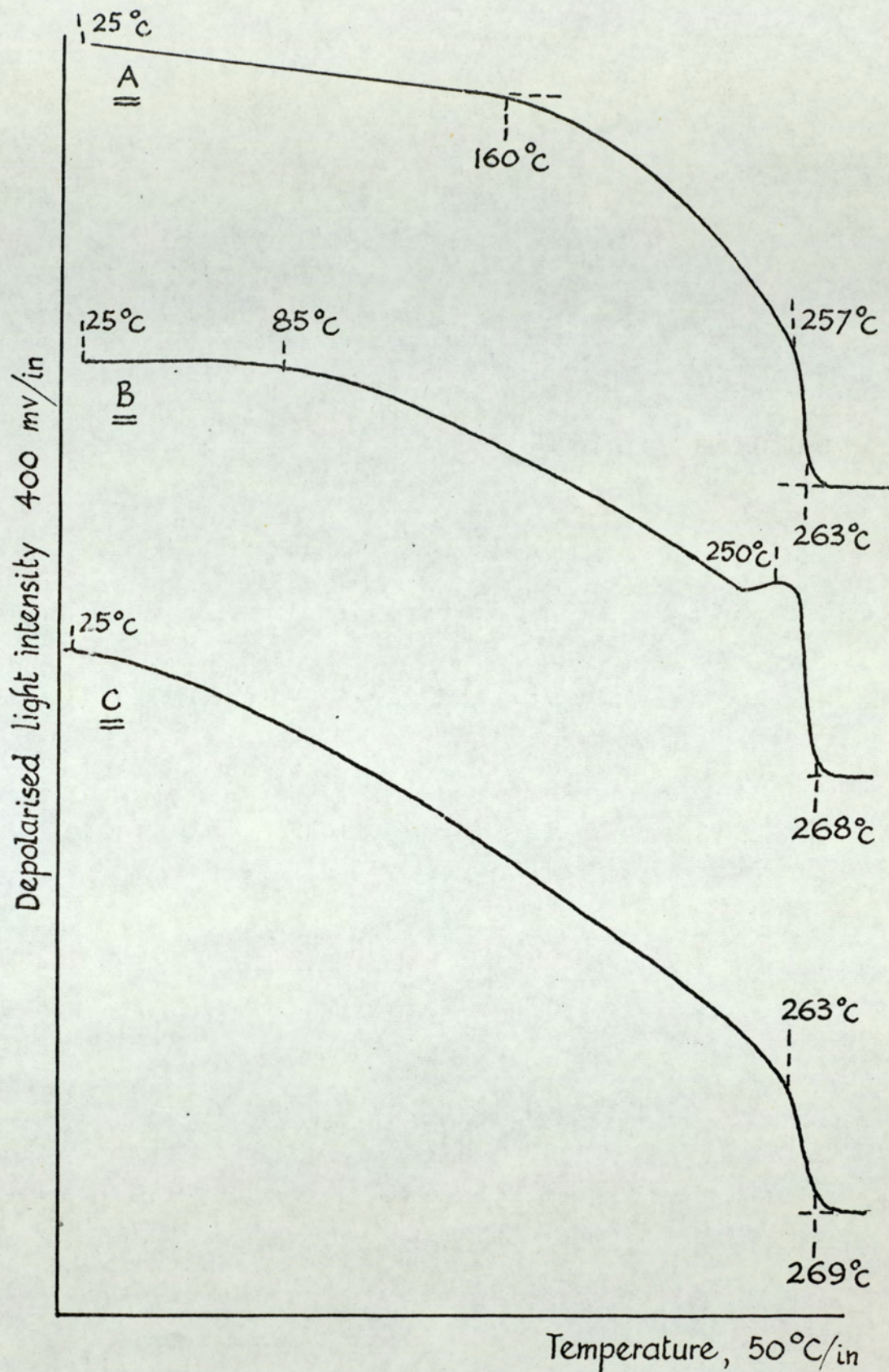


Fig.26. The melting of various forms of 66 nylon. A. Solution crystallized , B. Sample crystallized rapidly from a melt, C. Sample crystallized slowly from a melt. (2°/min. cooling.)

In a further investigation of the annealing of 66 nylon, a film of XP 10257 was crystallized by cooling the melt at 5°/min. from 290°C to 242°C. This sample was then held at 242°C for 14 hours. Table 24 gives the depolarised light intensity readings for the sample in this period. Owing to the lengthy time scale, these results will be discussed on a logarithmic time basis, and the logarithmic times have been inserted in table 24.

Table 24. Annealing of 66 nylon (XP 10257): depolarised light intensity changes as a function of time. Annealing temperature, 242°C.

Annealing time, min	0	5	10	30	75	14hrs.
Log (annealing time)	-	0.7	1.0	1.5	1.9	2.9
D.L.I. photocell mV	260	280	300	320	352	392
Increase in D.L.I., %	-	7.7	15.4	23.0	35.3	50.8

The depolarised light intensity traces for 66 yarn are shown in fig.27. Three samples of yarn were available for this study; two samples of high tenacity tyre cord, and a sample of normal yarn. The traces resulting from the three samples are very similar. The most significant feature of yarn is the high temperature for the onset of melting; fig.27 shows that this varied between 212 and 236°C depending upon the yarn sample, but this is significantly higher than the equivalent results for the melt crystallized samples shown in fig.26. In the melting process, there is initially a loss of birefringence, which is observed as a loss in colour. At 255°C the normal yarn appears to have low ordered birefringence, and this temperature corresponds approximately to the completion of the early D.T.A. peak (39). The main melting process follows this. With the present hot stage microscope the yarn is oxidised immediately after melting, so preventing optical

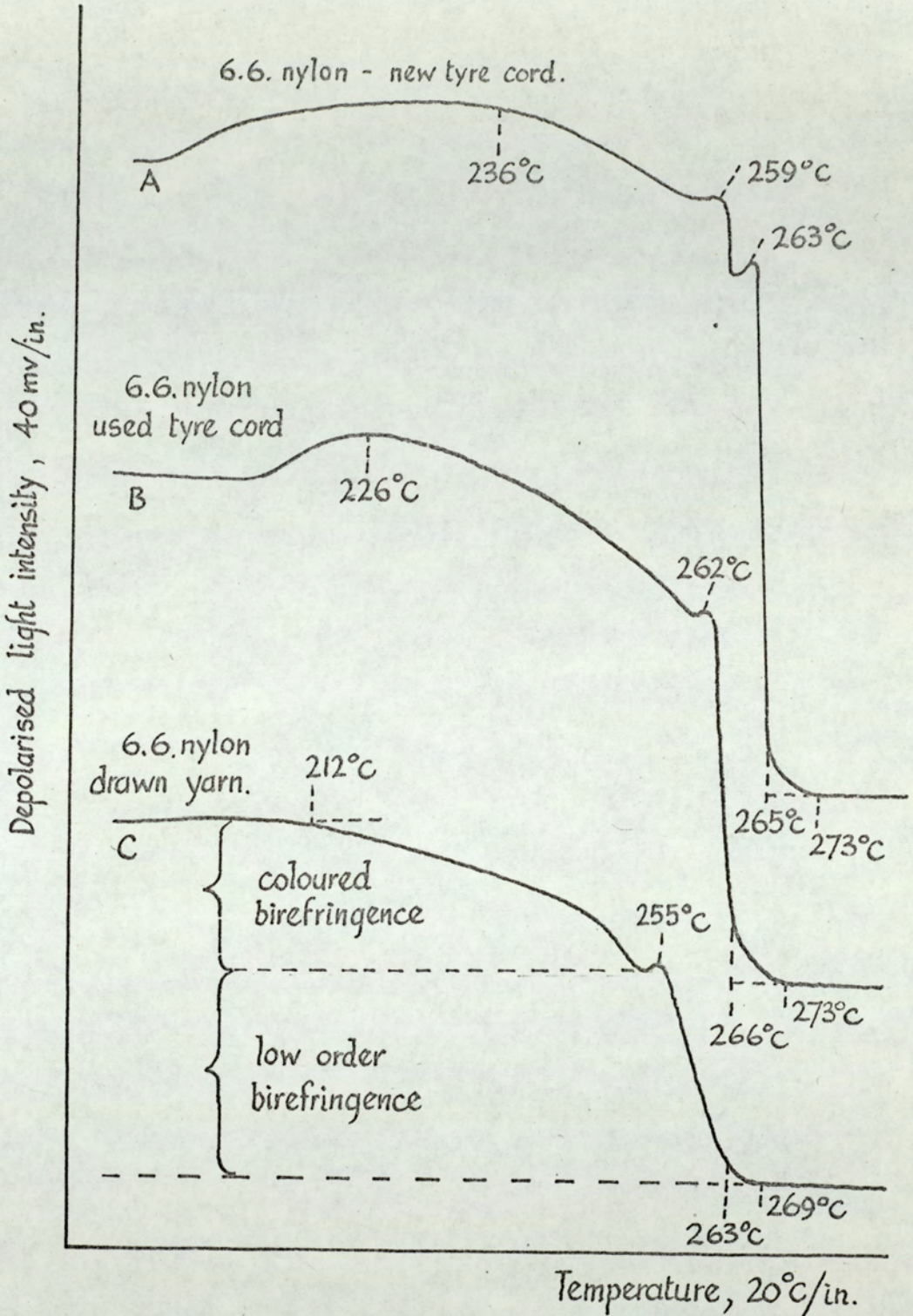


Fig. 27. Melting of 66 nylon yarn. Sample heated at 2°/min.

measurements of recrystallization. The melting of yarn was found to be complete at 263-266°C, although fig.27 shows that the baseline is not attained immediately, and the trace has been interpreted by extrapolating the lines. Tyre cord appeared to have a slightly higher melting point, and a sharper melting process. An interesting feature of the yarn graphs is the small peak occurring at 255° for normal yarn and 263° for tyre cord. This appears to be caused by the collapse of the rigidity of the yarn, which brings a larger area of sample into effective focus on the microscope. The precise shape of the peak is surprisingly consistent, however, and this may warrant further investigation.

Differential thermal analysis observations.

The shapes of the D.T.A melting endotherms for 66 nylon and the copolymers show some interesting features. Four examples of these are shown in fig.28, overleaf.

Fig.28A shows the normal trace for the laboratory polymer sample, with melting peaks at 255°C and 267°C. If commercial polymer or very rapidly crystallized samples of laboratory polymer were taken, the 255° peak was not noticed, but the 267° peak appeared in the same form as for the more slowly crystallized sample. This similarity of behaviour is explained on the basis that commercial polymer as supplied had been quenched after melt extrusion, whereas the laboratory sample of polymer had been crystallized at 2°/min from the melt.

The melting endotherm depends upon the crystallization conditions. Fig.28 B illustrates the remelting of 66 nylon which had been crystallized slowly at a rate of $\frac{1}{2}$ °/min. The 261° peak has become larger, and covers a wider temperature range, but the 267° peak has not been altered by the process. These observations are

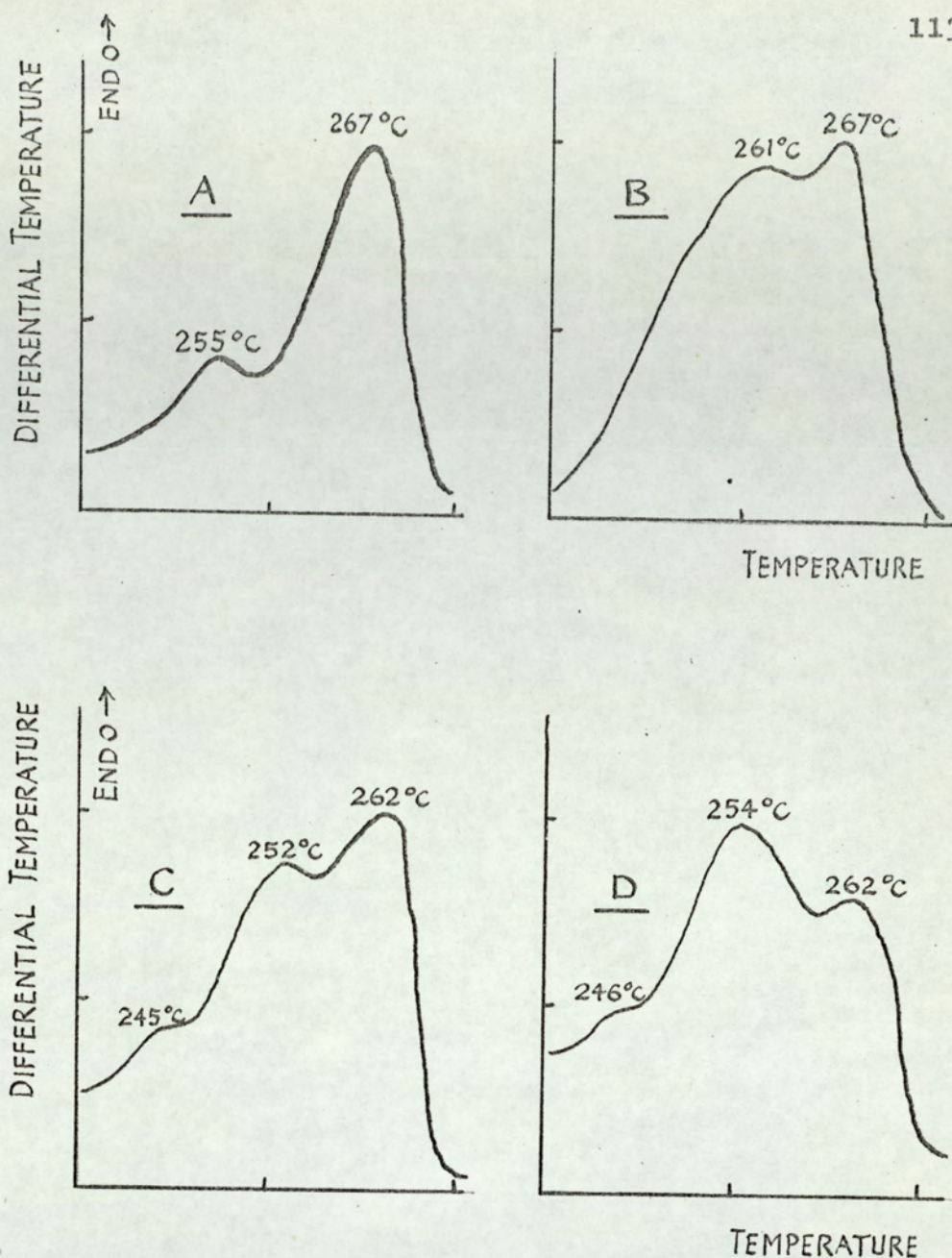


Fig.28. Differential thermal analysis of 66 nylon and a copolymer of 1% 6X nylon with 66 nylon. D.S.C.cell, heating programme, $5^{\circ}/\text{min}$.

A. Laboratory sample, first fusion.

B. Remelt of A from slow crystallization ($\frac{1}{2}^{\circ}/\text{min}$).

C. 1% 6X nylon, first fusion.

D. Remelt of C from slow crystallization ($1^{\circ}/\text{min}$ to 210°C)

very similar to those of Hybart and Platt (39) and Bell et al (93-95), although slight temperature variations can be noticed where different equipment has been used.

66 nylon in the form of aggregated single crystals which had been precipitated from a solution in butane diol, was heated at $5^{\circ}/\text{min}$. in the D.S.C. cell. A small peak at 248°C and a larger peak at 262°C were noticed. The low melting temperature may be due to residual butane diol. A second sample was annealed in the D.S.C. cell for 5 hours at 245°C , then cooled to 200°C . This sample was then heated at $5^{\circ}/\text{min}$; only a single peak, at 261°C , was noticed.

The 66/6 nylon and 66/6T nylon copolymers show similarly shaped D.T.A. graphs, although the sizes and temperatures of the peaks depend upon composition. The observations of Platt (39) for the annealing behaviour of 66 nylon appeared to hold also for these copolymers. During annealing, the higher temperature peak decreases in size, whilst the lower temperature peak increases significantly in size and appears at a slightly higher temperature.

The 6X / 66 copolymers show a different D.T.A. behaviour, with a greater tendency to form the lower temperature peak. Fig 28 C and D (page 113) shows that the lower temperature peak predominates on fusion of a slowly crystallized sample. A small peak at 245°C was also observed for the 1% 6X copolymer. Less reproducible peak shapes were observed for the 2 and 3% copolymers, and multiple melting endotherms were not easily resolved. Baseline variations also suggested that these copolymers melt over a very wide temperature range.

CHAPTER 5 , DISCUSSION.

Techniques for studying rates of crystallization of polymers.

The only technique which was found to be generally suitable for all the copolymers used for this study was the depolarised light intensity method. This proved to be acceptable for all copolymers which could be seen to crystallize with the development of birefringent structures, although the spherulites were frequently too small or too poorly defined to allow measurement of growth rates using a micrometer eyepiece or by the photographic methods. The 20/80 6T/6.10 nylon copolymer had the least birefringent spherulites, and light intensity measurements with this polymer were difficult, owing to the low amount of depolarisation. In order to increase the sensitivity of the apparatus for polymers of this type, it would be necessary to amplify the photoresistor output and to improve the lamp stability. It is doubtful whether the required stability could be obtained from an incandescent lamp.

Differential thermal analysis was suitable for the temperature-programmed studies, including the heats of fusion determinations, but isothermal D.T.A. was not practicable for 66 nylon crystallization. This is supported by the comments of Booth and Hay (51) who found the Differential Scanning Calorimeter manufactured by Perkin Elmer Ltd., to be a more suitable instrument for crystallization studies. The DuPont D.S.C. cell can, however, be used for some crystallization studies with isothermal operation. Some preliminary laboratory experiments had shown that the 11 nylon results of Hybart and Pepper (38) could be repeated by isothermal D.T.A. with the DuPont D.S.C. cell. Although 11 nylon and 66 nylon have similar heats of fusion, the 66 runs must be carried out at higher temperatures. Thus temperatures for 66

nylon are about 245°C and for 11 nylon are about 170°C . At the higher temperatures, the isothermal control of the D.S.C. cell becomes more variable due to increased heat requirements and convection currents, and the instrument response is reduced due to radiation heat loss. The latter is shown by the instrument calibration: equal areas for melting graphs were given by 2.78 m.cals at 235°C and by 2.10 m.cals at 159°C . Since 66 nylon cannot be suitable for crystallization studies by the D.T.A. technique due to erratic response from the differential temperature output, it is doubtful whether any copolymers of 66 nylon could be studied either.

Dilatometry and the other techniques mentioned for studying polymer crystallizations were rejected as a result of the literature review (Chapter 1).

Superposability of crystallization isotherms.

According to Russell (69), and Mandelkern (68), crystallization isotherms of volumetric fraction changes versus time on a logarithmic time axis should be superposable by rescaling the time axis. This property is said to be applicable to homopolymers only, as Mandelkern's isotherms for a butadiene copolymer (66) gave readings which were not superposable. In order to test the validity of this treatment for depolarised light intensity measurements on 66 nylon, the results for the laboratory-produced polymer have been rescaled on a logarithmic time base, and are shown overleaf in fig. 29. Within experimental error, isotherms of crystallization extent versus log. time are superposable, although the isotherm for 240°C appears to deviate from the normal behaviour. This is not surprising, as crystallization occurring at this temperature is rapid, and short times are difficult to determine accurately on the instrument.

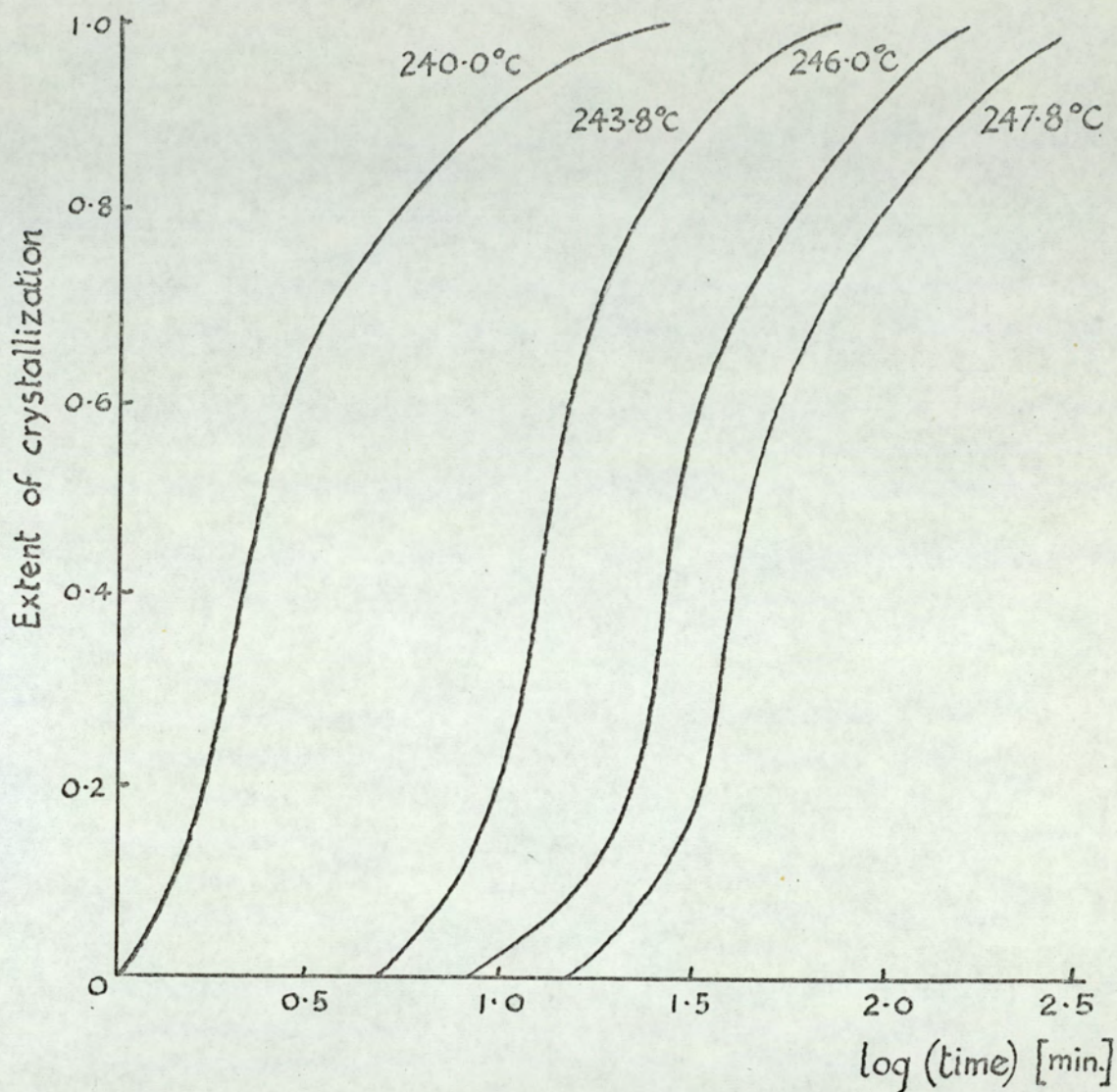


Fig.29. Crystallization isotherms for 66 nylon (laboratory polymer) using a logarithmic time axis.

A small amount of branching agent (6X) causes a large effect of breaking the superposability of isotherms. Fig.30 a (page 119) shows the isotherms for the copolymer of 3% 6X nylon with 97% 66 nylon. Only the early stages of the crystallization lead to superposable isotherms; as crystallization proceeds, the deviation from the behaviour of 66 nylon becomes pronounced. The extension of the crystallization process commences at about 50% completion at 232.2°C , as compared with 30% completion for 237.2°C . The effect is also more noticeable with the 3%6X copolymer than with the 2% and 1% samples, and it is attributable to the branching /cross-linkage feature rather than to copolymerisation. Fig.30 b shows that the isotherms for the 3% 6 nylon /97% 66 nylon copolymer are superposable on a log.time base, and these curves exhibit a behaviour similar to the results for 66 nylon homopolymer.

The branched copolymer shows comparable behaviour with the synthetic rubber results of Mandelkern (66). His crystallizations also proceed at a retarded rate at high conversions, and the onset of this retardation is reported to occur at a higher conversion for the lower temperature isotherms. A less prominent behaviour was noticed for branched polyethylene by Kovacs (67). For this polymer, branched units cannot enter the crystalline state, and as crystallization proceeds, the process is retarded due to the influence of the non-crystallizable branches. With branched nylon, the migration of crystallizable chain fragments is clearly retarded by the presence of branches and cross-links, and this leads to the extended isotherms.

It is interesting to postulate now that, if this retardation is attributable to branch chains or cross-links interfering with the main chain mobility, superposable isotherms should be obtainable from linear (unbranched) copolymers. Examples of these are the random 66/6

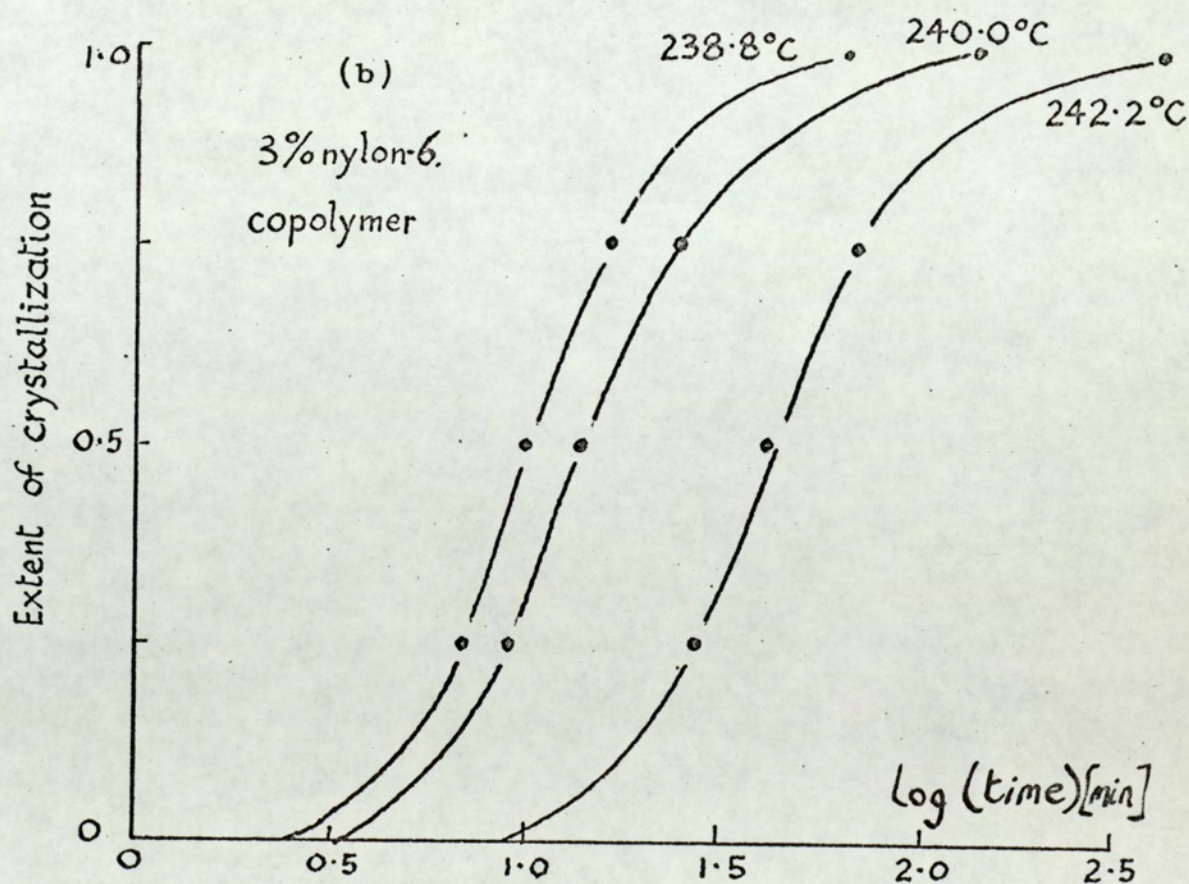
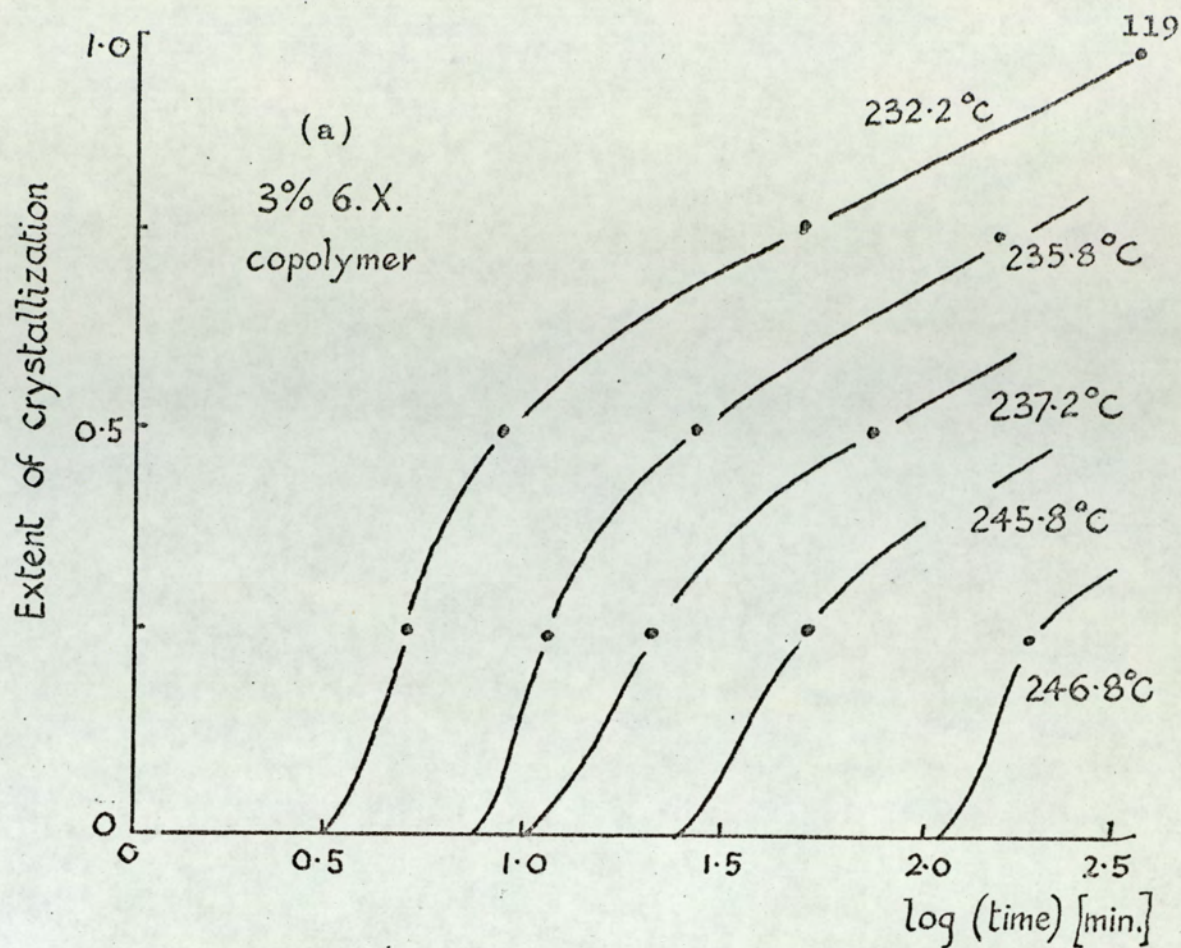


Fig. 30. Crystallization isotherms for 3% copolymers of 66 nylon with (a) 6X nylon and (b) 6 nylon. Log. time axis.

nylon copolymers or the 6T/66 copolymers, which were prepared without the addition of a branching agent. Fig.31 (overleaf) shows the re-scaled isotherms for two such copolymers, the 40/60 6/66 nylon copolymer and the 20% 6T /80% 66 copolymer. In each case the isotherms are superposable within experimental error. More surprisingly, however, the isotherms are practically superposable with the results for 66 nylon homopolymer.

If these observations are considered using Mandelkern's theory (66), not all the crystallizable units of copolymers are able to participate in the process, as there is a requirement for sequences of greater length than a critical nucleus parameter, which is itself temperature dependent. At the low supercoolings, the value of this parameter becomes large. Thus the 6X copolymer behaviour is consistent with a decrease in the availability of suitable crystallizable units as the process proceeds. This effect is also enhanced by the increased melt viscosity of the branched copolymers, which serves to reduce the crystallization rate over the complete process.

For random copolymers without branching or cross-linking, the crystallization behaviour may be considered to be comparable with the effect of adding an inert diluent to the system, as is encountered by plasticizer additions. There is a significant difference, as the melt viscosity is not substantially altered by copolymerisation except by its usual temperature dependence. For a concentrated solution of a polymer, Mandelkern (88) gave the free energy of nucleus formation as dependent upon the melting point reduction and the volume fraction of polymer, in addition to the usual terms encountered in the nucleation equation for a homopolymer. (equation 1.24). For these copolyamides, the effective polymer fraction is not reduced by the copolymer introduction, and hence the reduction in the nucleation rate is proportional to the reduction in the measured melting temperature. On

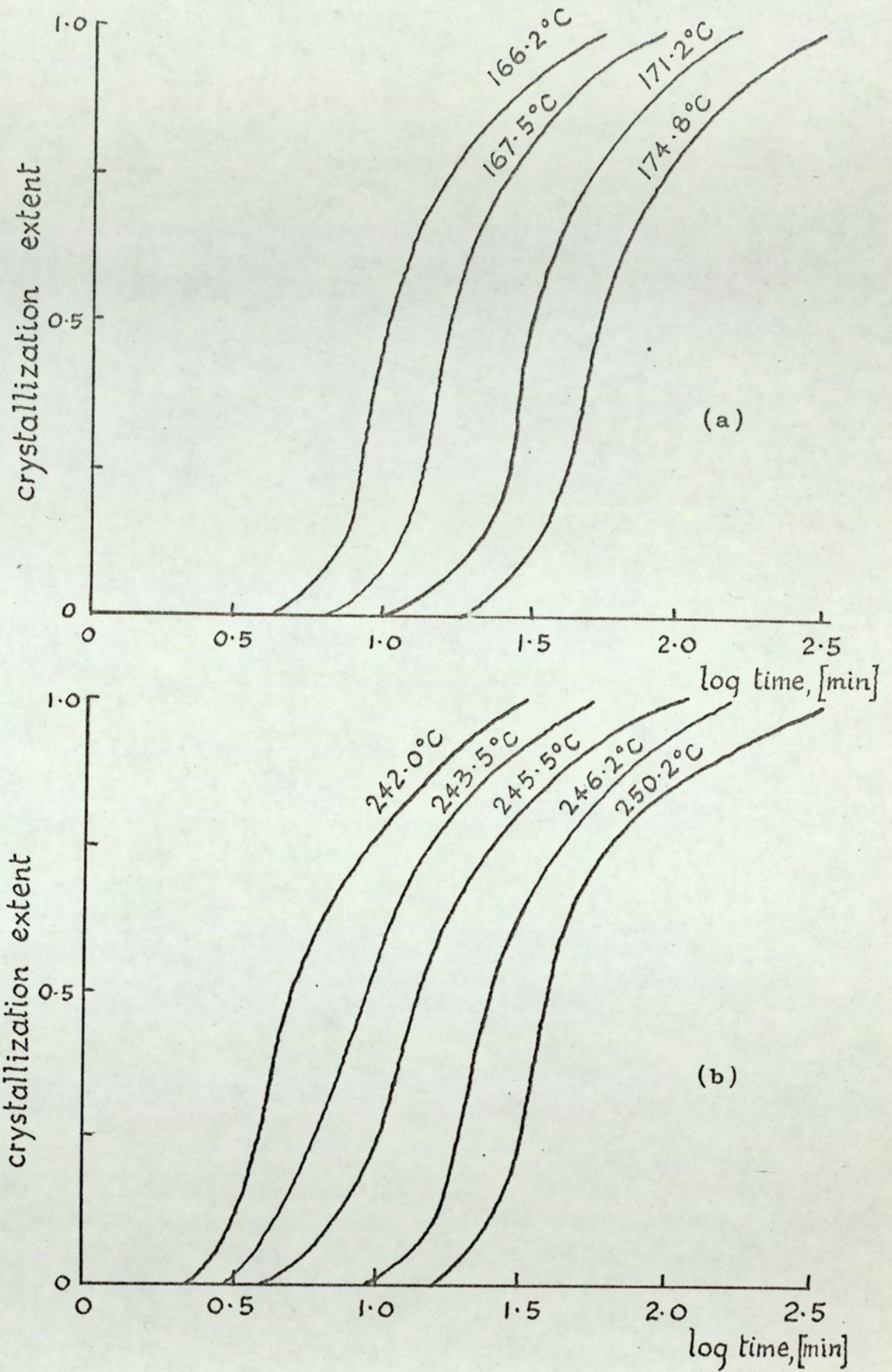


Fig. 31. Crystallization isotherms for (a) 40/60 6/66 nylon copolymer and (b) 20/80 6T/66 copolymer. Logarithmic time axis .

this basis, the superposable logarithmic time base isotherms are not anomalous, but are a feature of copolymerisations where the comonomer serves as a diluent without impeding the normal migration of polymer chain units through the melt.

Any deviations noticed from 66 nylon in fig.31 are easily attributable to the temperature dependence of the melt viscosity. Over the range of 160-250°C, these viscosity variations appear to have a surprisingly insignificant effect upon the shape of the crystallization isotherms.

Avrami analysis.

The Avrami plots of $\log (\ln \theta)$ versus \log time for 66 nylon and the 73/27 6/66 nylon copolymer are shown in fig.32 (page 123). The graphs show the usual format of Avrami graphs, with a linear portion having a slope of n , the Avrami integer, and a curved portion at a high conversion level, where there is a continuously decreasing value of the integer. A close inspection of fig.32 suggests that n is not constant, but changes throughout the process; it is useful, however, to consider the nearest integral value for n to describe the early section of the process.

For 66 nylon, deviation from linearity in fig.32.a has become significant at 55% completion for the 241.5°C isotherm, and at 50% completion for the 247.8°C isotherm. An Avrami integer of $n=3$ can be assigned to the process for 10-40% conversion. A tangent to the graph at 25% conversion has a slope of 3 to the nearest whole number.

For the copolymer, fig.32b, the Avrami analysis gives $n=4$ to the nearest whole number, with deviation occurring at about 50% conversion. The general results for 66/6 nylon copolymers indicate $n=4$ for copolymers composed mainly of 6 nylon and $n=3$

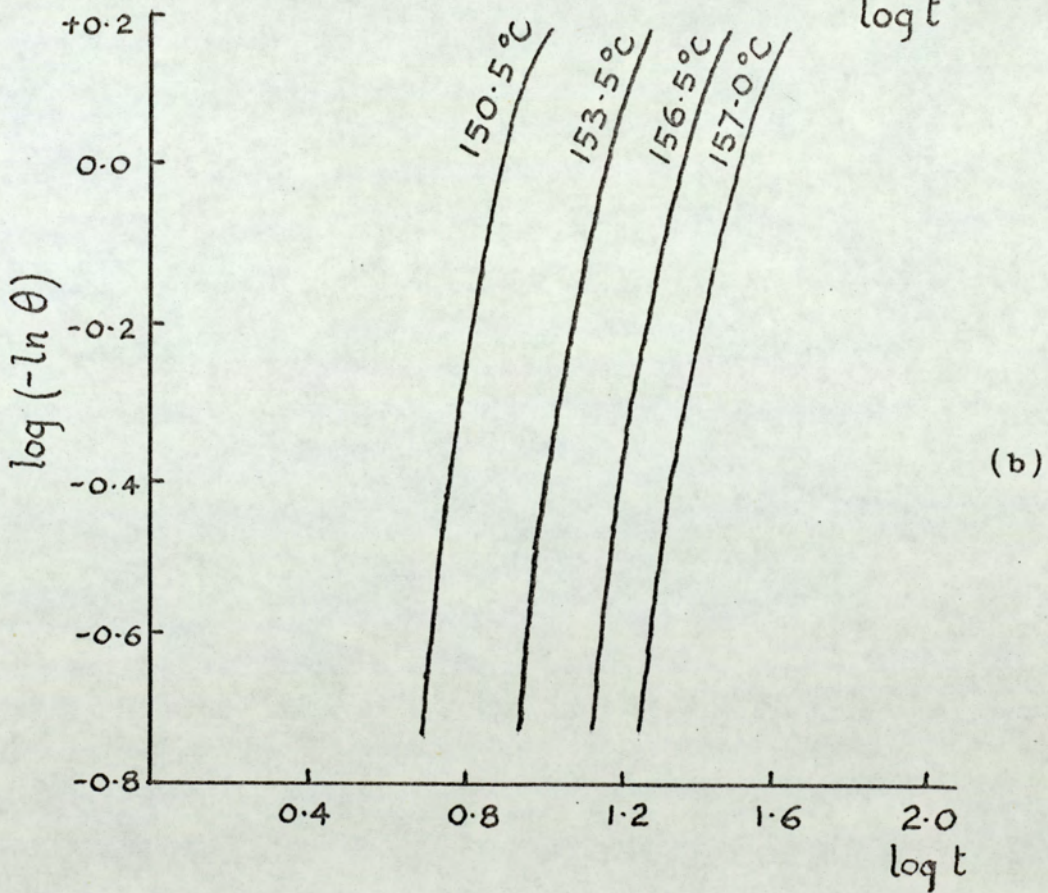
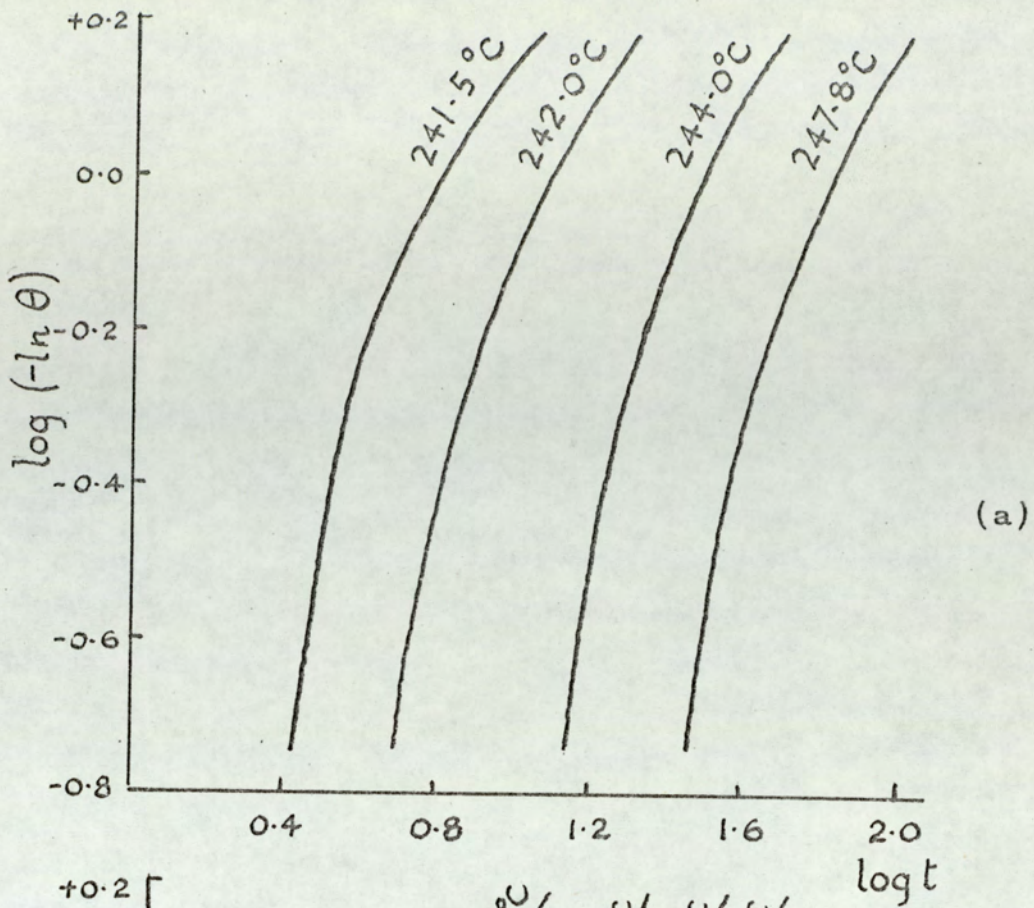


Fig. 32. Avrami graphs for (a) 66 nylon, laboratory sample and (b) the 73/27 copolymer 6/66 nylon.

for copolymers composed mainly of 66 nylon, taking the nearest integral values for n .

The inaccuracy of applying this treatment to polymer systems is fully discussed by Sharples (34), with reference to dilatometry. Difficulties arise in practice with deciding upon the initial and final values for the polymer volumes, and the deviation from linearity which is observed at high conversions, is attributable to the normal process of secondary crystallization. Pepper (38) found for 11 nylon and copolymers of 11 nylon with up to 20% 6 nylon, that the Avrami integer of $n = 4$ applied throughout to the first 66% of the crystallization process. These results were for volume contractions, and there was no evidence to suggest that deviation from the Avrami graph linearity commenced at an earlier conversion for the copolymers. Even so, time base measurements had suggested that secondary crystallization processes may be more pronounced in the case of copolymers.

The depolarised light intensity method for studying polymer crystallizations is seen to amplify the inadequacy of the Avrami treatment, as it appears to show a high sensitivity to the secondary crystallization process. As a consequence of this, deviation from linearity on the double logarithmic plots is observed at about 55% conversion, instead of the 65% value obtained from dilatometry. Also the recording apparatus gives less accuracy of both time and conversion than may be obtained using precision dilatometry, and good temperature control of a hot stage is more difficult to achieve than the thermostating of an oil bath. This loss of precision has the result of introducing more uncertainty into the value for the Avrami integer. Sharples (34) discussed the results of Gent (89) who proved that only a small error in the measurement of time or conversion can result in an incorrect assignment of the n value. For a crystallization half time of 120 minutes, an error of 10 minutes in $t_{\frac{1}{2}}$ leads to a change in

the n value from 4 to 3. With the apparatus used in this study, it is therefore inappropriate to consider fractional Avrami integer values.

The behaviour for a 6T / 66 nylon copolymer is shown in fig.33a, overleaf. This is seen to be very comparable with the graphs for 66 nylon homopolymer, both in slope and in the point of deviation from linearity.

A different situation is encountered if the Avrami analysis is applied to the 6X / 66 copolymers. Fig.33b shows the 3% 6X copolymer graph in this analysis. In the early stages of the crystallization process, the homopolymer value $n = 3$ is followed. Deviation occurs, with n decreasing at 35% conversion for the 237.2°C isotherm. At the faster crystallization rates, this deviation occurs at a higher conversion level (55% conversion for the 232.2°C isotherm), but the appearance of the graph is significantly different from the equivalent curve for a copolymer without branching agent. The decrease in n for the copolymers containing 6X is pronounced, with a value of $n = 1$ being approached at high conversion. These Avrami values are similar to the Avrami graphs of Buchdahl, Miller and Newman (53) for low density polyethylene.

The crystallization rate constant, Z , is usually defined by reference to the Avrami equation, and is given by

$$Z = \ln 2 / (t_{\frac{1}{2}})^n$$

The rate constants for the 66 nylon crystallizations have been calculated using this expression and with an Avrami value of $n = 3$, and the results are shown in table 25. (page 127). For comparison, the published results of Hartley, Lord and Morgan (86,90) are included. These results were obtained using the density balance technique for a commercial polymer having an M_n molecular weight value of 11,600.

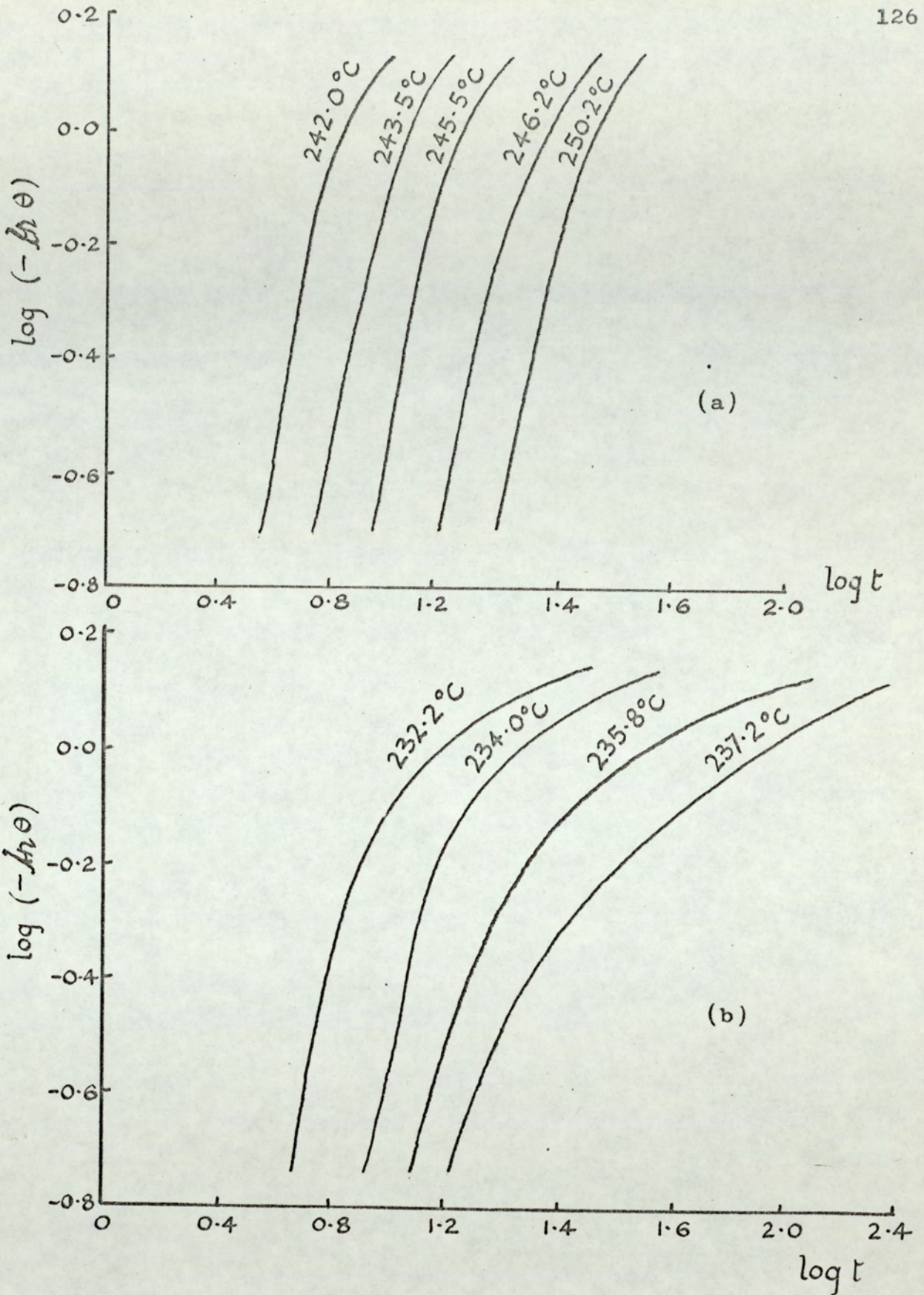


Fig. 33. Avrami graphs for (a) 20/80 6T/66 nylon copolymer and (b) 97/3 66/6X copolymer.

Table 25. Crystallization rate constants, Z, for 66 nylon.

Laboratory sample, code 32								
Temperature	247.8	246.7	246.0	244.0	243.8	242.0	241.5	°C
Z constant	.00655	.00935	.0293	.0624	0.401	1.05	10.8	$\times 10^{-3} \text{ min}^{-3}$
Commercial polymer, XP 10257								
Temperature	251.0	248.8	248.0	246.5	°C			
Z constant	.00252	.0176	.0316	.0651	$\times 10^{-3} \text{ min}^{-3}$			
Results of Hartley, Lord and Morgan, (reference 86)								
Temperature	250	247	243	°C				
Z constant	.0029	.037	.662	$\times 10^{-3} \text{ min}^{-3}$				

The $t_{\frac{1}{2}}$ values for copolymers containing up to 50% 6 nylon can be converted into rate constants using the same method, but it relies upon the correct value being selected for the Avrami integer. For copolymers having 66 nylon as the major component, including the 6T / 66 copolymers, n has been taken as 3. For 6 nylon and copolymers containing up to 30% 66 nylon, the Avrami integer has been taken as 4, and $Z = \ln 2 / (t_{\frac{1}{2}})^4$.

For the 6X copolymers, no certain value can be ascribed to the Avrami integer, as it is constantly changing, even before the crystallization half time. It is consequently inappropriate to describe a rate constant for the kinetics of crystallization of the 6X copolymers.

The dependence of crystallization rates on temperature.

The several expressions of Mandelkern, Quinn and Flory (Chapter 1, page 24) for the temperature dependence of crystallization rates all include the exponential with a $T_m^2 / T \Delta T^2$ function. The processes included are spherulitic or disc-like growth from spherical

or disc nuclei, and the equations may be simplified in the general case to equation 1.19:

$$\ln Z = \ln z_0 - f\left(\frac{T_m^2}{T \Delta T^2}\right)$$

where Z is the temperature dependent rate constant, and z_0 is another constant; T is the crystallization temperature, and f the functional term involving the nucleation and growth constants. In this expression, T_m is the thermodynamic melting point of the polymer, and ΔT is the value $T_m - T$. Owing to polymers behaving in a non-thermodynamic sense on melting, even at extremely slow heating rates, the thermodynamic melting point cannot be measured directly in practice. The loss of birefringence method used in this study leads to melting points which are higher than those obtained by D.T.A., but it is doubtful whether these are equivalent to the results of dilatometric measurements using slow heating rates.(35). The temperature dependence equation implies that a linear relationship exists in the $\ln Z$ versus $T_m^2 / T \Delta T^2$ graph, if the correct value has been selected for T_m .

For results utilising the half time, $t_{\frac{1}{2}}$, the general equation becomes

$$\ln \ln 2 - n \ln t_{\frac{1}{2}} = \ln z_0 - f\left(\frac{T_m^2}{T \Delta T^2}\right)$$

i.e.

$$\ln \frac{1}{t_{\frac{1}{2}}} = \frac{1}{n} (\ln z_0 - \ln \ln 2) - \frac{f}{n} \left(\frac{T_m^2}{T \Delta T^2}\right)$$

hence $\ln 1/t_{\frac{1}{2}}$ may be used as an alternative to $\ln Z$ in a graph versus $T_m^2 / T \Delta T^2$, to evaluate T_m .

Fig.34, overleaf, is a graph of the results for the commercial sample of 66 nylon, which had a measured melting point of 269°C by the disappearance of birefringence method. Neither 269°C nor 271.5°C is adequate to produce a linear graph in fig.34, but a good straight line results if the polymer T_m value is taken as 274°C. This is therefore taken to be the thermodynamic melting point of 66 nylon.

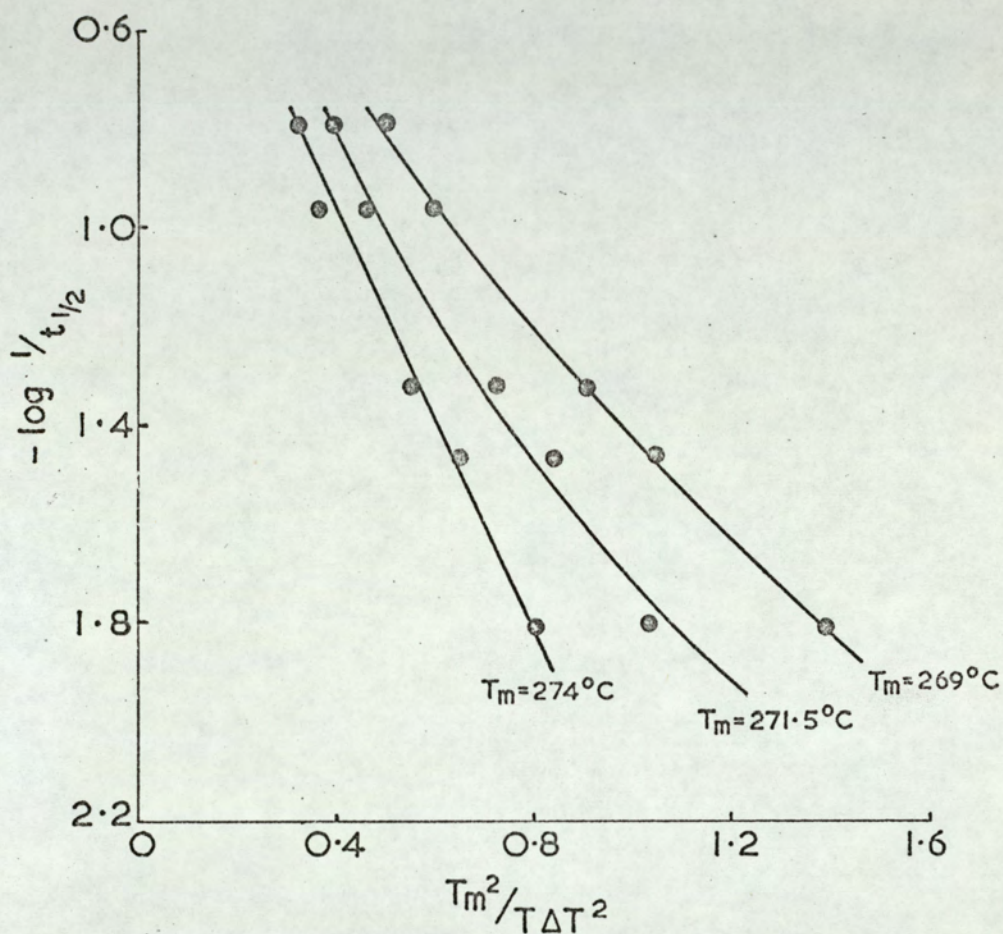


Fig. 34. Temperature dependence of crystallization rate for 66 nylon. Graph of $-\log 1/t_{1/2}$ versus $T_m^2 / T \Delta T^2$ for three temperature values of T_m . A linear graph results for $T_m = 274^\circ\text{C}$

McLaren (42) has given consideration to the determination of the thermodynamic melting point of 66 nylon, using the equilibrium melting method of Frank (66). This simply uses the supposition that the crystallization will proceed at an infinitely slow rate at T_m . Defining the temperature coefficient of crystallization, u , as

$$u = d \log Z / dT \text{ where } Z \text{ is the rate constant,}$$

for three dimensional nucleation $u = -k_2 (T_m - T)^{-3}$

or for two dimensional nucleation $u = -k_1 (T_m - T)^{-2}$, where k_1, k_2

are constants, McLaren found that a graph of $u^{-\frac{1}{3}}$ against T was linear for 66 nylon, and when extrapolated, intersected the temperature axis for an infinitely slow crystallization at 272.5°C . These observations for a polymer of molecular weight $M_n = 14,600$ were contrasted with a T_m value of 271.5°C for a polymer having an $M_n = 11,600$.

An attempt was made to determine the thermodynamic melting point of the laboratory sample of 66 nylon using this treatment, and assuming McLaren's observation of three dimensional nucleation. Unfortunately, the graph of $\log Z$ versus temperature was not sufficiently precise to allow the evaluation of $d \log Z / dT$ for a range of temperatures, and hence the suggested plot of $u^{-\frac{1}{3}}$ did not give a good linear portion which could be extrapolated to provide T_m . However, the value which was obtained by substitution of possible values of T_m using the Mandelkern, Quinn and Flory expression gave a result (274°C) in near agreement with McLaren's value, and showed that the thermodynamic melting point is a few degrees above the measured melting point value. This adds support to the Mandelkern Quinn and Flory theory.

The graphical plots of $\log 1/t_{\frac{1}{2}}$ versus $T_m^2 / T \Delta T^2$ can be extended to copolymers, apparently without loss of validity. This is illustrated in fig. 35, overleaf, which shows the determination of the thermodynamic melting point for the copolymer of 70% 66 nylon/30% 6 nylon.

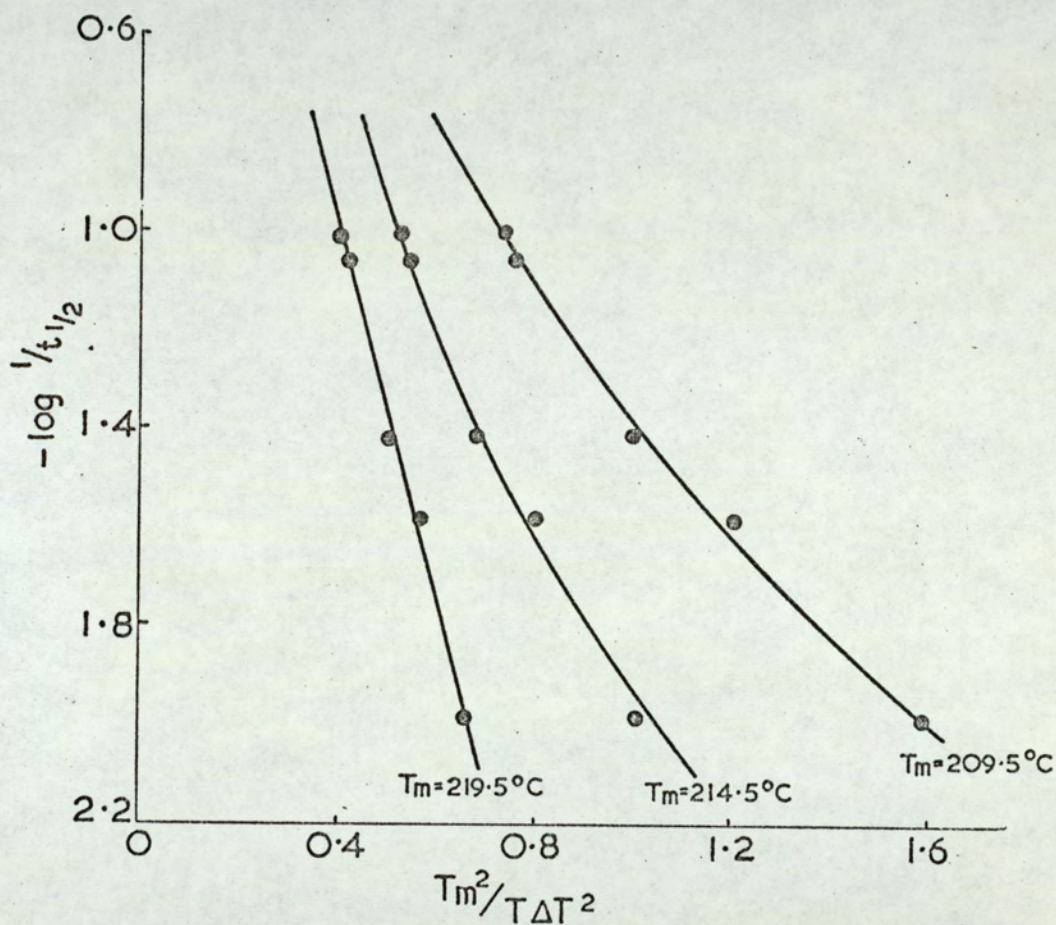


Fig. 35. Temperature dependence of crystallization rates for a copolymer of 70% 66 nylon and 30% 6 nylon. Graph of $-\log 1/t_{1/2}$ versus $T_m^2 / T \Delta T^2$ for three temperatures taken as T_m . A linear graph results for 219.5°C .

In order to produce a linear graph, it now becomes necessary to increase the value for the melting point by 10°C from the measured melting point of 209.5°C to 219.5°C . A smaller temperature increase was found to be sufficient for the 6T copolymers with 66 nylon. Fig.36, page 133, shows the $\log 1/t_{\frac{1}{2}}$ versus $T_m^2 / T \Delta T^2$ graph for the copolymer of 10% 6T / 90% 66 nylon. For this copolymer, the measured melting point is 274°C and a curved graph is obtained at this temperature. A nearly linear graph is obtained if the melting point is taken as 276.5°C , and a straight line results for the 279°C points. The thermodynamic melting point for this copolymer has therefore been taken as 279°C .

With 6.10 nylon and copolymers of 6.10 with 6T nylon, the thermodynamic melting points were found by the substitution method to be only 2°C above the measured melting points. This low increase is probably accounted for by the low molecular weights of the 6.10 nylon copolymers, although the same type of behaviour has been encountered with unfractionated polyethylene (35).

Table 26 (page 134) gives a summary of the thermodynamic melting points which have been estimated for the 66/6 copolyamides and for the 6T copolymers. All the results were obtained by substituting values for T_m in the $-\log 1/t_{\frac{1}{2}}$ versus $T_m^2 / T \Delta T^2$ graphs, and noting the minimum T_m temperature required to produce a straight line.

Mandelkern Quinn and Flory have considered the significance of the slopes of the $-\log 1/t_{\frac{1}{2}}$ versus $T_m^2 / T \Delta T^2$ graphs for homopolymers. In order to simplify the general expressions which give the temperature dependences of the disc or spherulitic nucleation and growth processes, it is first necessary to neglect the secondary crystallization component, which is recognised to be a serious error.

Using $-\ln t_{\frac{1}{2}} = \frac{1}{n} (\ln Z - \ln \ln 2)$, the two equations for disc nuclei

with disc growth and spherical nuclei with spherical growth (Chap.1) are

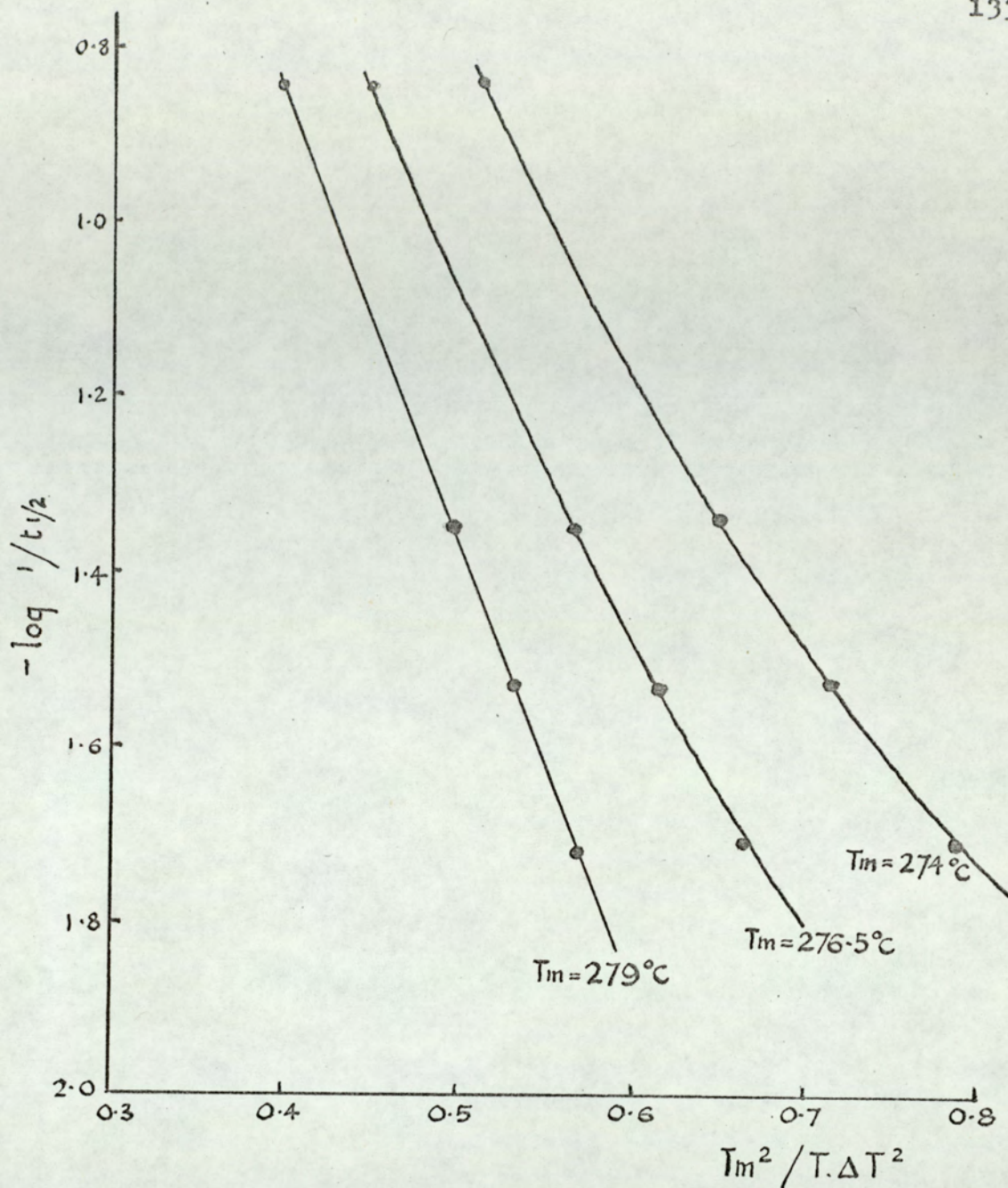


Fig. 36. Temperature dependence of crystallization rates for the 10% 6T copolymer with 66 nylon. Graph of $-\log 1/t_{1/2}$ versus $T_m^2 / T \Delta T^2$ for three values of T_m .

Table 26. Thermodynamic melting points of copolyamides; determined by substituting T_m values in $-\log 1/t_{\frac{1}{2}}$ versus $T_m^2 / T \Delta T^2$ graphs, until linearity resulted, Method of Mandelkern et al (35,62), e.g. figs. 34-36.

66/6 nylon copolymers.

% 66 nylon	100	93	85	80	70	60	50
code	32	26	25	24	33	31	37
measured melting pt, °C	268	256	235	227	210	188	178
thermodynamic m.pt, °C	274	262	249	240	219	203	189

6/66 nylon copolymers.

% 6 nylon	100	90	85	73	60
code	30	38	29	28	27
measured melting pt, °C	221	201	195	179	177
thermodynamic m.pt, °C	226	212	205	188	-

6T /66 nylon copolymers.

% 6T nylon	0	2	5	10	15	20
code	32	55	47	43	49	50
measured melting point °C	268	270.5	272	274	277	281
thermodynamic m. point °C	274	275	277	279	281	284

6.10 /6T copolymers

% 6T nylon	0	10	15	20
code	61	62	67	69
measured melting pt, °C	229	222	219	215
thermodynamic melting pt. °C	231	224	221	217

(for disc nucleus and disc growth, equation 1.18,)

$$-\ln t_{\frac{1}{2}} = \frac{\ln z_0 - \ln \ln 2}{3} - \frac{E_D}{RT} - \frac{8\pi \bar{\sigma}^3}{3(\Delta hu)^2} \frac{T_m^2}{(\Delta T)^2 RT}$$

(for spherical nucleus and spherical growth, eqn. 1.16)

$$-\ln t_{\frac{1}{2}} = \frac{\ln z_0 - \ln \ln 2}{4} - \frac{E_D}{RT} - \frac{4\pi \bar{\sigma}^3}{3(\Delta hu)^2} \frac{T_m^2}{(\Delta T)^2 RT}$$

where $\bar{\sigma}$ is the mean interfacial free energy for the surfaces, and E_D the transport activation energy.

Fig 37, overleaf, shows the result of taking the slopes of each graph used in the compilation of the 66/6 nylon results of table 26. The slopes for the homopolymer graphs were found to be 5.4 for 6 nylon, and 2.12 for 66 nylon. These appear to be representative of crystallizations which occur with $n = 4$ for 6 nylon and $n = 3$ for 66 nylon. According to the above equations, 66 nylon would be expected to show the greater slope, and this clearly does not apply. The discrepancy may be due to the significantly different crystallization temperatures. However, an interesting situation arises in the cases of the lowest melting copolymers of the 66/6 series, (codes 27, 28 and 37). It has already been seen (page 122) that the Avrami analysis of the copolymers leads to an Avrami integer which is a characteristic of the homopolymer which forms the major ingredient, and for the 73% 6 nylon copolymer n is 4, whereas for the 50% copolymer n is 3. These two compositions and the 60% copolymer all have closely similar melting points (177-179°C), and so they are representative of a changeover region. The slope of $\log 1/t_{\frac{1}{2}}$ versus $T_m^2 / T \Delta T^2$ against composition graph (fig. 37) shows a discontinuity in this region, and using the above equations it can be predicted that the slope should change from 4/3 to 8/3 times the functional group including $\bar{\sigma}$. This implies that the slope should double on passing from the 6 nylon characteristic region to the 66

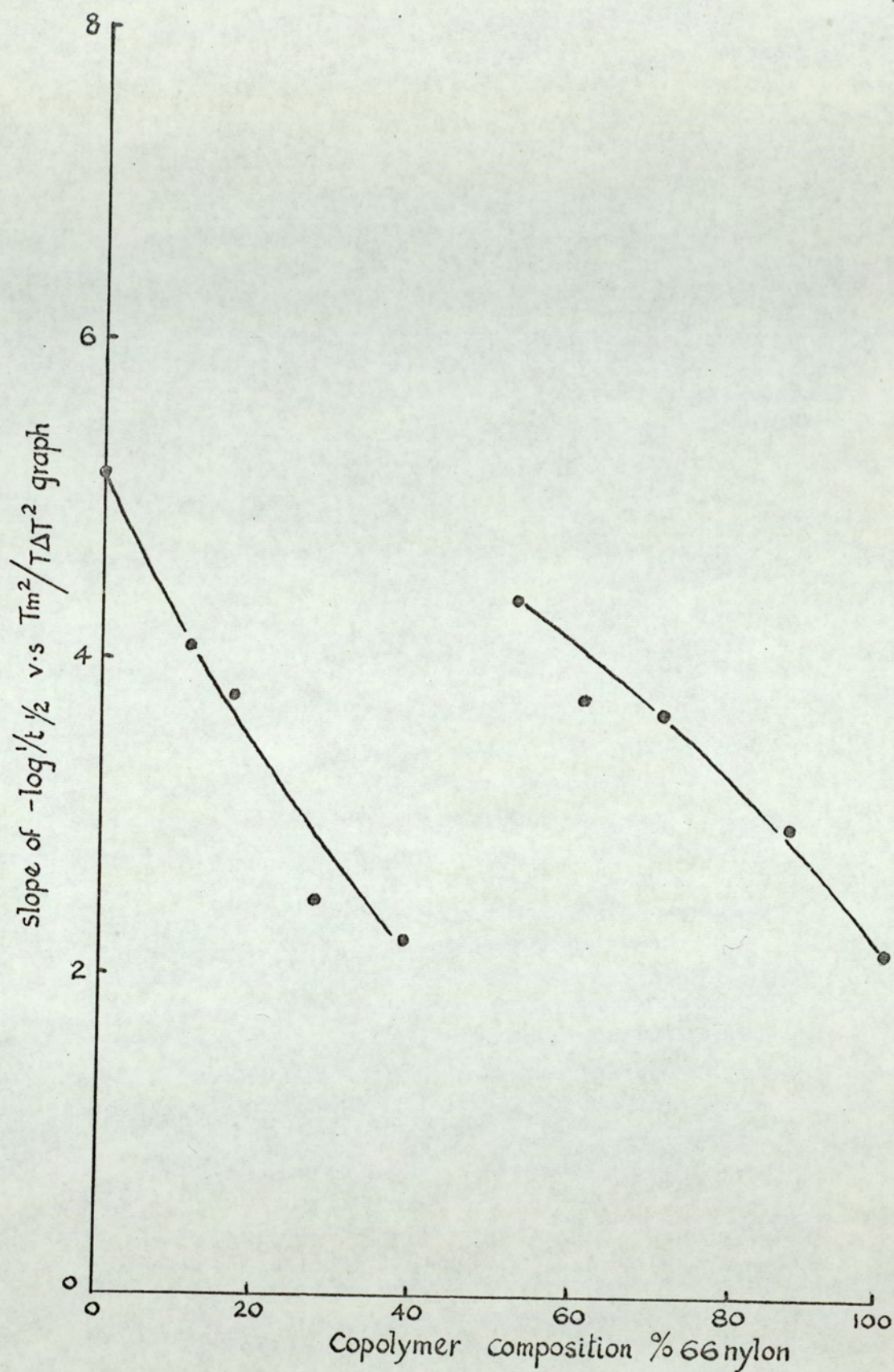


Fig. 37. Graph of the slope of figs. 34-36 versus composition for 66/6 nylon copolymers.

nylon region. Fig 37 shows that the slope changes from 2.3 to 4.4 over this region. This agreement between the theoretical prediction and the practical observation may be fortuitous, but it is now interesting to consider the actual $\log l/t_{\frac{1}{2}}$ versus $T_m^2/T\Delta T^2$ graph for the copolymer which has a composition inside the transition zone, i.e. the 60%66/40%6 copolyamide. Fig.38, overleaf, shows the curves which were obtained for three values of T_m selected for this copolymer. As the curves tend to bend in the reverse direction, there is no approach to linearity obtainable for any reasonable value of T_m , and it appears that the treatment of this theory is inapplicable. This observation suggests that a single Avrami integer may not apply to the primary crystallization process for this copolymer. With the results of the present experiments, it is not possible to differentiate between minor variations in the Avrami integer, and consequently the hypothesis cannot be confirmed.

A second interesting case arises with the 6X/66 copolymers, which were seen to show poor adherence to the Avrami treatment, owing to the extensive and lengthy secondary crystallization processes which dominate the depolarised light intensity traces. The $\log l/t_{\frac{1}{2}}$ versus $T_m^2/T\Delta T^2$ graphs for the 6X copolymers show the same general form as the 66/6 graphs (figs.34-36). However, the predictions of the thermodynamic melting points from the T_m values needed to produce straight lines give misleading results, which even suggest that the thermodynamic melting point is below the measured melting point. The values for T_m for these copolymers by the substitution method are shown in table 27.

Table 27. T_m values for linearity in the temperature dependence graphs for 6X copolymers. (Method as in table 26.)

% 6X nylon	0	1	2	3
measured melting point, °C	268	267.5	265	263.5
T_m for linear graph, °C	274	270.5	265	258.5

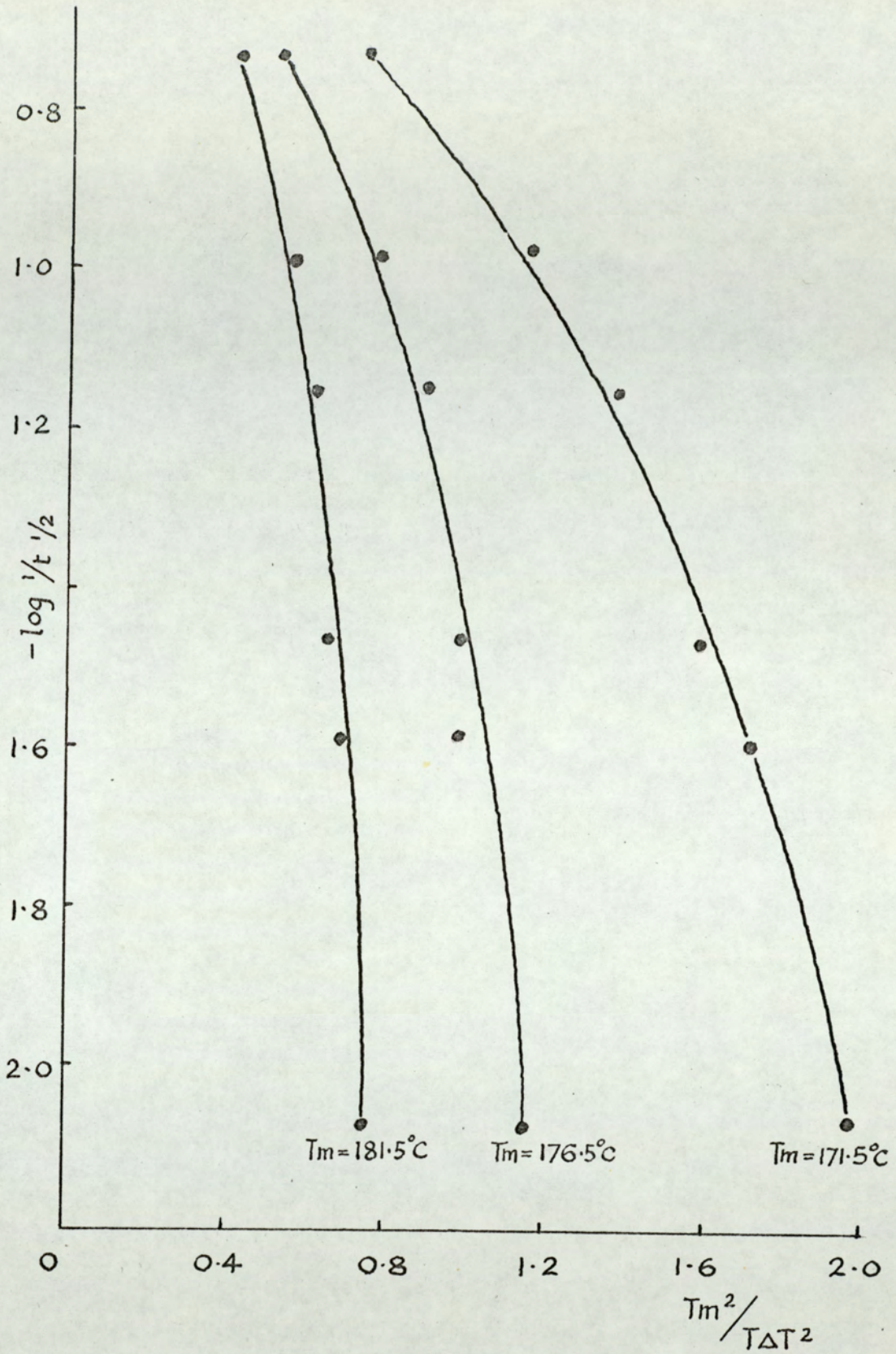


Fig. 38. Temperature dependence of crystallization rates for the 60/40 6/66 nylon copolymer. Graph of $-\log 1/t^{1/2}$ versus $T_m^2 / T \Delta T^2$ for three possible values of T_m .

The conclusion supported by this analysis is that, as deviation from the Avrami equation becomes more pronounced, the temperature dependence equations, which are themselves based on the Avrami equation become inapplicable. This is particularly noticeable in the case of the 3% 6X copolymer, which showed deviation from the Avrami behaviour before $t_{\frac{1}{2}}$ time had elapsed, and on the temperature dependence test the copolymer appeared to have a thermodynamic melting point which was 5°C below the measured value.

The Flory equation applied to 66/6 nylon copolymers.

The equation of Flory for the dependence of the melting temperature on the concentration of crystallizable units (page 32) is:

$$\frac{1}{T_m} - \frac{1}{T_m^{\circ}} = - \frac{R}{\Delta H_u} \ln X_A \quad (1.25)$$

where T_m is the copolymer melting point and T_m° the homopolymer melting point, X_A is the mole fraction of the crystallizing component and ΔH_u the crystalline heat of fusion.

For a non-random copolymer system, the equation is inappropriate. In order to test the validity of the Flory equation to the 66/6 nylon copolymers, the melting points of the copolymers have been used to construct a graph of $1/T_m$ versus $\ln X_A$, which is shown overleaf, as fig.39. From the figure it can be seen that the treatment is applicable to 66 nylon containing up to 40% copolymerised 6 nylon, and 6 nylon containing up to 30% copolymerised 66 nylon. The interpolated heats of fusion for the crystalline regions of the polymers are 28.1 cal/g for 66 nylon and 31.9 cal/g for 6 nylon.

If the thermodynamic melting point values from table 26 are used in the Flory treatment, slightly higher heats of fusion can be obtained, and this is also illustrated in fig.39. The crystalline heats of fusion then obtained are 31.8 cal/g for 66 nylon and 32.0 cal/g for

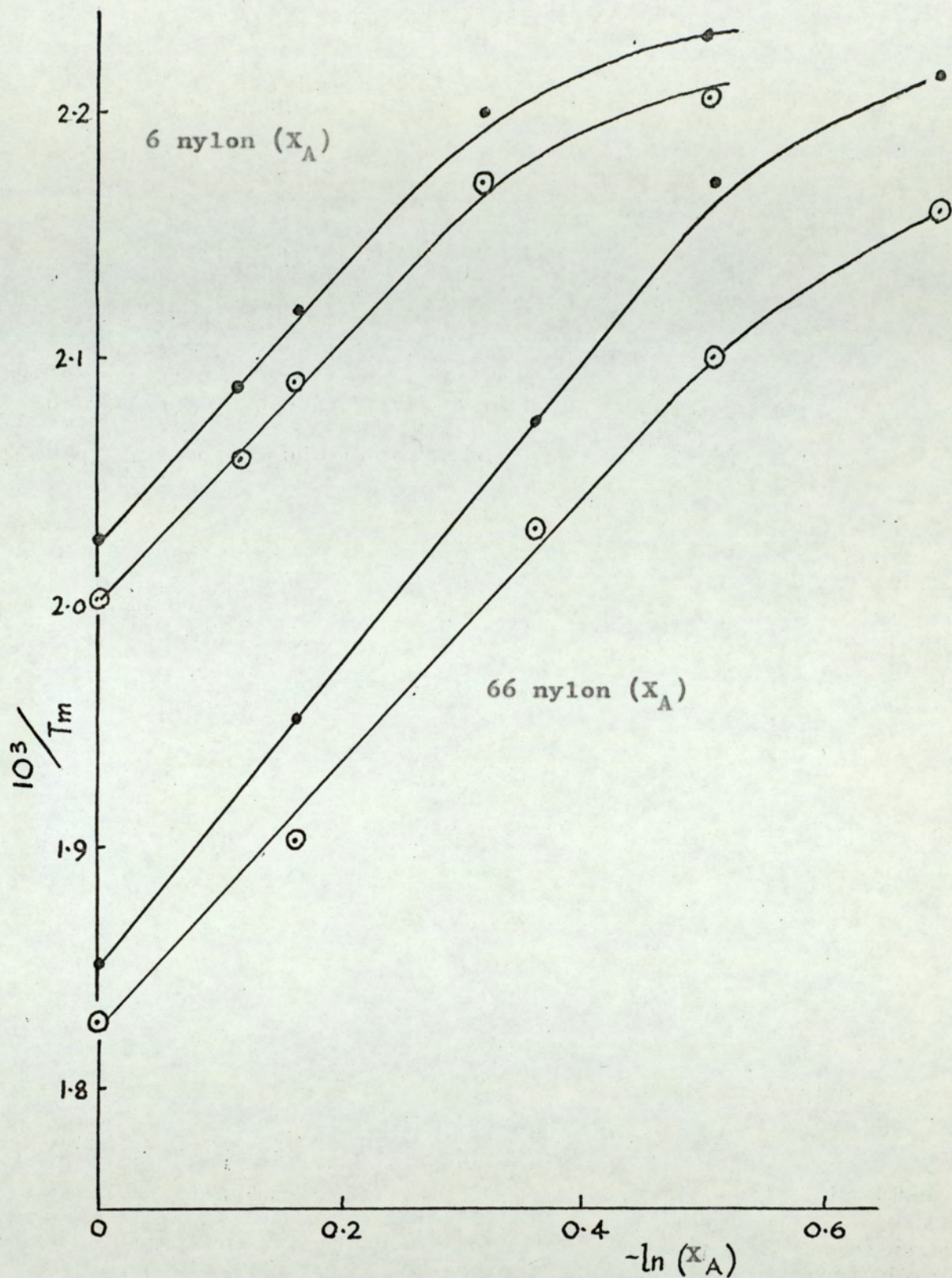


Fig. 39. Copolymer - composition curves according to Flory's equation, 66/6 nylon copolymers.

- measured melting points.
- ⊙ estimated thermodynamic melting points.

6 nylon. These results are still much lower than the results published by Inoue (91) using differential thermal analysis of polymers of known densities, which gave 46.8 cal/g for 66 nylon. Low heats of fusion have been reported previously from copolymer melting point data, and Mandelkern (35) pointed out that the use of non-polymeric diluents generally leads to more reliable melting points for insertion into the Flory equation.

The isomorphous character of 66/6T nylon copolymers .

The results for the 66/6T copolyamides show a considerable retention in the crystalline melting point values as the 6T comonomer is introduced, as discovered by Edgar and Hill and others (29). Behaviour of this type is regarded as the test for isomorphism (27). Two observations in general in the results of the 6T /66 copolyamides are contrary to the expectations for isomorphous replacements. (i). There is a decrease in the heat of fusion (measured by D.T.A.) as the comonomer is introduced, although this decrease is less pronounced if the sample is annealed before fusion. Total isomorphous replacement would suggest that the heat of fusion value for the homopolymer should be retained through the copolymer series. (ii) Crystallization rates for the 2 - 10 % copolymers occurred at lower temperatures than the rates for the equivalent half time value for 66 nylon homopolymer. Complete isomorphous replacement would imply a retention in this temperature, or an increase in the crystallization temperature for these copolymers.

The melting point of 6T homopolymer is thought to be 371°C (92), although decomposition occurs rapidly as 6T homopolymer melts. 66 nylon has a melting point of 268°C, so isomorphous copolymers should ideally show an increase in melting point of 1.03°C for each percent of comonomer added (35). However, the 20% copolymer melted at 280°C, which is 8°C below this prediction, and from the melting point /

crystallinity data for the 66/6 copolyamides, this can be estimated to be representative of a reduction of about 5% in the percentage crystallinity from 62% to 57%. For comparison, the equivalent introduction of 20% 6 nylon into 66 nylon resulted in a reduction in the percentage crystallinity of 12%, to 50% crystalline.

A possible explanation of the partial crystallinity loss with 66/6T copolymers may be the 0.4 Å carbonyl group separation difference (27). Complete co-crystallization is consequently not favoured, although there is a significant re-introduction of crystallinity by annealing. The heats of fusion data illustrate this, and calculations of percentage crystallinities may be made assuming Inoue's data for 66 nylon (91) is also valid for these copolymers. For the 20% copolymer of 6T nylon, the heat of fusion is increased from 7.0 cal/g to 15.5 cal/g on annealing, corresponding to a percentage crystallinity change of from 22.5% to 49.8%, whereas 66 nylon homopolymer under the same conditions showed a smaller increase of 5.8 cal/g. The values for the crystallinity of 6T are still low by estimation using the copolymer melting points. No estimates of the crystallinities of the 6T copolymers from the density measurements has been possible, because no published information on the densities of the crystalline and amorphous regions of 6T homopolymer was available. 6T homopolymer was not prepared for this work.

The 6.10/6T copolymers are not isomorphous, as the melting point of 6.10 nylon is reduced by copolymerisation with up to 20% 6T nylon.

Fusion of 66 nylon, and D.T.A. multiple melting endotherms.

A few results on the melting of 66 nylon using the depolarised light intensity apparatus may be usefully compared with the differential thermal analysis measurements of Platt (39), Bell et al (93-95)

and White (87). This D.L.I. technique has the advantage over differential thermal analysis that the sample may be viewed, and physical changes taking place at optical magnification dimensions may be correlated with temperature. It was seen in Chapter 2 that the instrument accurately correlated D.L.I. measurements of transition temperatures with the D.T.A. peak temperatures, provided simple substances were used, and approximate correlation with polymers should be a reasonable assumption.

Fig. 40, overleaf, shows the results for annealing 66 nylon from table 24 (page 110) using D.L.I. measurements, and a comparison with the D.T.A. results of Platt (39) has been made. Platt used the DuPont Calorimeter Cell, which is less sensitive than the more modern D.S.C. cell, but the results are comparable and show a small increase in the heat of fusion of 66 nylon after annealing at 242°C for several hours. Bell et al (93), using a Perkin Elmer instrument, annealed 66 nylon at 220°C , and found a slower but more consistent increase in the total peak area for this polymer. The present optical observations show an increase of 36% in the total birefringence of 66 nylon after annealing for 5 hours at 242°C . Using the D.S.C. cell at 245°C , a 30% increase in the heat of fusion was noted for the same annealing time (table 20). Platt found only a 20% increase in the heat of fusion at 242° for this annealing time.

The temperature range in which the lower D.T.A. peak occurs was found to be within the region where birefringence is being lost from 66 nylon without loss of the spherulites. It is suggested that this corresponds to the loss of secondary crystallites from the exposed parts of the spherulites, as the more strongly bonded primary crystallites which form the basic spherulitic structure have insufficient free energy to allow them to enter the melt state. It follows

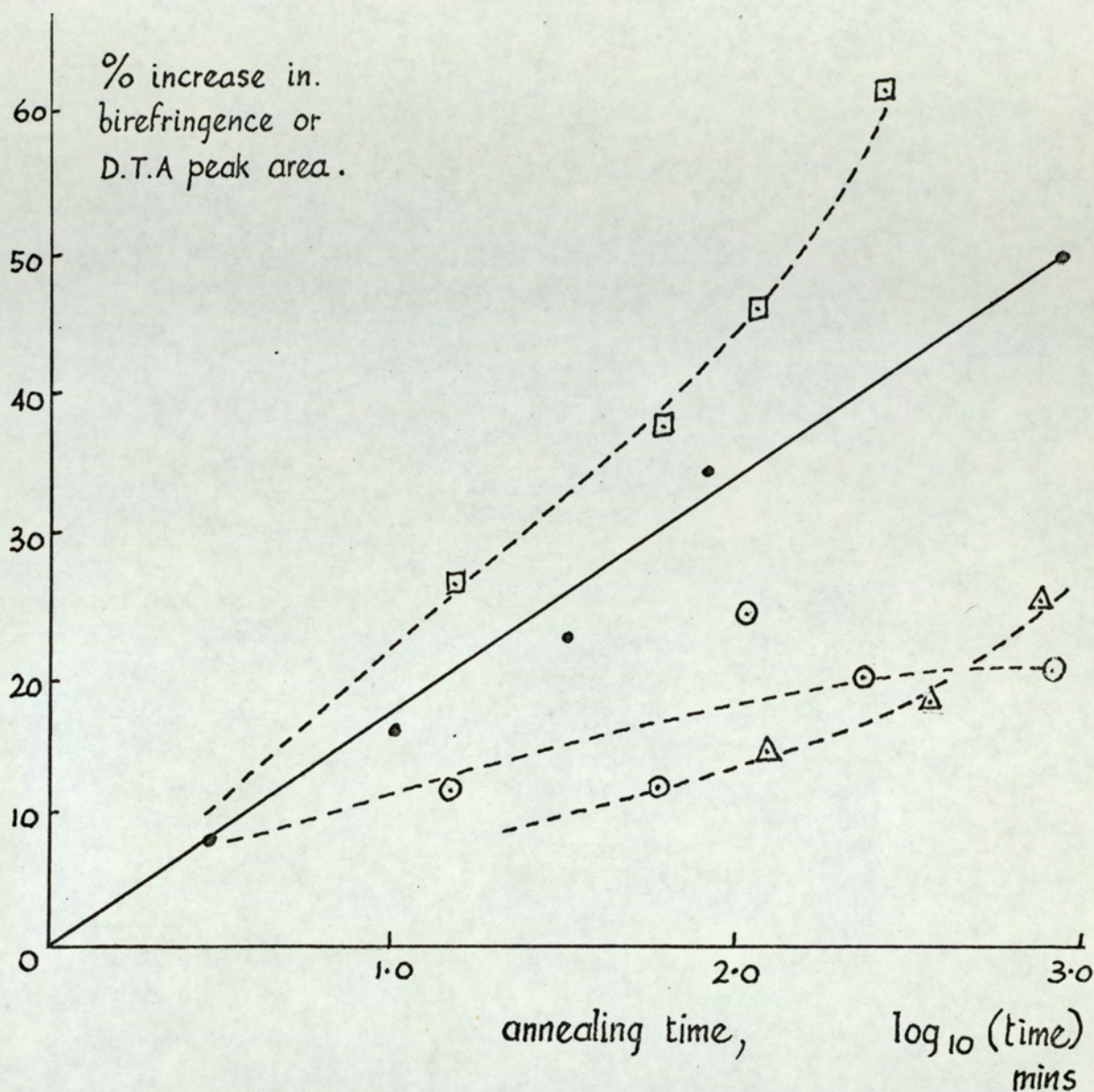


Fig.40. Annealing of 66 nylon. Data of programmed microscopy and D.T.A results of Platt (39) and Bell et al (93)

- Increase in birefringence after annealing at 242°C (table 24, page 110)
- Increase in the total D.T.A. peak area after annealing at 242°C (ref.39)
- △ Increase in total D.T.A. peak after annealing at 220°C (ref.93)
- Increase in low temperature DTA peak at 242°C (39)

that annealing has the effect of improving the perfection of the spherulites, and allowing further secondary crystallization to take place. In order to explain the two melting peaks which are observed for 66 nylon it is necessary to consider two separate processes which may take place during annealing :- (1) Additional crystallization from the melt may take place upon the existing faces of the spherulites. There is no evidence from microscopy to suggest that new spherulites are forming during the annealing period. (2) Imperfect primary crystallites within the existing spherulites may remelt and reform as secondary perfection lamellae, indistinguishable from the material forming in process 1. The evidence for process 2 is less certain than the evidence for secondary crystallization, but three observations using optical microscopy give definite support to the complete melting of poorly formed primary crystallites: (a) Many annealed spherulites have very low birefringence or complete absence of birefringence in the inner regions, implying that crystalline migration has taken place. (b) A substantial loss of birefringence from 66 nylon is observed in the 250 - 260°C range, as shown in fig. 26. After this, the amount of birefringence remaining may be very small if the sample has been carefully annealed. (c). Single crystal like entities are occasionally found in partially crystallized melts which have been held at temperatures close to the melting point (12). At these temperatures, the spherulite bonding forces are clearly weak, and lamellae crystals may form individually; these readily act as centres for spherulite formation upon cooling.

This two process hypothesis appears to explain the D.T.A. observations that the lower melting peak grows and the higher melting peak shrinks during the annealing process. Merger of the peaks after much annealing may occur, due to the small temperature separation of

the peaks ,and the observation that the lower temperature peak rises in temperature as its size increases. Rapidly crystallized polymer shows no low temperature peak,and no loss of birefringence in the appropriate region. Crystallization studies confirm that rapidly crystallized polymer contains less secondary crystallized material,as a better adherence to the Avrami equation is obtained.

The authors of the published D.T.A. observations (39,93-95) also consider three further explanations of the occurrence of multiple melting peaks,which now appear to be less probable on applying the depolarised light intensity observations.

1.The existence of positively and negatively birefringent spherulites , which themselves have different internal structural bonding and hence different primary melting points,can be seen in very slowly crystallized 66 nylon.No changeover is noticed on annealing,and some other polyamides,e.g. 6 nylon, which show multiple melting points ,do not crystallize in more than a single spherulitic form.(10).

2.The possibility of interconversion between the α and β crystalline forms of 66 nylon (Chapter 1) is proposed by Bell et al(93),but is rejected on two considerations : (i) the multiple melting endotherms are not confined to 66 nylon,but are also seen for polymers which are thought to exist predominately in a single crystal form (e.g. 6 nylon) and (ii) the lower melting form is not likely to predominate after annealing. There is also some current controversy over the existence of these forms of 66 nylon.

3.A process involving the folding or unfolding of polymer chains within already formed crystallites may be occurring,thus altering the shape of the crystals comprising the spherulite. Keller and Priest (96) have found that annealing of single crystals results in lateral coarsening, due to the unfolding of some of the chains. Since more lengthy

crystalline sequences then result, it would be reasonable to postulate that they should have a higher melting point, unless the unfolding process has led to their re-location away from the main bonded section of the spherulite. Lower melting point amplification, as is observed in practice, would be expected only if folding processes are taking place, contrary to the observations on single crystals. It is difficult to envisage why either process should lead to an increase in the heat of fusion and the depolarised light intensity, whilst at the same time resulting in a lowering of the melting temperature. The considerations of Booth, Dodgson and Hillier (97) of the production of more lengthy chain sequences on annealing, which leads to higher dilatometric melting points, are in agreement with the theories of Mandelkern and Baker (73), and lend support to the practical observation that the lower peak is observed to increase its temperature upon annealing.

The statement of Bell et al (93) that the higher melting form is kinetically preferred, whilst the low melting form is thermodynamically preferred is obvious on considering the D.T.A. observations. This statement gives no useful information about the nature of these preferred forms. It may be suggested that in the extreme cases, they correspond respectively to spherulites composed only of primary crystallites and formed by a true Avrami process, and perfect single crystals located in a non-bonded spherulite. All the observations can then be considered as representing a partly transformed state, composed of a mixture of imperfect specimens of these two forms.

The D.T.A. of single crystals supports these theories. Because the precipitate from butane diol is a non-spherulitic form of 66 nylon, it does not give a peak which would correspond to the melting of spherulites. In the non-annealed sample (page 114), the early

melting peak (248°C) is probably attributable to poorly formed crystalline material which had been precipitated upon the single crystals, and this may be responsible for the aggregation of the crystals. The true melting of the single crystals probably accounts for the higher melting peak (262°C). On annealing, a perfection process can occur, but observations using the polarising microscope suggest that spherulite formation does not take place. The more perfect crystals now have a single D.T.A. melting peak, although it is surprising that it appeared at a slightly reduced temperature (261°C).

The D.T.A. of nylon yarn follows a pattern similar to that of annealed polymer, with a large low temperature peak, followed by a smaller higher temperature peak. The depolarised light intensity trace is similar to the integrated form of the D.T.A. trace, and visually there is a loss of coloured birefringence from the yarn at around 250°C . This high ordered birefringence had been introduced to the yarn by the changes taking place during the drawing process, as it is not seen in undrawn yarn. It is therefore reasonable to suggest that the D.T.A. peak observed for yarn at 250°C is attributable to the melting of the crystallinity which had been introduced during the drawing process or converted from the original spherulites by that process. The higher D.T.A. peak is representative of the normal melting temperature for very rapidly crystallized polymer, and may be attributed to the loss of the spherulitic crystallinity which had originated during the spinning process.

Fusion of copolymers and multiple melting endotherms.

The copolymers of 66 nylon with 6 nylon and 6T nylon all showed D.T.A. fusion graphs which had the same shape as the equivalent 66 nylon homopolymer graphs, although the peak temperatures were dependent

upon the copolymer compositions. On annealing, each of the 66/6T copolymers showed a large development of crystallinity which contributed to the low temperature peak upon fusion. This difference in behaviour encountered between 66 nylon and 66/6T copolymers was not noticeable with the equivalent composition 66/6 nylon copolymers, which behaved more like 66 nylon. This suggests that the same features which cause multiple melting peaks in 66 nylon are present in similar proportions in the 66/6 copolymers, but in slightly different proportions in the 6T/66 copolymers. It may be suggested that the copolymers would favour shorter sequences of chains in the formation of crystallites, and on Mandelkern and Baker's theories (73), these would have low melting points and would not favour the unfolding process on annealing. This further supports the theory that spherulite changes are responsible for the two melting endotherms developing on annealing.

The different behaviour observed on melting branched nylon (fig.28) appears at first to be anomalous, as there is a much greater tendency to form the lower melting peak, even without annealing. However, there is also an overall reduction in the heat of fusion, and whilst spherulites still form, their optical intensities are low. This suggests that there is an increased tendency to reject branched polymer chains from the growing spherulite and a proportionally larger fraction of the melt may later crystallize in the slower secondary process.

The D.T.A. observations with copolymers lend support to the hypothesis that the separate melting of spherulite primary crystallites and secondary crystallites is the reason for the multiple melting endotherms seen in the differential thermal analysis of polyamides.

CHAPTER 6 . CONCLUSIONS .

The crystallization and melting of copolyamides.

From the present study of the three modified forms of 66 nylon, the following conclusions have been made.

1. Crystallization occurs in random copolymers of 66 nylon with 6 nylon and with up to 20% 6T nylon or up to 3% trimesic acid as a copolymer-branching agent. Crystallization is accompanied by a depolarised light intensity change if the sample is viewed using a polarising microscope.
2. Random copolymerisation normally results in a reduction in the temperature at which crystallization occurs, as illustrated by 66/6 nylon copolymers and 6T/6.10 nylon copolymers. This reduction is high in the case of the branched copolymers, where a high supercooling occurs before crystallization may take place. When isomorphous copolymerisation occurs, as with 6T/66 copolyamides, the crystallization temperature may not fall significantly from the homopolymer crystallization temperature.
3. Random copolymerisation results in a reduction in the total crystallinity. Compared with the values found for the copolymers of 66 nylon with 6 nylon, the reduction is less pronounced when isomorphism occurs and more pronounced for the branched copolymers.
4. The Avrami equation for the time dependence of crystallizations applies to approximately the same extent in the cases of 66/6 nylon copolymers and 66/6T nylon copolymers as is encountered with 66 nylon homopolymer. The depolarised light intensity method for studying crystallization rates is sensitive to observations of the deviations from Avrami behaviour. This theoretical treatment is inapplicable to branched copolymers.

5. Isotherms which show reasonable adherence to the Avrami equation are also superposable if the time axis is expressed logarithmically and rescaled.
6. Secondary crystallization plays an important part in the crystallization process of these polyamides. Particularly lengthy crystallization times have been encountered with branched copolymers, and this has been attributed to lengthy secondary crystallization.
7. The temperature dependence of the crystallization rates follows a systematic trend, and leads to reasonable values for the thermodynamic melting points using a theoretical treatment of Mandelkern, Quinn and Flory. This adds support to the theory, but as it assumes the Avrami theory, it is not applicable to the branched copolymers.
8. Flory's equation for evaluating the heat of fusion of nylon homopolymer from copolymer melting points gave poor agreement with the experimentally determined heat of fusion.
9. Melting of nylon and copolyamides is accompanied by a loss of depolarised light intensity, when the samples are viewed using a polarising microscope. The melting point, as defined by the final disappearance of birefringence from a sample, varies according to the copolymer composition, but is a useful and reproducible measurement for each copolymer. With 66 nylon and its copolymer derivatives, a surprisingly high amount of melting activity was noticed at temperatures substantially below the final melting point. This activity was not detected by means of the differential thermal analysis equipment.
10. Differential thermal analysis shows that two endothermic transitions occur with the melting of these polyamides. The proportional sizes of the transitions depends upon the crystallization history rather than copolymer composition for the 66/6 nylon and 66/6T nylon copolymers. The branched 66 nylon copolymers show melting behaviours

which are different from the observations for 66 nylon homopolymer.

The general importance of nylon polymers.

World production of nylon polymers in 1970 is estimated to be about half a million tons (98). The British consumption of nylon for plastics applications was 6,750 tons in 1968 (99) of which 4,500 tons was 66 or 6.10 nylon for moulding or extrusion. The remainder was mainly 6 nylon (1,500 tons), monofilament and 11 nylon (750 tons).

Two new monomers for producing amorphous polyamides have been introduced recently. These polymers are an interesting class of high temperature transparent moulding materials, with high glass transition temperatures and no crystallinity. They are derived from the terephthalic 'salts' of 3-amino 3,5,5 trimethyl cyclohexylamine, and 2,2,4 trimethyl hexamethylene diamine. The latter is the monomer for Dynamit-Nobel's 'Trogamid' T. (20,100).

Nylon polymer appeared again at Interplas Exhibition in 1969. (101). Most of the exhibits were produced from homopolymers, although a new film grade copolymer, and a composition for hot melt adhesion were seen. New additives are extending the general applications of polyamides, with weather resistant, lubricated and flame retardant glass-filled grades.

The polymers used in large quantities for fibres are 66 nylon and 6 nylon, although 66/6 nylon copolymers and 66/6T copolymers are thought to be of importance for specialised applications. Cross-linked fibres are known to show elasticity (102), which would make them potentially useful, but their development has been impaired by the impossibility of melt spinning. Cross-linked polymer formation in 66 nylon is thought to be responsible for some of the difficulties occasionally encountered in the spinning process. The introduction of cross links by an irradiation process on spun fibre must be rated as

expensive and impracticable.

The technological implications of the work.

It is well known that crystalline polymers lose their mechanical strength if a plasticizer is added. This may take the form of the incorporation of a non-crystallizing comonomer, and the 66/6 nylon copolymer system was found to be an example of this behaviour. The observations of loss of crystallinity and reduced melting points were indicative of copolymers with lower mechanical rigidity and tensile strength, and poorer thermal rigidity by comparison with the properties of the homopolymer. There are a few advantages with materials of this type: they possess more flexibility than homopolymers, and may be processed over a wider and lower temperature range. Thermal decomposition is sometimes troublesome with the processing of 66 nylon, but the favoured solution to this problem would be to change to 6, 11 or 6.10 nylon rather than to use a copolymer.

The isomorphous copolyamides of 66 nylon with 6T nylon gave only a partial retention of the total crystallinity as the comonomer was introduced, although a substantial recovery of this lost crystallinity occurred on annealing. This unexpected conclusion implies that a loss in mechanical strength may be expected with these materials, unless annealed. It may be unreasonable to extend this speculation to include drawn fibres.

The information from 66/6X nylon copolymers supports the technological observations of the disadvantages of incorporating any branched or cross-linked polymer into the melt for spinning. These copolymers were found to be slow to crystallize and they developed comparatively small amounts of crystallinity. The melt viscosity of these copolymers would also make spinning impracticable.

A few implications may be drawn from the melting traces

for the homopolymers. The maximum temperatures for continuous service of polyamides are significantly below their melting points, and may correspond approximately with the temperatures of the commencement of depolarised light intensity changes in the samples. For 66 nylon and 6 nylon in moulded form, this loss of birefringence commences at about 120°C , but for fibres it is significantly higher, with 230°C for 66 nylon (and 185°C for 6 nylon). The traces predict that, in an oxygen free atmosphere drawn 66 nylon fibre should be resistant to stress deformation at temperatures between 120 and 200°C , whilst a moulded sample may show stress relaxation in this temperature range. No transitions which could be equated with the onset of depolarised light intensity changes were detected by using the differential thermal analysis equipment.

Recommendations for further work.

Polymers and copolymers :- An extensive review of polyamides is given by Morgan (103). In the present study, it has been an objective to base the copolymers upon the commercial nylons, hence the study has included only derivatives of 66 nylon, and 6 and 6.10 nylons. Many polyamides exist for which there is no reported information on crystallinity or crystallization rates.

Modified polymers :- of the polymers studied, branched/cross-linked nylon showed the most prominent departure from the expected crystallization behaviour. Two ways of producing cross-links in nylon are irradiation and oxidation. Reaction with formaldehyde also introduces cross-links; and it is anticipated that these polymers would show interesting departure from the regular crystallization behaviour, which could be compared with the trimesic acid copolymer results.

Apparatus and methods :- The depolarised light intensity method

has proved convenient and useful for this study, and it is doubtful whether the work could have been carried out with the thermal and dilatometric techniques. The dielectric change in crystallization is another technique which could usefully be introduced. With all high temperature crystallization studies, temperature control is a problem, and in this study the results could have been more precise if a more efficient temperature controller had been designed.

Technological basis:.- There is no practical correlation between the rates of crystallization determined experimentally using isothermal microscopy or dilatometry, with the rapid crystallizations used in industrial practice. Research is needed to enable the optimum moulding and extrusion conditions to be achieved.

Mechanical properties:.- the influence of crystallinity upon the strength of polymeric materials has not been satisfactorily evaluated.

Theoretical analysis:.- the interpretation of crystallization data is complicated by the inadequacy of the basic Avrami theory; any more satisfactory treatments require an extensive mathematical treatment which includes computerised approximations.

REFERENCES.

1. P.H.Geil, Polymer Single Crystals, Interscience, 1963.
2. A.Keller, J.Polymer Sci., 1959, 36, 361.
3. P.H.Geil, J.Polymer Sci., 1960, 44, 449.
4. A.Keller, Private communication.
5. A.D.Keith and F.J.Padden, J.applied Physics, 1963, 34, 2409.
6. E.H.Boasson and J.M.Woestenenk, J.Polymer Sci., 1957, 24, 47.
7. J.H.Magill, J.Polymer Sci., pt A2, 1966, 4, 243; J.Polymer Sci, 1965, A3, 1195.
8. B.Kahle, Zeits. Elektrochem., 1957, 61, 1318.
9. B.B.Burnett and W.F.McDevit, J.applied Physics, 1957, 28, 1101.
10. J.H.Magill, J.Polymer Sci., pt.A2, 1969, 7, 123.
11. J.H.Magill, Polymer, 1962, 3, 43.
12. J.H.Magill and P.H.Harris, Polymer, 1962, 3, 252.
13. A.Keller, Polymer, 1962, 3, 393.
14. P.Meares, Polymers- Structure and bulk properties, VanNostrand, 1965.
15. D.R.Holmes, C.W.Bunn and D.J.Smith, J.Polymer Sci., 1955, 17, 159.
16. C.W.Bunn and E.V.Garner, Proc.Roy.Soc.Lond., 1947, A189, 39.
17. W.P.Slichter, J.Polymer Sci., 1958, 35, 77.
18. D.C.Vogelsong, J.Polymer Sci., 1963, A1, 1055.
19. D.C.Vogelsong, J.Polymer Sci., 1962, 57, 895.
20. Materials supplement to British Plastics, Jan.1970, 77.
21. W.E.Catlin, E.P.Czerwin and R.H.Wiley, J.Polymer Sci., 1947, 2, 412.
22. S.Sonnerskog, Acta.Chem.Scand., 1956, 10, 113.
23. W.O.Baker and C.S.Fuller, J.Amer.Chem.Soc, 1942, 64, 2399.
24. M.Baccaredda and E.Butta, J.Polymer Sci., 1956, 22, 217.
25. C.W.Deeley, A.E.Woodward and J.A.Sauer, J.applied Physics, 1957, 28, 1124.
26. P.J.Flory, J.Amer.Chem.Soc., 1941, 63, 3083.

27. G. Allegra and I. W. Bassi, *Adv. in Polymer Sci.*, 1969, 6, 549.
28. G. J. Howard and S. Knutton, *Polymer*, 1968, 9, 527.
29. O. B. Edgar and R. Hill, *J. Polymer Sci.*, 1952, 8, 1.
30. H. Plimmer, R. J. Reynolds et al, *Brit. Pat. appl.* 1949/604.
31. L. F. Fieser and M. Fieser, *Organic Chemistry*, Reinhold, 1956.
32. A. J. Yu and R. D. Evans, *J. Polymer Sci.*, 1960, 42, 249.
33. F. B. Cramer and R. G. Beaman, *J. Polymer Sci.*, 1956, 21, 237.
34. A. Sharples, *Introduction to polymer crystallization*, Arnold, 1966.
35. L. Mandelkern, *Crystallization of Polymers*, McGraw Hill, 1964.
36. E. D. Harvey, *M.Sc. thesis*, University of Aston in Birmingham, 1965.
37. C. N. Holmes, *M.Sc. thesis*, University of Aston in Birmingham, 1966.
38. F. J. Hybart and B. Pepper, *J. applied Polymer Sci.*, 1969, 13, 2643;
B. Pepper, *M.Sc. thesis*, University of Aston, 1967.
39. F. J. Hybart and J. D. Platt, *J. applied Polymer Sci.*, 1967, 11, 1449;
J. D. Platt, *PhD. thesis*, University of Aston, 1968.
40. M. Inoue, *J. Polymer Sci.*, 1961, 55, 753.
41. G. Allen, *Brit. Polymer J.* 1969, 1, 168.
42. J. V. McLaren, *Polymer*, 1963, 4, 175.
43. J. H. Magill, *Nature*, 1960, 187, 770, *Polymer*, 1961, 2, 221.
44. F. L. Binsbergen and B. G. M. de Lange, *Polymer*, 1970, 11, 297.
45. B. Y. Teitelbaum and N. A. Palikhov, *Vysokomol. Soedin. pt. A*, 1968, 10,
1468.
46. E. M. Barrall, J. F. Johnson and R. S. Porter, *Applied Polymer Sympos.*,
1969, 8, 191.
47. J. N. Hay, *J. Sci. Instruments*, 1964, 41, 465.
48. L. A. J. Ireland, *Practical Wireless*, 1970, 45, 690
49. R. P. Miller and G. Sommer, *J. Sci. Instruments*, 1966, 43, 293.
50. J. H. Magill, *Brit. J. applied Physics*, 1961, 12, 618.
51. A. Booth and J. N. Hay, *Polymer*, 1969, 10, 95.
52. P. W. Allen, *Trans. Far. Soc.*, 1952, 48, 1178.

53. R.Buchdahl,R.L.Miller and S.Newman,J.Polymer Sci.,1959,36,215.
54. B.I.Sazhin and N.D.Podosenova,Vysokomol.Soedin,1964,6,137.
55. DuPont Instruments,Wilmington,Delaware,U.S.A. Sales literature and 900 Handbook,1964 and 1969.
56. M.Avrami,J.Chem.Physics,1939,7,1103.
57. W.Banks,J.N.Hay and A.Sharples,J.Polymer Sci.,1964,A2,4059.
58. J.N.Hay,M.Sabir and R.L.T.Steven, Polymer,1969,10,187.
59. M.Gordon and I.Hillier,Phil.Mag.1965,11,31.
60. I.Hillier, Polymer,1968,9,19.
61. D.Turnbull and J.C.Fisher,J.Chem.Physics,1949,17,71.
62. L.Mandelkern,F.A.Quinn and P.J.Flory,J.applied Physics,1954,25,
830.
63. J.D.Hoffman,J.Chem.Physics,1958,29,1192.
64. L.B.Morgan,Chemy.Industry,1951,796.
- 65.F.D.Hartley,F.W.Lord and L.B.Morgan,Trans.Roy.Soc.Lond,1954,A247,
243.
66. L.Mandelkern in Growth and Perfection of Crystals,ed.R.H.Doremus,
B.W.Roberts and D.Turnbull,Wiley,1958.
67. A.Kovacs,Ricerca Sci. Suppt.A, 1955,25,668.
68. L.Mandelkern,Chem.Reviews,1956,56,903.
69. E.W.Russell, Trans.Faraday Soc.,1955,47,143.
70. N.A.Plate,T.Kheu and V.P.Shibaev,J.Polymer Sci,ptC,1967,C16,1133.
- 71.F.Gornick and L.Mandelkern,J.applied Physics,1962,33,907.
72. P.J.Flory,Trans.Faraday.Soc.,, 1955,51,548.
73. C.H.Baker and L.Mandelkern,Polymer,1966,7,7.
74. Handbook of Chemistry and Physics,The Chemical Rubber Co,44th
edn,1963.
75. S.Drake,in the Encyclopedia of Philosophy,Vol.3,Macmillan,1967.
76. P.W.Allen,Techniques of Polymer Characterisation,Butterworths,
1959.
77. W.R.Sorenson and T.W.Campbell,Preparative Methods of Polymer
Chemistry, Interscience,1961.

78. H.G.Elias and R.Schumacher, *Makromol.Chemie*, 1964, 76, 23.
79. J.J.Burke and T.A.Crofino, *J.Polymer Sci.*, pt.A2, 1969, 7, 1.
80. R.Bennewitz, *Faserforsch.Textil.technol.*, 1954, 5, 155.
81. P.W.Morgan and S.L.Kwolek, *J.Polymer Sci.*, 1963, A1, 1147.
82. A.Keller, *Kolloid Zeits.*, 1969, 231, 386.
83. C.W.Hock and J.F.Arbogast, *Anal.Chem.*, 1961, 33, 462.
84. M.L.Miller, *Structure of polymers*, Reinhold, 1966.
85. H.W.Starkweather and R.E.Moynihan, *J.Polymer Sci.*, 1956, 22, 363.
86. *Polymer Handbook*, eds.J.Brandrup and E.H.Immergut, Wiley, 1967.
87. T.R.White, *Nature*, 1955, 175, 895.
88. L.Mandelkern, *J.applied Physics*, 1955, 26, 443.
89. A.N.Gent, *Trans.Inst.Rubber Ind.*, 1954, 30, 139.
90. F.D.Hartley, F.W.Lord and L.B.Morgan, *Ricerca Sci. suppt.A*, 1955, 25, 577.
91. M.Inoue, *J.Polymer Sci.*, 1963, A1, 2697.
92. V.E.Shashoua and W.M.Eareckson, *J.Polymer Sci.*, 1959, 50, 343.
93. J.P.Bell, P.E.Slade and J.H.Dumbleton, *J.Polymer Sci. pt A2*, 1968, 6, 1773.
94. J.P.Bell and J.H.Dumbleton, *J.Polymer Sci*, pt.A2, 1969, 7, 1033.
95. J.P.Bell and T.Murayama, *J.Polymer Sci*, pt.A2, 1969, 7, 1059.
96. A.Keller and D.J.Priest, *British Polymer Physics Conference*, Shrivensham, 1969, *J.Polymer Sci*, pt.B, 1970, 8, 13.
97. C.Booth, D.V.Dodgson and I.Hillier, *J.Polymer Sci*, pt.A2, 1970, 8, 519.
98. *Modern Plastics*, Jan.1970, 47, 97.
99. *British Plastics*, Jan.1969, 42, 57.
100. A.H.Wilbourn, *Plastics and Polymers*, 1969, 37, 417.
101. *British Plastics*, July.1969, 42, 86.
102. E.L.Whitbecker, R.C.Houtz and W.W.Watkins, *Ind.Eng.Chem.*, 1948, 40, 878.
103. P.W.Morgan, *Condensation Polymers*, Wiley, 1965.